SHRINKAGE AND CREEP CHARACTERISTICS

OF

SOIL-CEMENT

A thesis presented for
the degree of Doctor of Philosophy
in Civil Engineering
in the University of Canterbury
Christchurch, New Zealand

by

R.J. Dunlop

1973

ABSTRACT

The work presented in this thesis is an initial investigation into the development of shrinkage and creep in a soil-cement pavement slab, and the consequent internal stresses which are induced.

A survey is made of the relevant material which has been researched on soil-cement and a limited study on the shrinkage and creep of concrete.

By examining shrinkage, creep and strength with respect to the moulding conditions, recommendations for the mix proportions of loess soil-cement and sandy pumice soil-cement are presented.

The existing methods for predicting shrinkage stresses within a soil-cement base were found to be totally inadequate so a new method of stress prediction, based on experimental results and fundamental theory is presented. This new method is shown to adequately predict shrinkage stresses, provided the moisture distribution within the soil-cement slab is known.

Studies on moisture flow both in soil-cement prisms and soil-cement slabs are shown to be very accurate provided the initial flow parameters have been accurately obtained.

It is shown that a combination of traffic loading, temperature changes, shrinkage and fatigue failure must be taken into account when designing a soil-cement pavement slab.

Present design methods have been criticized and additions have been proposed.

ERRATA

VOLUME I

Page	Description
viii	∞ missed as subscript from Q_∞ and S_∞
viii	x_1 should read $f/\sqrt{k}$.
3	line 10 - "coarse aggregate particles" should read "coarse-grained soils".
17	line 9 - "soils" should read "soil-cements".
24	line 8 - after "laboratory samples" add "of cohesive soils dry of OMC".
40	Para. 2, line 6 - "latter" should read "Latter change".
54	line 20 - "Redwood" should read "Redward".
94	line 7 - one closing parenthesis missed.
130	Section 8.1.1, line 14 - "for a sample of 4 gm or less" should read "for a sample".
142	3rd last line - stop not comma before Klute.
163	6th last line - "rainfall were represented by 4th order equations, as shown in fig. (8.36)" should read "rainfall, as shown in fig. (8.36), was represented by a 4th order equation".
173	Section 9.1.8, line 9 - "fig. (6.4)" should read "fig (6.5)".
174	line 5 - equation should read: "$\frac{\text{original MC} - \text{MC}^{(t)}}{(\text{original MC}/\Delta t)}$" where t is in days
174	6th last line - "(b) restrained" should read "(b) internally restrained".
188	3rd from last line - "10%" should read "10% of the surface moisture content".
204	line 3 - "highly" should read "over-compacted".
213	line 13 should read "Base requires minimum cover = 19 mm".
217	lines 10 and 15 - "Possions" should read "Poisson's'

Page	Description
224	4th from last line - "acceptance" should read "suitability".
225	Section 11.7.2, line 2 - "From the results" should read "From the computer results".
228	line 4 - "3.29 M" should read "3.29 m".
228	line 6 - "2.98 M" should read "2.98 m".

ACKNOWLEDGEMENTS

I wish to gratefully acknowledge the assistance given to me by the many people and organizations throughout the period of study.

Professor H.J. Hopkins, Head of the Civil Engineering Department for overall supervision of the project and personal interest.

Professor R. Park for his personal interest and advice.

Messrs. J.P. Blakeley, T.A.H. Dodd and Dr. P.J. Moss, my supervisors, for their personal interest, encouragement, assistance and direction.

The remaining members of the Academic Staff of the Civil Engineering and especially Dr. R.O. Davis for his advice and assistance in preparing this thesis.

All members of the Technical Staff of the Civil Engineering Department who have worked on or in connection with this project. Special thanks must be attributed to the Technical Officers, Messrs. H.T. Watson and P.C. Dawson for their help in planning and obtaining the necessary help and equipment. Also Messrs. C. Bennett, H.H. Crowther, V. Gavars, R.P. Hall, K.L. Marrion, N.W. Prebble, P.J. Robinson, S.R. Robinson, J.S. Sheard, G.W. Sim, J.G.C. Van Dyk for their competent approach to the construction of the large quantity of equipment used in this project and the dedication displayed in carrying out the testing under sometimes difficult conditions. Mr. H. Patterson for photographic preparation and Mr. W. McClelland for assistance in preparing this document.

Mr. F. Downing of the Chemistry Department for his skill and assistance in building the large quantity of glass apparatus used in this project.

Dr. D.P. Seed of the Geology Department who painstakingly analyzed the chemical properties of the soils used in this project.

The many members of the University Maintenance Staff and especially Mr. L.C. Johnston for his assistance in speedily rectifying failures in the constant temperature room, curing room and fog room plant.

The many members of the University Computer Staff for their excellent assistance in punching cards, de-bugging programs and running the numerous computer programs.

Also the staff of the Engineering Faculty Library for their assistance.

The National Roads Board for a Postgraduate Scholarship in 1969 and for substantial financial contributions to this project.

The Ministry of Works for a Study Award for 1970-72 and the University of Canterbury for financial assistance.

Many individuals and organizations for their contribution in the supply of materials and technical assistance including Roading Division, Christchurch Laboratory and Hamilton Laboratory - of the Ministry of Works; New Zealand Portland Cement Assn; N.O. Pierson Ltd Refrigeration and Air Conditioning Engineers, Christchurch; Dunlop (N.Z.) Ltd and Hamilton City Council.

My brother, Bevan Dunlop for typing the draft and continued assistance with the preparation of this thesis and Mrs. I. Bean for typing this thesis.

Finally, I wish to thank my parents and friends for their encouragement and especially my wife, Elizabeth, for her dedicated loyalty in assisting with the large amount of laborious laboratory testing.

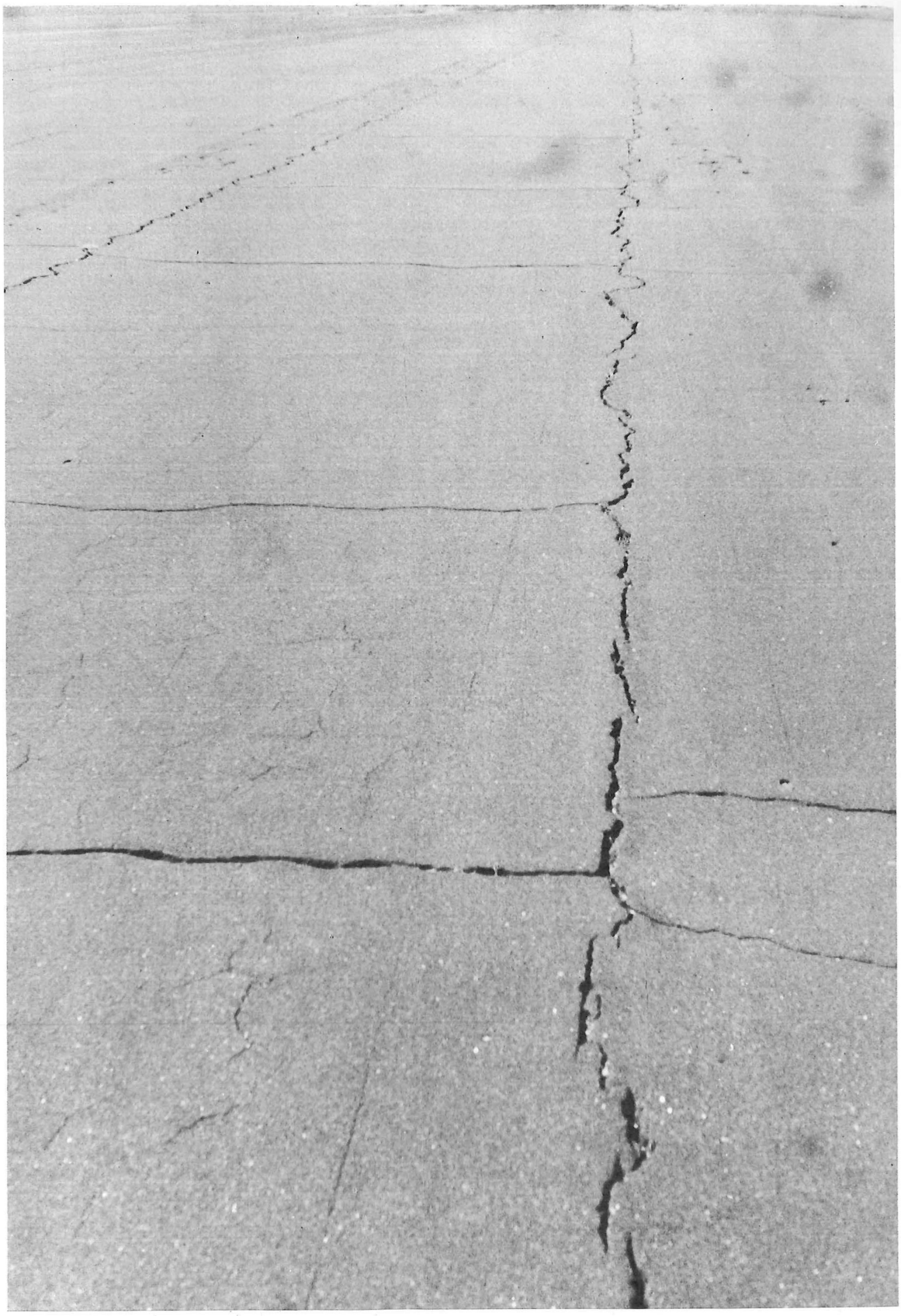

Frontpiece: CRACKING OF SOIL-CEMENT IN THE WANGANUI AIRFIELD

INDEX OF NOTATION

B	:	fb/K
b	:	width of a prism.
C_v	:	coefficient of consolidation.
C_5	:	$(\frac{\partial h}{\partial \theta})_5$: inverse differential water function at point 5.
D	:	diffusivity.
$(EI)_1$	:	$\int_{-y_c}^{b-y_c} E(t)\, y^2 dy$
E_c	:	modulus of elasticity in compression.
E_k	:	modulus of elasticity for the Maxwell model (fig. (9.16)).
E_m	:	modulus of elasticity fig. 7.1.
E_k	:	modulus of elasticity fig. 7.1.
E_t	:	modulus of elasticity in tension.
erfc(u)	:	$2/(5\pi)\int_u^\infty e^{-u2}\, du$
e_x	:	measured strain in the x direction.
e shoulder	:	evaporation at the shoulder.
E sat	:	evaporation from a free water surface.
f	:	surface factor.
hl	:	ratio: impedance of sample/impedance of membrane or plate.
h	:	suction.
H	:	the relative humidity.
H_a	:	relative humidity of the atmosphere.
I	:	infiltration.
I_T	:	transformed moment of inertia.
k	:	diffusivity coefficient of shrinkage.
K_x, K_y, K_z	:	permeabilities in the x, y and z directions.

Index of Notations (cont.)

K	:	permeability.
K_1	:	soil layer in computer program of road cross section.
l	:	length of a prism.
M	:	molecular weight of water.
MC	:	moisture content.
M'	:	moment.
n	:	numerical number.
P	:	linear differential operator.
pF	:	suction.
Q	:	linear differential operator.
Q_t	:	outflow at time t.
Q_∞	:	ultimate outflow at $t = \infty$.
R	:	gas constant.
S	:	free unrestrained unit linear shrinkage strain.
S_∞	:	value of S when $t = \infty$.
S_{av}	:	average shrinkage = $1/b \int_0^b s\,dy$.
S'	:	$S(t)$.
t	:	time.
T	:	Kt/b^2.
T_a	:	absolute temperature.
u	:	excess pore pressure.
V_{max}	:	maximum deflection at $l/2$.
V	:	volume of sample.
V_x, V_y, V_z	:	macroflow velocities in the x, y, z direction.
x, y, z	:	co-ordinates of a prism (fig. (7.4)).
x_1	:	$f/\sqrt{K}$.
y_p	:	curvature.

Index of Notations (cont.)

y'	:	distance of fibre from the neutral axis.
y_c	:	distance from the sealed surface to the neutral axis.
z	:	height above datum.
ε_t	:	creep strain.
ε_x	:	strain produced by stresses.
η_m	:	modulus of viscosity (fig. (7.1)).
η_K	:	modulus of viscosity (fig. (7.1)).
η_k	:	viscoelastic coefficient of the Maxwell model (fig. 9.16).
τ	:	η_K/E_K = relaxation time.
σ	:	$\sigma(t)$ = sustained stress.
σ_f	:	$\sigma_f(t)$ = ultimate compressive strength.
σ_x'	:	stress in a prism restrained from deflecting.
σ_x''	:	stress in each fibre.
θ	:	volumetric water content.
ξ	:	σ/σ_f
α	:	$f/\sqrt{K}$.
α_n	:	solutions of $(hl = \alpha' \tan \alpha')$.
β	:	$[(1-(y/b))](b/K)$.
φ_1	:	E_m/η_m.
φ_2	:	E_m/η_K.
φ_3	:	E_K/η_K.
Φ_1	:	$(-(\varphi_1+\varphi_2+\varphi_3) + \sqrt{(\varphi_1+\varphi_2+\varphi_3)^2-4\,\varphi_1\varphi_3})/2$.
Φ_2	:	$(-(\varphi_1+\varphi_2+\varphi_3 - \sqrt{(\varphi_1+\varphi_2+\varphi_3)^2-4\,\varphi_1\varphi_3})/2$.
$\partial\rho$	:	pressure or suction increment.
ψ	:	$h + z$ = total potential.

VOLUME I

SHRINKAGE AND CREEP CHARACTERISTICS

OF

SOIL-CEMENT

CONTENTS

CONTENTS (cont.)

CONTENTS (cont.)

CONTENTS (cont.)

CONTENTS (cont.)

CONTENTS (cont.)

VOLUME II

FIGURES

TABLES

APPENDICES

CHAPTER ONE

INTRODUCTION

1.1 General

Probably the earliest recorded use of cement stabilization of soil was in England about 1917, where cement was applied to muddy tracks to provide a usable road. The first recorded, scientifically controlled project was undertaken in 1935, near Johnsonville, South Carolina, United States of America. Since this time, many miles of roads and airport runways throughout the world have been built on bases and sub-bases which have been stabilized with cement.

In New Zealand, the first recorded placing of cement stabilized pavement was in 1943-44, at the Ardmore airport in Auckland, where 53,000 square feet of airfield was laid by the Ministry of Works, Auckland. At the time this airport was under construction, research on cement stabilization was being carried out in the laboratories of the Department of Scientific and Industrial Research in New Zealand, under the control of K.S. Birrell. The testing program comprised appropriate tests taken from the Standards of the American Society for Testing Materials; these tests were applied to soils obtained from twenty-nine airfield locations throughout New Zealand.

This early work was an excellent start in the right direction, but, unfortunately, it was not followed by more

NOTE: text on original also missing on far right (20/12/20)

1.1 (cont.)

research, especially on the suitability of different soil types for stabilization. Work along these lines has only been started in the last few years. In the meantime, construction of cement stabilized pavements began to increase up to the boom period in the early 1960's, as local bodies, government and private contractors realized the benefits to be gained from this new process. This boom period was followe by a sharp recession starting about 1968 and continuing until the present time, where the amount of stabilization being carr out is hardly worthy of mention. The main reason for the decrease in cement stabilized pavement construction has been attributed to the substantial increase in the number of pavements which have cracked over the last decade.

The increase in failures of cement stabilized pavements has been attributed to inadequate knowledge of the cement stabilized soils before the commencement of pavement construct Failures take the form of cracks within the stabilized base, and have often been attributed to shrinkage. (Frontpiece). In some cases, shrinkage causes cracking, but any or all of the following may also cause cracking:

i) failure of the subgrade

ii) fatigue failure owing to heavy traffic loading

iii) internal stress build-up owing to temperature and shrinkage-induced stresses.

The cracks so formed cause the following problems:

i) Undesirable appearance and riding quality.

ii) Fragmentation into short slab lengths which no longer represent a rigid pavement.

1.1 (cont.)

iii) Allow water ingress to the subgrade.

1.2 Definition of Soil-Cement

A cement-stabilized soil is defined as a tightly compacted mixture of pulverized soil, water and portland cement. As the cement hydrates, a hard, durable structural material is formed. A cement-stabilized material is usually named according to the size of the soil particles to which the cement is added. Thus, soil-cement is a mixture of water, cement and fine-grained soil, while cement-treated material is a mixture of water, cement and coarse aggregate particles.

1.3 New Zealand Approach to the Use of Soil-Cement

Cement stabilization has been confined largely to the North Island of New Zealand, where there exists a shortage of good quality aggregate suitable for conventional pavement construction. A summary of the construction techniques, laboratory tests, design procedures and pavement performances is presented in Appendix I.

In New Zealand, laboratory testing of soils for stabilization appears to be very limited and has been confined to simple tests only. The results obtained in the field were mostly satisfactory, but many instances of cracking were evident.

Research work on soil-cement in New Zealand has been very limited. The Department of Scientific and Industrial Research has carried out some laboratory tests on a number of soils, while at the University of Canterbury, some small

1.3 (cont.)

projects on cement stabilized soils have been undertaken.

1.4 Overseas Research

When this research project was initiated, only three papers on shrinkage in soil-cement were found. One paper by Nakayama and Hardy[92] briefly outlines experimentally-obtained results on some of the factors which influence shrinkage. Two papers by George[50,53] discuss the influence of some factors on shrinkage, then propose an elastic theory for predicting shrinkage cracking in a soil-cement base. From the limited information provided by these papers on the factors which influence shrinkage, it appeared that a reduction in shrinkage could be obtained by constructing a pavement with these factors optimised. However, from a study of the theory for shrinkage cracking presented by George[50], it was evident that many significant factors such as differential drying, non-uniform development of shrinkage stresses, and creep, had been ignored.

During the course of this project six further papers have been published on the subject of shrinkage and shrinkage stresses in soil-cement. George[51], in a later paper, introduced the influence of viscoelastic properties on the stresses induced in soil-cement. Unfortunately this study was not realistic, but a still later paper by George[52] did briefly discuss differential drying. Shrinkage was related to drying time by the diffusion equation while creep was represented by the Burger model.

A paper on shrinkage stresses in soil-cement prisms was presented by Okada and Kawamura[98], and although inadequate

1.4 (cont.)

in many aspects, it was a great step forward in understanding and expressing the occurrence of shrinkage and creep within a prism. The recognition of differential drying characteristics across a sample drying from one side indicated the complexity of the problem, but the stresses derived using the developed theory were not verified by experimentally-obtained results.

A later paper presented by Kawamura[72] again used the diffusion equation to relate shrinkage to drying time, but creep was represented by the Burger model instead of by a series of experimentally-obtained creep curves as used previously (98). Unfortunately, this method also had shortcomings, as shown later in this thesis (Chapter 7).

Bofinger and Sullivan[17] have presented a report on shrinkage and cracking for one moist cured soil-cement mix, while Pretorius and Monismith[108], in a report just received have used the finite element technique in an attempt to predict shrinkage cracking. The use of finite elements had been considered for this thesis, but firstly many other factors needed investigating. Pretorius and Monismith[108] have carried out their study without investigation of the many physical parameters, thus rendering the bulk of the work invalid.

1.5 Scope of this Study

Because of the limited research and the concern indicated by New Zealand roading engineers as to the cause and control of cracking in cement stabilized soil bases, it was decided to investigate shrinkage of soil-cement and the many factors which influence this shrinkage. Therefore, a program of laboratory

1.5 (cont.)

tests was set up to examine the effects of such variables as moulding density, moulding moisture content, cement content etc., on tensile and compressive strength and ultimate shrinkage. These tests were followed by determinations of shrinkage stress build-up using specially developed equipment. Results were obtained for two fine grained soils, namely a Canterbury modified loess and a Hamilton sandy pumice.

As results from the above work became available, new ideas and problems were investigated so that the original test program needed revision. It soon became apparent that available moisture and its movement within the soil cement greatly influenced the shrinkage, creep and strength so investigations were initiated into the techniques for measurement of suction and permeability of soil-cement, for later use in predicting moisture migration.

A stress prediction hypothesis for the development of internal stresses in small soil-cement prisms was then proposed as follows.

The prism is considered to be long and narrow so that the stresses which develop internally are considered to be independent of the longitudinal co-ordinate. The Maxwell Model has been used to represent the visco-elastic effects in a soil-cement with the viscoelastic coefficient being both time and moisture content dependent and the elastic modulus being moisture content dependent. By considering the strain changes within a prism as drying occurs, stresses are predicted at different positions across the prism.

In order to use the above proposed stress prediction hypothesis a considerable amount of data is required. This data includes, moisture content profiles with respect to drying time for a soil-cement prism, the compressive and tensile strengths with respect

1.5 (cont.)

to the moisture content, the free unrestrained shrinkage with respect to the moisture content, the viscoelastic coeffficient with respect to time and the moisture content, the elastic modulus with respect to the moisture content and the strain changes which occur across a drying prism.

To obtain this data, the following experiments were planned. Many prisms were dried for specific periods of time before being broken to obtain the moisture content profiles. The compressive strengths were obtained from 13mm diameter samples broken in unconconfined compression, while the tensile strengths were also obtained from 13mm diameter samples using the indirect tension test. The free unrestrained shrinkage was recorded with respect to the moisture content as a 13mm diameter 100mm long sample dried. Viscoelastic coefficients and elastic modulii were obtained from tension creep tests, while the strain changes which occur as a prism of soil-cement dries were recorded using a demec gauge measuring between two demec points glued to the soil-cement. Therefore, a simplified study of the stresses caused by both traffic loading and differential temperatures is presented in this thesis.

The aim of this project was

(a) to enable a pavement designer to predict the possibility of cracking, and

(b) to enable a pavement designer to minimise cracking and crack spacing.

CHAPTER TWO

PAVEMENT CONDITIONS AS THEY EXIST IN THE FIELD

2.1 Road Pavements and their Construction

A road pavement can be designed in several ways, depending on the traffic loading and the subgrade conditions. A rigid pavement is generally constructed of concrete in the form of a slab, which rests on either a sub-base or the subgrade, thus acting as a bridge over soft spots. On the other hand, a flexible pavement usually consists of a sub-base placed on the subgrade followed by a compacted base and bituminous surfacing. It carries little load by slab action, relying on a consistent load bearing ability of the sub-base and subgrade. For most soil-cement pavements, the subgrade is either compacted or weakly stabilized with small quantities of either lime or cement and then compacted. If a sub-base is required, it may also be weakly stabilized, while the base itself is of a good quality soil-cement.

For discussion purposes, a soil-cement pavement will be considered as overlying an unstabilized sub-base and subgrade. The soil-cement base is usually constructed as continuous slabs in runs approximately 1.5 metres wide and 400 metres or so long. Other similar soil-cement slabs are placed edge to edge until the necessary carriageway width is formed.

2.2 Environmental Effects

Changing environmental conditions can seriously affect

2.2 (cont.)

the performance of a soil-cement pavement. Consider first the water table, which could be high when the pavement is placed, yet in the drier seasons the water table will drop, causing a drying out of all pavement layers. If evaporation is greater than infiltration, drying out of the shoulder can result in the drying of the remaining pavement layers. One side of the road may be situated very close to a hill, e.g. in a cutting. This will cause accumulation of water on that side of the road, with likely migration across the road pavement beneath the sealed surface. Vegetation may alter the moisture distribution also, with large trees providing a water sink. Any form of existing drains may provide an outlet for water, thus altering the moisture distribution.

Any loss of moisture from the soil-cement base will cause shrinkage, which is resisted by subgrade restraint, at the frictional contact between base and subgrade, so that most of the slab is fully restrained in the direction of the road centreline. Thus, tensile stresses develop within the soil-cement slab and, wherever the tensile stress in the slab exceeds the tensile strength of the material, a crack will form.

An apparent loss of moisture occurs when soil-cement is cured without any external moisture loss. This process, known as self-desiccation, occurs when a cohesive soil is stabilized. The unstabilized soil lumps lose some of their moisture to the hydrating cement grains, so that these unstabilized soil lumps shrink, thus causing an overall shrinkage of the soil-cement base even though it is fully protected from evaporation. This so termed 'self desiccation' effect is important. Self desiccation will

2.2 (cont.)

develop stresses which are uniform throughout the pavement section, but drying shrinkage stresses never develop uniformly. Therefore, once drying of a soil-cement base has been initiated, the moisture distribution throughout the base will be non-uniform, thus causing the development of non-uniform stresses.

2.3 Stresses Developed in a Soil-Cement Pavement

When a pavement slab is subjected to a wheel load at any interior point, a compressive stress is developed at the top of the slab and a tensile stress at the bottom. If the pavement slab is cracked, corner loading will cause a tensile stress to develop at the top of the slab and a compressive stress at the bottom. As soil-cement is weak in tension, the bottom layer of the slab will be critical for interior loading and vice versa for corner loading.

Temperature changes may produce considerable contractions or expansions, depending on the direction of the change. The temperature effects may be divided into two parts; (a) uniform contraction experienced in mid-winter, compared with uniform expansion in mid-summer and (b) the effect of differential temperatures which occur daily over the slab depth. When the top of the slab is warmer than the bottom, the slab tends to rise in the centre, but it is restrained by its self weight and the weight of the adjoining continuous pavement sections. Tension develops in the bottom face of the slab. The reverse process occurs at night when the top of the slab cools faster than the bottom.

2.3 (cont.)

Differential settlement of a subgrade after a pavement is placed causes stresses similar to differential temperature stresses. If a soft spot develops in the subgrade and settles below the surrounding subgrade, the soil-cement base acts as an unsupported slab, deflecting downwards when under traffic loading. This will add considerably to the tensile stresses occurring in the bottom face of the pavement slab.

By combining these stresses with those due to shrinkage, the critical stress conditions can be obtained. Moist curing shrinkage and uniform temperature changes will develop a uniform tensile stress throughout the pavement slab. Non-uniform stresses, on the other hand, are extremely difficult to account for, because of the lack of appreciation as to how they develop in a soil-cement base. By examining all the stresses which occur at both the top and bottom of a soil-cement slab, it is found that the tensile stresses at either the top or the bottom of the slab will be critical depending on the position of the wheel loading. It is usually the combined effect of some or all of these stresses which causes cracking, and not just one, as has so often been assumed.

2.4 Internal Stress Build-up

The effects of internal stress build-up caused by temperature changes and by moisture movement during drying and moist curing, have been briefly outlined above. The internally induced stresses resulting from moisture changes normally develop over a period of time, thus allowing creep to occur within the soil-cement under stress. Some pavements have failed completely under internal

2.4 (cont.)

stresses, indicating that either the material was not suitable for a cement stabilized base, or the slab was incorrectly cured.

Even though a soil-cement pavement may be adequately designed to withstand the maximum wheel loads likely to be imposed, including an adequate allowance for fatigue, it may fail within a few months, because the designer has failed to include the internal stress build-up caused by temperature and moisture changes. Because of the importance of these internal stresses and especially the shrinkage stresses caused by drying, the work described in this thesis is concentrated on a meaningful evaluation of such stresses.

CHAPTER THREE

REVIEW OF PREVIOUS RESEARCH

Before commencing experimental work on soil-cement, it is evident that the strength tests and type of compaction to be adopted need to be fully understood. Also an understanding of the likely structure of soil-cement is essential, but existing studies in this field are very limited.

Concrete research has received a great deal of attention in such fields as structure, shrinkage, creep and strength development, but research work in soil-cement specifically on shrinkage, creep and cracking is extremely limited. From preliminary investigations into the causes of shrinkage, it was apparent that an understanding of moisture flow in a soil-cement base was required, but as there appeared no mention of this in the existing literature, moisture flow in soils was investigated.

3.1 Compaction

Samples compacted in the laboratory need to reproduce the strength characteristic of the field compacted material. This means that the compaction method should simulate the type of roller which is most likely to be used on the particular material under study. For a clay material, the sheepsfoot roller is normally used, while for a sandy material a vibrating roller is used. For the compaction of clayey material, the roller action is generally one of a build-up of pressure,

3.1 (cont.)

followed by a dwell period, then a shearing motion as the roller moves on. This effect is termed a kneading action; therefore, a kneading compactor would be required to produce soil-cement samples. Differences in the structure resulting from different laboratory compaction methods have a pronounced effect on the engineering properties of a soil. It was observed by Lambe[79] that soils compacted dry of optimum moisture content shrank appreciably less than those compacted wet of optimum. It was also found by Seed and Chan[127] that both the degree of particle orientation and the axial shrinkage increase, as the moulding moisture content increases. From Fig. 3.1 by Seed and Chan, one may see that the kneading compactor gives the lowest strength and the highest shrinkage for a particular material when compacted wet of optimum moisture content, thus producing the worst conditions in the compacted sample. It was, therefore, concluded that a kneading compactor would be required for work on soil-cement. A brief design of a kneading compactor, similar to the Californian compactor[134] was prepared in 1968 by Redward[110] and a compactor was subsequently constructed to this design.

3.2 Strength Tests on Soil-Cement

The compressive strength of soil-cement has been the main acceptance standard for many soil-cement pavement projects. The use of the compression test may seem a little pointless, when one considers that both flexural stresses and internal stresses within the pavement will produce tensile stresses. Therefore, the compression test should be supplemented by a

3.2 (cont.)

tensile test.

The unconfined compressive test described in British Standard[19] is the normal test used in many countries for soil-cement samples, but no allowance is made for reducing end restraint. When a sample is loaded between parallel steel plattens, the ends of the sample are restricted from expanding by the friction developed between the steel platten and the end of the sample, with consequent bulging of the sample in the centre.

For obtaining the tensile strength, the following tests have been used: direct tensile test, bending test and indirect tensile test. The direct tension test would appear to be the best way of measuring the tensile strength, but two main problems are encountered. These are the likelihood of including bending stresses, owing to misalignment of the applied load, and the method of gripping the sample. Mitchell[88] has shown, using photoelastic studies, that large stress concentrations occur at the loading grips on a figure-eight briquet. Use of epoxy glue to attach special swivel ends to the sample has proved reasonably successful. This method has recently been improved by Bofinger[13] using plates glued to the two opposite sides of each end of the sample. This develops shear in the glue between the plates and the sample, thus providing a much better bond. However, photoelastic studies might show that this method of gripping a sample causes non-uniform stress distribution across the sample.

The bending test involves applying a constant bending moment to a prismatic beam specimen. Many engineers favour this method

(3.2 cont.)

of tensile strength determination because it is obtained in a way similar to the conditions imposed by traffic loading, but the tensile strengths obtained by this method are considerably higher than those obtained by the direct or indirect tension tests.

The indirect tensile test involves the diametral loading of a cylindrical sample with a compressive force (applied along two opposite generators) (Fig. 3.2). A number of research workers (137), (65), (91), (13), (74), (88) have discussed the indirect test and brought forward points for and against its use. Bofinger[13] points out that Ec and Et are not equal, yet no attempt has been made to analyse the true stresses. Apart from this, the test has many major advantages, such as:

(a) Failure occurs in a region of uniform tension.

(b) Failure is not seriously affected by surface conditions.

(c) The co-efficient of variation of the test results is low.

(d) An ordinary compression tester is used for the test.

Hudson et al[65] have made an investigation into the factors affecting the indirect tension test and have produced the following recommendations:

i) Samples should have as large a diameter as possible.

ii) The loading strip should be contoured stainless steel, of width one inch.

3.2 (cont.)

iii) The loading rate should be 2.0 inches per minute.

iv) The testing temperature should be room temperature, in the range of 75° to 77°F.

3.3 The Structure of Soil-Cement

The complex chemical reactions which occur when cement is mixed with a soil make it difficult to predict exactly what the reaction products will be; nevertheless, a number of writers have suggested structures for soil-cement. Davidson et al[31] attributed the stability of silty and clayey soils to the strong skeletal matrix which encases the unpulverized soil lumps. The matrix forms a honeycomb effect, which provides most of the strength, while the unstabilized soil lumps contribute little strength to the soil-cement mix. This "surface coating" prevents contraction and swelling with removal or addition of water. Indication of increase in strength with time and cement content was the only experimental evidence produced to substantiate the proposed model.

Herzog[63,64] suggested the following model:
In the case of a cement grain situated in a newly compacted clay-cement, the pore water in contact with the cement grain propagates the formation of hydrated cement gel and simultaneous release of lime. As hydrated gel occupies twice the volume of unhydrated cement, the growing cement gel may "key in" the surrounding flocculated clay mass, establishing strong bonds at cement-clay interfaces. Thus, the hydrated cement particles would be surrounded by a layer of "glued on" domains of clay particles. The hydration of cement to form hydration products

3.3 (cont.)

has been termed the primary reaction, while the reaction of the released lime with the clay particles is the secondary reaction. This leads to the formation of a "sea-urchin-like body", in which the hardened cement core is surrounded by a zone of domains of flocculated clay particles, glued together by secondary cementation at inter-domain contacts. From the outer boundary of this zone conduits, formed by interconnecting macropores, protrude into the unstabilized clay mass. When lime is released by the hydration process, it tends to line the walls of the conduits, thus stabilizing them. If enough cement is present, the grain spacing is reduced to such an extent that protruding arms of the skeleton unit intermesh and join to form a continuous skeleton. From experimental tests on the strength of clay-cement, it has been found that, when the cement contents are very low, matrix yield occurs and the clay is the only source of strength. Once the cement content reaches a certain level in a clay-cement sample, there is no matrix yield, indicating that a skeleton structure must have been formed.

Bofinger[11] likewise proposed the development of a skeleton structure in a clay-cement. He found that significant strength gains were obtained, even for 1% cement content, from the soaked tensile tests. Therefore, he assumed that the skeleton must be continuous. However, the tests were carried out on an artificially blended soil with a very low clay content and a high ratio of cement to clay, so it is difficult to extract any meaningful results.

3.3 (cont.)

Croft[27] after studying thin sections cut from soil stabilized with cement and with lime, concluded that stabilization is basically achieved by skeleton formation.

Stocker[129] predicted that there are two important modes of cementation developed in stabilized soils - skeletal and diffuse. The former is likely to occur in cement-stabilized soils with adequately high cement contents. The latter can occur only in lime reactive soils and would be the dominant mode of cementation produced by lime, whether this is derived from added hydrated lime or from cement. The relative importance of either mode in a stabilized system is a combined function of type of additive, content of additive, type of soil and of time. Stocker has shown that diffuse cementation occurs by the diffusion of lime throughout the matrix and lumps, leading to attack by the lime on the clay particles at their edges, followed by deposition of cementitious reaction products at or near these edges. This explanation of soil stabilization for cement and lime appears to be most acceptable, as it is backed by experimental observations, optical and electron-optical evidence. The most important point brought forward by Stocker is that lime can diffuse into unpulverized clay lumps and stabilize them against volume changes. There is no suggestion of conduits being required to transmit lime in solution, as had previously been proposed by other writers in this field.

3.4 Shrinkage, Creep and Structure of Concrete

Research into shrinkage, creep and structural changes of concrete has received considerable attention, especially over

3.4 (cont.)

the last few years. In order to explain such deformations as creep and shrinkage, the structure of concrete has been widely investigated, and as concrete is very similar to soil-cement, it seemed that a study of this research work would be worthwhile. Many research workers have put forward hypotheses (87), (95), (68), (123), (58), (142), (106) which attempt to explain creep and shrinkage deformation using the structure of concrete. Unfortunately, there appear to be arguments for and against all these hypotheses, thus making the actual situation anything but clear.

One point on which all researchers seem certain is that the water present in a concrete mix greatly influences both the shrinkage and the creep. The two main hypotheses concerning the way in which this water affects shrinkage and creep may briefly be described as follows: The first one is commonly known as the seepage theory, in which the water in the concrete is thought to exist in two main states, (a) that called adsorbed water, in which a water layer only a few molecules thick is adsorbed on the solid particle surfaces, and (b) capillary water, which exists in cavities between two solid particles, as shown in fig. (3.3). When water is removed from the wedge shape in fig. (3.3), the attractive forces are altered so that the wedge tends to close. Likewise, when an external load is applied in the direction of the arrows, fig. (3.4), the wedge also will tend to close, causing the water meniscus to change and forcing the water from the point of the wedge out into the remainder of the void space. The loss of this water causes the whole wedge to become deformed in the direction of the

3.4 (cont.)

external applied load, thus representing creep. The other hypothesis explains shrinkage in the same way, but creep is examined along different lines. The adsorbed water is regarded as lubrication for the solid particles which, under load, tend to slide over one another, thus permitting deformation in the direction of the applied load.

Many studies have been published on various aspects of shrinkage and drying in concrete (96), (139), (76), (54), (85), (97), (95), (89), (94), (22), (59), (93), (71), (121), (90), (107) and (58) which cover many experimental points of interest. However, other researchers have turned their attention to such effects as drying on concrete strength (70) and the prediction of shrinkage stresses in concrete (102), (72), (20), (100) and (7).

3.5 Shrinkage, Creep and Cracking in Soil-Cement

Soil-cement is a relatively unresearched material, compared with concrete, especially in the fields of shrinkage and creep, and only a handful of publications are available to act as guidelines for future research. Nakayama et al[92] and George[50] have carried out studies of shrinkage characteristics on a number of soil-cement mixes, by varying such parameters as moisture content, moulding density and cement content. Research on creep in soil-cement has received even less attention, such that only one full study has been reported. This was carried out by Bofinger[15] for creep in tension in which he concluded that, once a sample had moist cured for 7 days or more, no creep was apparent. George[51] and Kawamura[73], on the other hand,

3.5 (cont.)

found considerable creep present in soil-cement after 7 days moist curing when they carried out compression creep tests in conjunction with their crack prediction experiments. Both these writers assumed that creep in tension is the same as creep in compression, but did not investigate this.

Other work on soil-cement has taken the form of crack prediction and allowance for shrinkage in actual roads (73), (51), (53), (14). The findings presented in these studies are, unfortunately, gross simplifications of the real problems, with no field results to back the theoretical studies. George[53,51] has made attempts to predict cracking within a soil-cement base by equating the forces caused by shrinkage stress build-up and subgrade restraint with the tensile strength of the soil-cement. No attempt was made to account for non-uniform stress development. On the other hand, Kawamura[73] has taken into account non-uniform shrinkage stress build-up, creep and non-uniform strength gain. This is an excellent study which goes a long way towards the understanding of soil-cement behaviour in a road pavement.

3.6 Moisture Movement

In early studies of shrinkage stresses in soil-cement, the very important moisture content parameter had been ignored. It became evident that shrinkage, creep and strength of soil-cement were more dependent on the moisture content than on time. Therefore, studies of moisture flow in soil-cement appeared necessary; however, no record of any such work was in the literature. Consequently, the initial investigations were along

3.6 (cont.)

the lines employed for determination of moisture flow in natural soil. The theory of moisture flow in natural soil is extremely complex and is probably even more so in soil-cement, but many researchers (62), (3), (113), (115), (109), (18), (143) and (133) have shown that the diffusion process, analogous to heat transfer to and from a body, satisfactorily predicts moisture flow in natural soils, provided the necessary moisture flow parameters have been carefully obtained. Before the diffusion equation can be used, the moisture content parameter must be represented in terms of suction, and the moisture flow parameters in terms of permeability and inverse differential water function. The suction is expressed in centimetres head of water and necessitates the determination for each soil of a moisture content vs. suction curve, for which laboratory tests have to be used. Croney et al[30] have produced a comprehensive coverage of the common experimental procedures. The laboratory techniques for measurement of the moisture flow parameters are much less satisfactory, even though considerable research has been carried out on them, (111), (78), (69), (25), (3), (112), (36), (141). Indications of large discrepancies between laboratory determinations and field determinations of flow parameters have attracted continuing research into the field techniques for obtaining the flow parameters, and more reliable results can now be produced. A number of research workers have presented results and/or developed methods to predict moisture movement below the ground surface in the field, (47), (114), (10), (115), (125), (136), (49), (22), (1), while other workers have concentrated on laboratory

3.6 (cont.)

moisture flow studies (61), (140), (122), (37), (8) . Among papers published, suitable techniques were found which,when modified to suit this particular research,enabled moisture flow parameters to be determined for small soil-cement samples. This could then be extended to full scale pavement studies.

3.7 Summary

From the studies on compaction techniques,it was evident that laboratory samples should be manufactured using a kneading compactor, even though most soil-cement samples have in the past been compacted using other techniques.

Strength tests for determining the suitability of a soil-cement have been widely used in laboratory research, but only the unconfined compression test is specified by pavement designers.

The action of cement on clays appears to be two-fold; the primary reaction in which skeletal formation occurs and the secondary reaction brought about by the diffuse cementation of the lime, produced by the hydration of cement throughout the matrix and lumps. By studying the research completed on the structure and the behaviour of concrete, it could be concluded that the theory for moisture movement under conditions of stress or drying can account for shrinkage and creep of soil-cement.

In order to fully understand this movement of moisture in soil-cement, new investigations would be required as no relevant literature appeared available.

CHAPTER FOUR

THE STRUCTURE OF SOIL-CEMENT

By considering separately the structure of soil and of cement gel, the structure of their combination, soil-cement, can be better understood. A brief review of existing knowledge of the structure of soil-cement and of concrete is presented in this chapter, while the influence of moisture on the structural arrangement within both these materials is discussed. From the comments and experimental results of previous researchers, a proposed structure for soil-cement is presented.

4.1 Composition of Soil-Cement

Soil-cement is composed of combinations of all or some of the following materials and constituents:- sand, silt, clay, unhydrated cement grains, hydrated cement (gel), water in different states, and air voids. Therefore, in any soil-cement mix there exists a complicated many-phase system. All sand and most silt particles will act as rigid inert inclusions within the soil-cement, whereas the remainder of the silt particles and all the clay will react with lime produced by the hydration of the cement.

When cement and water are added to the soil, the following reaction is thought to take place (67) .

$$\left.\begin{matrix} C_2S \\ \\ C_3S \end{matrix}\right\} \xrightarrow[\text{Lime Soln.}]{\text{Saturated}} C_2SH \xrightarrow[\text{soln.}]{\text{weak lime}} CSH$$

where C = CaO, S = SiO_2, H = H_2O .

4.1.1 Physico-chemical Properties of Clays

Before any attempt is made to explain the mechanism of cement stabilization, a brief mention of the clay structure appears appropriate. Clay minerals can be approximately divided into three main groups; kaolins, illities and montmorillonities. These clay minerals with an average thickness of 30 Å are crystalline in nature and are built-up principally from two structures, the silica tetrahedron and the octrahedral unit of brucite (Grim[55]).

These clay layers or platelets are thought to exist as domains composed of bundles of coherent parallel orientated clay platelets in close packing, and these domains are believed to behave as structural units and not as individual clay platelets (Stocker[132]).

4.1.2 Composition of Cement Gel

The hydration of cement produces a coherent porous mass composed of poorly crystallized, colloidal reaction products, together with some non-colloidal products, principally calcium hydroxide (Powers[106]). This heterogeneous material in its densest form is called "cement gel"; it occupies more than twice as much space as the cement from which it was derived, and thus, when the hydration process is complete, it fills the space once occupied by the grains of cement plus some or all of the interstitial space originally filled with water.

The structural nature of the cement gel is of special interest. The gel appears to exist in laminar form, and these laminae are probably layers of impure colloidal tobermorite,

4.1.2 (cont.)
with an average thickness of about 30 Å. The spaces between laminae have been termed gel pores and were found by Powers[106] to have an average width of 15 Å. It may appear that the tobermorite gel laminae and the clay platelets are physically similar, but the mineral properties of clay particles in the colloidal state are very different from those of hydrating cement particles.

4.2 Chemical Reactions in Lime-Clay-Water Systems

Work carried out by Diamond and Kinter[33] indicated that chemical reactions between lime and clay lead to the formation of various calcium aluminate hydrates and calcium silicate hydrates, similar to those formed by the hydration of Portland cement. There is preferential attack of lime on clay crystal edges, as shown by electron microscope studies (Diamond, White and Dolch[34], Sloane[128]) and by chemical analysis (Stocker[131], Ruff and Ho[124] and Plaster and Noble[103]).

It would appear that the lime solution attacks the clay crystals on their edges, generating small accumulations of cementitious calcium silicates and aluminates at or near these edges, thus bonding neighbouring crystal edges. Portland cement has been shown to release lime on hydrating, so it is indirectly a source of cementitious material, which can be deposited at distances remote from the original cement grains. This reaction is termed diffuse cementation. Stocker[130] states that, as a first approximation, Portland cement is one-third as effective as hydrated lime, as a source of lime for pozzolanic reaction with clays.

4.3 Reactions Between Cement and Clay

Portland cement stabilizes clays by rapid formation of a skeletal structure.

Herzog[63] attempted to explain strength development and volume stability in soil-cement by assuming that, as each cement grain hydrates, the hydrated cement gel which forms occupies twice the volume of the original cement grains and in doing so established strong bonds at the clay-cement interfaces, so that each cement grain is surrounded by a zone of domains of flocculated clay particles glued together by lime cementation of inter-domain contacts. Outside this zone, adjoining macropores develop conduits in the unstabilized clay; solutions of the released lime diffuse along these conduits, stabilizing their walls. As this stabilizing process penetrates through the unstabilized clay, similarly stabilized conduits from other cement grains will link up, provided the cement content is high enough. The more conduits that intermesh, the stronger will be the mix.

Stocker[130] has disagreed with these ideas and has proposed the following explanation of cement stabilization of a clay soil. The primary reaction is the development of a skeleton in a soil matrix, and this depends entirely on the position of the cement grain and on the development of the hydrated cement gel. This hydration is rapid, with much of the hydration and expansion of the cement grains being complete in six hours or less. If early disturbance of the immature skeleton occurs as in compacting a soil-cement layer, healing of the skeletal damage will be much more effective than if the disturbance occurs later within this period. The secondary reaction is one of

4.3 (cont.)

diffuse cementation, brought about by lime attacking the clay edges, to cause cementation of adjoining clay particles as described above for the action of lime on clays. Skeletal and diffuse cementation appear to be independent spatially; skeletal cementation depends on the distribution of the cement grains with respect to one another, while diffuse cementation appears to occur anywhere throughout the stabilized mix.

4.4 The Influence of Moisture in the Micro-structure of Soil-Cement

In order to understand and explain the mechanism of both creep and shrinkage, an understanding of the influence of moisture in soil-cement appears to be essential. Since little research work appears to have been carried out on moisture movement and moisture retention in soil-cement, the literature on concrete research in this field was examined. Also, it is necessary to understand the hydration process of cement in order to determine the movement and retention of moisture in soil-cement.

4.4.1 Water as it Exists in Concrete

Clay platelets are of the same order of thickness as the individual sheets of impure colloidal tobermorite in the cement gel, having an average thickness of 30 Å (Herzog[63]). These tobermorite laminar sheets, separated by gel pores of average width 15 Å, have been assumed to compose the cement gel. Copeland and Chang[26] have concluded that the masses of cement gel which form on calcium hydroxide crystals soon after the start of the hydration process are not necessarily related

4.4.1 (cont.)

in position to the original cement grain.

Concrete research workers have established that shrinkage and creep are dependent only on the cement gel, with the aggregate being regarded as an inert rigid inclusion. Ishai[68] proposes that evaporable water exists in a cement gel in the following four ways:-

(a) Pore water in the capillary and gel voids, at a distance of at least 10-20 Å from the solid surface, therefore outside the range of van der Waals forces of adhesion.

(b) Water adsorbed onto the crystal surface in layers 1-2 molecules deep.

(c) Inter-crystalline adsorbed water, i.e. water confined between mutually adjoining crystal surfaces in narrow spaces up to two molecules wide. This type of water, subject to two sets of forces, is more strongly bound than (a) or (b).

(d) Intracrystalline zeolitic water (water one molecule thick embedded in the tobermorite crystal). This water is very strongly bound and not removable by ordinary drying.

4.4.2 Research Into the Presence of Water in Cement Gel

Coincidentally, three different research workers, Powers[106], Ishai[68] and Ruetz[123], all working independently, brought forward three different hypotheses to explain creep and shrinkage at the same conference in London in 1965.

4.4.2 (cont.)

Powers' hypothesis[106] provides an excellent description of the occurrence of shrinkage as a cement gel dries. This hypothesis for shrinkage is basically similar in context to that presented by the two other researchers. On the other hand, for the mechanism of creep Ruetz[123] and Ishai[68] have produced similar hypotheses, but these disagree with that of Powers[106].

4.4.2.1 Shrinkage

For a discussion of shrinkage in cement gel (Powers[106]), the evaporable water is considered as existing in two broad forms, capillary water and adsorbed water.

When a sample of cement gel is completely dried, it is observed that total collapse of the structure does not occur, thus indicating that bearing points must exist in a cement gel. It is likely that the cement gel grows as a structure of crumpled laminations, thus explaining the existence of points of contact. Provided capillary water is present and the relative humidity of the system remains above 50%, then water a few molecules thick is adsorbed on the surface of these contacts. On an unobstructed surface, adsorption of water molecules can build up an adsorbed film about 13 Å thick, thus requiring double that distance between opposite surfaces, if adsorption is to proceed unhindered. The thickness of the layer of adsorbed water varies from 2.0 Å at a relative humidity of 5% to 13.0 Å at a relative humidity of 100%. As the average space between solid cement gel surfaces is 15 Å, there is obviously some water hindered from free

4.4.2.1 (cont.)

adsorption in wedge-shaped pores. For the system to be in equilibrium such that different thicknesses of adsorbed water layers can co-exist, the water film must be under variable pressures. In the areas of hindered adsorption, extra pressures are brought about by the tensile stress in the bond that holds the structure from swelling without limit. This extra pressure in areas of hindered adsorption is called disjointing pressure, while the water in films in which disjointing pressure exists is called load-bearing water. As mentioned above, the adsorbed water layer thickness varies with the humidity of the cement gel, so it could safely be predicted that, at saturation when the thickness of the adsorbed water layer is a maximum, the disjointing pressure should be a maximum. Therefore, Powers concludes that volume change is predominantly influenced by disjointing pressure, especially in the lower humidity range, while capillary water affects the volume change in the higher humidity range.

Experimental evidence has shown that, after a cement gel has dried, its permeability is greatly increased and after subsequent wetting its shrinkage with re-drying is considerably reduced. Powers[106] suggests that first drying tends to create connecting channels between originally isolated cavities. Thus, if this first drying develops a continuous capillary system, second and subsequent dryings will empty the larger cavities without developing tension in them. The shrinkage for second and later dryings for cement gel is found to be very similar, indicating that hydrostatic tension in capillary cavities fails to develop. Therefore, shrinkage in these cases can be attributed

4.4.2.1 (cont.)

to tension developed in adsorbed films and to any effect of change of the surface tension of the solid particles.

The hypotheses put forward by Powers[106] and Ruetz[123] suggest two similar possible mechanisms for shrinkage. On the other hand, creep has provided researchers with many problems.

4.4.2.2 Creep

The hypothesis by Powers follows on from the above description of shrinkage in a cement gel. By considering an external compressive load being applied to any wedge, as shown in fig. (3.4), one can observe that slight closing of the wedge shape will decrease the radius of the capillary meniscus and increase the area of hindered adsorption. The water will tend to be squeezed from the hindered water film and thicken the unhindered film, raising its relative humidity. This closing of the wedge, situated just outside a compressed area, locally reduces film tension, and by opposing the external force tends to displace the compressed water. The force required to close the wedge can be considered as an increase in adjoining pressure, and it tends to produce a stiffening of the whole structure. Pressure gradients created in the compressed water films by such changes, set in motion a diffusion process, whereby excess water molecules in these compressed films are gradually transferred to unhindered adsorbed films or to capillary water. While this diffusion process proceeds, the specimen exists in a swollen state with elevated internal humidities, until longitudinal shortening is completed. The immediate deformation is termed elastic creep and the slow deformation irrecoverable

4.4.2.2 (cont.)

creep. If the system is sealed against drying, the excess water must remain in the system adsorbed on unhindered films or as capillary water. If drying is permitted, the excess water is lost to the atmosphere and the film tension and the disjoining pressure return to their unloaded values. The reverse process should occur when the load is removed.

When the solid surfaces are forced together, new molecular bonds form at new points of contact. These bonds have a variety of strengths, with the majority being relatively weak, thus some of them can be broken if a sample is allowed to take up water again. Therefore, the drier the sample becomes, the greater the number of bonds formed. This indicates that, more than likely, the bonds will remain unbroken, thus producing higher irrecoverable creep. In order to record the same longitudinal strain for both creep and shrinkage, only small loss of water from the sample is required for the creep sample, compared with the large moisture loss required for the shrinkage sample. Therefore, Powers[106] concludes that the mechanisms of creep and shrinkage are similar; shrinkage being caused by increased internal tension, which tends to pull adsorbed water from load bearing areas, while creep is caused by external forces which tend to push adsorbed water from these areas. When the two act together, complications occur; as the shrinkage is triaxial while the load is usually uniaxial.

A different hypothesis has been proposed by Ruetz[123], who argues that the seepage theory is defeated because creep strains occur not only in the torsion test, in which there is

4.4.2.2 (cont.)

no volumetric stress component, but also in the tension test, where the tensile force is working against the hypothetical extrusion of water. Experiments by Ruetz and others have shown that the process of shrinkage will orientate itself in the direction of the applied load. However, this process cannot promote the increase in creep with drying because in the tensile creep test, the creep deformation and shrinkage process are working in opposite directions, yet considerable creep still occurs. Experiments on vapour flow through samples with no net gain or loss of moisture produce no influence on creep, yet when there is a flow of moisture either into or out of the specimen, there is a marked increase in the creep strain. This phenomenon occurs under any stress capable of producing creep. Therefore, it cannot result from vectorial addition of the stresses present, but must be a property of the material.

Ruetz introduces the concept of a coefficient of viscosity of the hardened cement paste, which changes with the drying rate. The creep mechanism is thought to be one of sliding of the sub-microscopic gel particles over one another with the sliding taking place in the thin, multi-molecular layer of adsorbed water. A rise in temperature causes an increase in the number of particles capable of sliding, which can be explained by a change in the degree of aggregation of the gel particles. At room temperatures many of the gel particles are restricted in their movements. This can be explained by the formation of a structure of the connecting water layers

4.4.2.2 (cont.)

with small spacings between the limiting solid particle surfaces; thus resistance to deformation is considerably increased. Depending on the interaction between solid particle surfaces and adsorbed water molecules, the extent of the orientation with respect to the solid surface of these water molecules differs greatly. The orientation can be disturbed by increasing temperature - at elevated temperatures, the thermal inelasticity becomes sufficiently large for viscous flow to occur. The orientation can also be disturbed by mechanical deformation and disturbances originating on the outer surfaces, e.g. externally applied load or evaporation.

If, during drying, large quantities of water are extracted from the cement gel, so that the bonding water layer is greatly contracted in the lateral direction, then the orientation may finally thrust forward to the outside surface, where if a further rapid loss of water occurred it could result in disturbance of the surface water orientation. By diffusion of foreign ions in the lattice, an extensive transport of material may take place within the lattice structure. An application of a shear stess at this time will cause a quasi-viscous flow to take place. Neither Ruetz' or Powers' hypotheses can be regarded as incorrect in that both have a good understanding of the composition of cement gel.

4.5 A Proposed Hypothesis for the Structure of Soil-Cement

From the above literature available on soil-cement and cement gel structure, it appears reasonable that a new model

4.5 (cont.)

structure for soil-cement can be envisaged. This model for soil-cement will be examined in the light of experimental results presented later in this thesis, not with intent to completely confirm the accuracy of the model, but to ensure that the structure and mechanism for soil-cement proposed in this thesis does fit in with the experimental results.

4.5.1 The Stabilization Process

Most researchers in the field of cement stabilization of soil agree that there are two modes of stabilization occurring in any soil-cement mix. The primary mode is the reaction where the hydration products expand to fill empty voids around the original cement grains in such a way as to key in unstabilized clay domains, silt or sand particles. The secondary mode is the attack of hydrated lime on the clay domains. Various researchers take different views on the action of this lime in causing stabilization, but the very extensive work carried out by Stocker[130] seems to indicate that clay lumps are stabilized by diffusion of lime into them. Stocker was able to observe colour changes from the outer portions of large lumps to the central core. Also, when the sample was oven-dried at that stage, cracks appeared between the matrix and the clay lump and between the outer portion of the clay lump and the core at the position of colour change.

From the limited preliminary tests carried out for this project, on samples containing lumps of different maximum size, it was soon apparent from the results obtained that little

4.5.1 (cont.)

difference in strength properties resulted when smaller clay lumps were replaced with much larger clay lumps, provided the cement content was not low. For a low cement content, it can be assumed that little lime is produced by the hydration process. Therefore, diffuse cementation would not be able to develop adequately to stabilize all the clay lumps. The conclusion reached is that, provided enough lime is available for complete diffuse cementation, and adequate curing time is given, then mixes containing different clay lump sizes will exhibit very similar properties.

To summarize, the proposed structure is as follows:- A typical soil of sand, silt and clay is mixed with water and cement. From the spatial distribution of the original cement grains, hydration occurs with the hydration products expanding into the empty voids close to each cement grain and keying in the surrounding unstabilized clay. The lime released by the hydration process attacks the unstabilized clay crystal edges, generating small accumulations of cementitious calcium silicates and aluminates at or near these edges, and bonding the edges to adjacent edges and faces.

4.5.2 Explanation of Shrinkage and Creep

In concrete, research workers have concluded that the cement gel is entirely responsible for shrinkage and creep. Therefore, one can assume that the cement gel will play an important part in the shrinkage and creep of soil-cement. Unlike concrete which contains clean aggregate particles,

4.5.2 (cont.)

cement grains and cement gel, soil-cement contains colloidal clay particles cemented together by the action of released lime. As the colloidal clay particles are very similar in size and shape to the impure tobermorite laminae of which the cement gel is composed, it would seem reasonable to assume that the pattern of moisture retention and movement around clay particles will be similar to that in cement gel.

By assuming for the purpose of studying moisture flow and moisture retention that domains of clay particles and cement gel are very similar in their laminar arrangement, the following behaviour of soil-cement will be considered for a uniformly composed sample. Experimenters have shown that a soil-cement does not completely collapse on extensive drying, thus indicating that many internal bearing points must exist. This will probably be due to the crumpled nature of the gel laminae among the clay particle domains. As Powers[106] suggested, wedge-shaped voids in the cement gel contain both capillary water and adsorbed water. Mills[87], 1968, carried out saturation and drying tests on concrete with liquids of different molecular sizes. He found, using the molecular sieve device, that liquids of large molecular size would be absorbed to a limited extent only. As a highly polar liquid would react with the clay fraction present in a soil-cement, the exact significance of Mills' results cannot be determined without experimentation. Nevertheless, the cement gel will play a large part in a soil-cement, such that Mills' work will still be valid. Associated with this limited absorbtion of the large molecule fluids

4.5.2 (cont.)

there resulted only a small expansion and no strength reduction. As the origins of the strength and volume changes lie in the short range primary bonds existing at the apex of the wedge and the large range secondary, (van der Waal's) forces acting over the remaining areas of the solid surface, it is evident that only fluids of small molecular size, such as water, can influence the volume change and strength of a cement gel. Such bonds tend to close the wedges, this closure being resisted by the disjoining pressure in the adsorbed water and the elastic force in the solid.

Water is removed from the wedge either by evaporation or by being squeezed out under externally applied load. Evaporation causes a reduction in the amount of capillary water present in the wedge, thus decreasing the radius of the water meniscus, and at the same time, reducing the adsorbed layer thickness; the latter results in a decrease in disjoining pressure. Therefore, the overall effect is a closing of the wedge shape under the increased surface tension of the water meniscus and the increased van der Waal's forces. This gives rise to shrinkage, and takes place in every wedge shape present in a soil-cement mix, regardless of the orientation of the wedge to the drying face.

When a external compressive load is applied to a soil-cement sample, wedge shapes orientated perpendicular to the direction of the load will partly close, while wedges parallel to the direction of the load will tend to open. Consider first the situation where no evaporation occurs while the sample is

4.5.2 (cont.)

under load. Any wedge shape perpendicular to the direction of load is partly closed by the external load, causing a decrease in the radius of the capillary meniscus and an increase in the area of hindered adsorption. It is considered that this situation must arise irrespective of whether creep is caused by viscous flow or by moisture diffusion from areas of hindered adsorption. Therefore, it seems justifiable to adopt the mode of moisture retention and movement, as specified by Powers[106] and summarized in section (4.4.2.1) above. This infers that each partly closed wedge shape is kept open by capillary water unless evaporation is permitted.

Unfortunately, most research workers have ignored the wedge shapes which are parallel to the direction of the externally applied load. These wedges are slightly expanded by the external load and therefore are in a state of moisture shortage, so that the mode of moisture retention is the direct opposite to that experienced in wedge shapes which are perpendicular to the direction of the applied load. It would therefore seem reasonable that even though no evaporation takes place, creep could still occur, as moisture would tend to move from compressed wedges into expanded wedges. When evaporation does occur, the expanded wedges remain virtually unaffected, but surplus moisture in the compressed wedges is lost quickly and creep is greatly increased.

In this way creep in compression can be adequately explained using a form of the seepage theory, but the mode of creep for a sample loaded in tension still presents problems.

4.5.2 (cont.)

Ruetz in the discussion at the Structure of Concrete Conference in London, 1965,[135] considered that the seepage theory could not explain the creep which occurs when a sample loaded in tension is dried out and then resaturated. As resaturation occurs, creep rapidly increases, but the tensile load is opposing water removal from the wedge shaped pores.

One must bear in mind that shrinkage causes an isotropic collapse of the structure while creep is accompanied by a collapse of the structure in the direction of the applied load and dilation of the structure in the other two directions. This is because some wedges will be closing while others are opening. When a sample is dried, high pore water suctions are developed; therefore the presence of a tensile stress which is relatively small compared with the high suction is virtually unnoticeable. Consequently, when resaturation of this dried sample occurs, moisture will penetrate all the wedge shaped spaces regardless of the presence of a tensile stress, but when the suction of the sample is lowered by resaturation to be equal to the tensile stress, then moisture absorption into all the compressed wedge spaces should cease. On the other hand, moisture should continue to be absorbed into the expanded wedge spaces until they are fully saturated. In order to check that moisture absorption for a loaded sample was less than for an unloaded sample as suggested above, a number of experiments were carried out. These experiments did in fact confirm the suggestion that the presence of a load restricted absorption just as if it was an applied suction.

4.5.2 (cont.)

Probably the most important point missed by Ruetz is that, when a dried concrete or soil-cement sample is re-saturated with moisture, the strength decreases, as explained earlier in this chapter. Therefore, if a dried sample is resaturated while under the influence of a tensile stress, it would seem obvious that the creep rate must increase, because in effect the tensile externally imposed stress remains constant but the strength decreases. This has the same effect as applying an increasing tensile stress to a sample, under which creep would increase. Therefore, Ruetz's criticism of the seepage theory appears invalid.

Nevertheless, favourable consideration should still be given to Ruetz's[123] proposed mechanism for representing creep, in which sliding of the sub-microscopic gel laminae upon one another occurs in the very thin multi-molecular layers of adsorbed water. If equilibrium is ever to be attained, the above mentioned movements of moisture must take place while the sample is under load, but not all creep can be attributed to this moisture diffusion. Indications are that moisture diffusion accounts for most of the creep, especially in the upper humidity range, but sliding of gel particles over one another appears to occur in the adsorbed water layers, especially in the low humidity range. When a sample is at a low humidity, there is very little likelihood of moisture diffusion under load, yet small creep strains are still recorded. Therefore, one may assume that inter-particle sliding can contribute to creep. This sliding will occur with clay particles in the same

4.5.2 (cont.)

way as for gel laminae.

4.5.3 The Theoretical Prediction of Shrinkage and Creep

In order to represent both shrinkage and creep theoretically, more than just a proposed structure of soil-cement is required. Any theoretical method of predicting shrinkage must examine the amount of moisture contained in a sample, together with the average spacing and distribution of wedge shaped voids. Assuming that the diffusion equation adequately predicts the internal movement of moisture, then a relation between the moisture present and the size of the voids must be found. It would seem reasonable that the diffusion equation in one form or another should be able to account for creep, provided creep can be entirely attributed to moistrue diffusion. But it has just been established that sliding of particles over one another is also likely to contribute to creep. Therefore a theoretical method of predicting creep is not likely to be simple. Bažant[7] has presented an approach to concrete shrinkage and creep using thermodynamics of multi-phase systems, but the assumptions made, together with the large number of coefficients required to fit the many thermodynamic equations, make this approach in its present form unworkable. Furthermore, the theoretical analysis carried out by Bažant[7] has not been backed up by experimental work. Other research workers have used the diffusion equation to predict shrinkage without making allowances for the non-linear relationship between shrinkage and moisture content. For the theoretical representation of creep, many research

4.5.3 (cont.)

workers have attempted to use rheological models, but every mix of soil-cement has different properties, thus making difficult any representation without changing the parameters for each particular mix. The use of these rheological models has been limited, even in concrete research where variations due to soil properties are absent.

CHAPTER FIVE

MATERIAL PREPARATION AND SAMPLE MANUFACTURE

When soil materials for the testing program of this project were being selected, their suitability, availability and homogeneity had to be assessed. Also, the procedures for preparation and compaction of the soil-cement samples for laboratory tests must simulate those used in the field if meaningful results are to be obtained.

5.1 Materials and Their Preparation

5.1.1 Cement

Ordinary Portland cement from a single batch was stored in a sealed container and used for all the experiments. The cement was manufactured at the Milburn works in New Zealand.

5.1.2 Soils

A readily available soil, free from organic impurities, was desired for the initial testing program on soil-cement samples. A modified loess from Heathcote in Christchurch was finally chosen as a suitable material. After carrying out a large number of tests on the loess soil-cement, it was decided that similar tests should be done on another type of material for comparison, and that this should preferably be a sandy material, as the loess contains mostly clay and silt particles.

For this research project time did not permit the laying

5.1.2 (cont.)

of a trial section of road, so it was decided that an existing soil-cement pavement slab would be chosen for analysis of possible cracking occurrences. After studying many sites, a road in Hamilton, built of cement-stabilized sandy pumice, was finally selected for full-scale studies. Sandy pumice was thus the obvious choice as the second material for study. Therefore, 400 kg of the material was removed from the unstabilized sub-base of the actual road and transported to Christchurch. The particulars of the two test soils are summarized in Table 5.1.

5.1.3 Soil Preparation

Before using either soil in the laboratory, the following pretreatment was adopted. All the material was spread out on polythene sheeting on a concrete floor. It was mixed initially by hand shovelling, and finally by using a rotary hoe. This was followed by several passes of an 8 ton, steel-wheeled roller. The rotary hoe followed by the roller served to break down many of the lumps to a grading one would expect to find in the field after compaction of a soil-cement pavement. This material was bagged and stored in a fog room at its natural moisture content. Some large lumps still remained, but the grading was fine enough to be satisfactory for the largest moulds used on the project. For the 102mm x 51mm diameter and 102mm x 13mm diameter samples, a maximum particle size of 1.6mm was used, while for the 286 x 76 x 76mm prisms, the maximum particle size was 9.5mm.

5.2 Pulverization

In the early stages of this research project, it became evident that pulverization would play an important part in influencing the structure of a soil-cement mix, so particle size analyses were made of both the soil lumps and the fully pulverized soil. With the importance of lump sizes in mind, lump grading analysis was carried out for varying degrees of pulverization. It was soon evident that, once the soil had been compacted, it required a large amount of work to break it down to a similar grading to that which originally existed. Also it was found that drying the natural soil caused a break-down of lumps to 4mm diameter or less, so that there was a much higher percentage of fine lumps in a dry sample, compared with a wet sample.

Direct tension tests were carried out on loess soil-cement specimens which were compacted from a mixture containing 50% fully pulverized soil and 50% lumps with a grading between 16mm and 3.2mm. Results indicate that specimens containing larger lumps tend to give a lower tensile strength than those with smaller lumps, but the greatest reduction from the strength obtained for fully-pulverized material was only 5%. These tensile strengths were measured after 7 days moist curing. From this limited amount of testing, it could be assumed that lumps of natural soil included in soil-cement are not particularly detrimental to the strength of the mix.

Stocker[130] has pointed out that little evidence of an experimental nature is available on which to base specifications for pulverization of a soil to be stabilized. The two studies

5.2 (cont.)

on which most specifications rely are those by Felt[46] and Grimer and Ross[57]. As shown by Stocker[130], both these studies are misleading, yet they have greatly influenced the writing of specifications in which fine pulverization is said to be essential for good stabilization. Stocker investigated the effects of natural soil lumps in test samples, and found that lime produced by the hydration of cement diffused into these lumps, and eventually reached their centre, thus causing complete stabilization. In this project, the measured difference in tensile strength between samples with and without lumps may have vanished if the samples had been moist cured for a longer period, thus allowing more time for the lime to diffuse into the centre of the large natural soil lumps.

From the comments presented above, together with the experimental work carried out by Stocker[130], it is evident that soils with lumps which are difficult to break down do not, in fact, need to be finely pulverized for successful stabilization.

5.3 Sample Preparation in General

5.3.1 Mix Proportions

Before mixing cement, water and soil together in a batch mix, the exact quantities of each must be measured out. For this project, as in all laboratory testing the proportions of both added water and cement were calculated with respect to the dry weight of the natural soil.

It was found that a rapid method of determining the moisture content appeared desirable for controlling the

5.3.1 (cont.)

preparation of soil-cement samples. The only commercial device readily available was the Speedy moisture content tester. This device was only designed for use with sands and not surprisingly gave totally unreliable results on loess. In a search for a more reliable moisture content tester the device described in Appendix (II) was developed. This device was found to be suitable for most soils, provided their moisture content was lower than optimum, but because of this limitation it does not totally answer the rapid moisture content determination problem. In the interest of both laboratory and field control tests, a reliable method for rapidly determining the moisture content of soils and soil-cement is still greatly needed.

5.3.2 Mixing

A number of unconfined compression tests were carried out to determine what effect the mixing time had on the sample characteristics of compacted soil-cement. It was found that 3 minutes mixing of the cement with the precured soil, followed by 7 minutes mixing after the addition of the extra water, provided the best results. An allowance for evaporation from the mixing bowl was necessary because of energy dissipation as heat in the mixer and the exposure of the mix to the environment during the mixing process.

5.3.3 Sample Manufacture

All the loess samples were compacted with the kneading compactor built especially for this project. On the other hand, only the 102mm x 51 mm diameter sandy pumice soil-cement

5.3.3 (cont.)

samples were compacted with the kneading compactor. A kango hammer was found necessary to compact the larger prisms of sandy pumice soil-cement, as with the kneading compactor it was found to be impossible to achieve the required densities. Consequently, all the sandy pumice samples used for the shrinkage stess predictions were prepared using vibrational compaction.

Many different moulds were used throughout this project, but the following points are common to all. All samples were mixed, compacted, and packed for curing within one hour from wetting the cement. When samples were compacted in layers, the top of each layer was deeply scratched to provide a key for the next layer. Removal of samples from moulds was always a problem. An aerosol teflon spray proved very effective in parting the sample from the mould, but it was feared that the teflon spray might affect the rate of drying of the samples. Therefore, all moulds were hard chrome plated, to provide an extremely smooth surface.

5.4 Packing, Curing and Drying Samples

5.4.1 Packing and Curing

After compaction, all samples were vacuum packed and sealed in a plastic bag which was itself vacuum sealed in a second plastic bag. The use of the two bags ensured that osmosis did not occur through the plastic. By vacuum packing samples, air spaces around the sample were eliminated,thus preventing both condensation on the loose plastic and humidity changes

5.4.1 (cont.)

within the bag. A small electrically-driven vacuum pump was found to be suitable for removing the air from the plastic bags before they were completely sealed with an electric sealer.

Metcalf[82] concluded that by increasing the temperature of curing, the rate of gain of strength of both lime and cement-stabilized soils also increases. Thus, a higher strength would be attained by a sample cured at a higher temperature, age being equal. In the field, conditions are such that curing of a soil-cement pavement is likely to occur over a range of temperatures which depend on the season of the year. Metcalf[82] found that cyclic curing between a maximum and a minimum temperature was equivalent to curing samples at a constant intermediate temperature. Therefore, provided this discrepancy between the adopted laboratory curing temperature and the field temperature is kept in mind, appropriate allowances can be made.

5.4.2 Drying Samples

Variable conditions of drying have been used throughout this research project. To simulate the daily temperature variations experienced in the field, a small curing room was set up in which the samples were cooled to 0°C at night and heated to 27°C during the day. Details and specifications of the curing room and its plant are included in Appendix III.

This curing room functioned extremely well; the only problem encountered was that of trying to measure specimen strains while the room temperature was changing, and this was overcome by taking all readings at a set time of the day.

5.4.2 (cont.)

The curing room was used only for drying the loess samples; all the sandy pumice samples were dried in the constant temperature room at 20°C and relative humidity of 53%.

When prisms were being dried for determination of moisture content profiles or shrinkage, drying was allowed from one or two sides only and the other sides were sealed against evaporation. The sealing was carried out by brushing on two or three coats of a pliable wax heated to 60°C.

The loess prisms were laid in the same steel cradles which were used to restrain the samples (Chapter 6, section 6.2.3) and fig. (5.1)), for drying in the curing room. The sandy pumice samples were also laid in steel cradles, but drying was carried out by enclosing them in large perspex boxes in the constant temperature room. A large tray of sodium hydroxide was placed in each perspex box to remove the moisture from the air; each day the sodium hydroxide was changed and the whole box was thoroughly blown through with dry nitrogen.

Drying experiments were carried out on prisms 38 x 76 x 286 mm to detect the occurrence of carbonation during drying. A water-operated vacuum pump sucked dried air through the perspex boxes (fig. (5.2) containing the samples, see Chapter 9, section 9.1.1. The recorded shrinkages obtained from identical samples drying in these boxes were within 5%, thus indicating that controlled drying would enable reproducible results to be obtained. An earlier experiment, involving the drying of 60 cylindrical samples (102 mm x 51 mm diameter) for shrinkage determinations, failed

5.4.2 (cont.)

because the results obtained appeared inconsistent. The errors in the results occurred because the large air flow used to dry the samples caused non-homogeneous drying across the sample section and this in turn caused inconsistent shrinkage results. An old vacuum cleaner was used to circulate the air, while a humidity chamber was used to control the relative humidity of the air flow as shown in fig. (5.3).

5.5 Compaction

5.5.1 Building an Automatic Kneading Compactor

As mentioned in Chapter 3, kneading compaction was adopted for this research project. The only kneading compactor which existed in the laboratory was a small hand-operated 13 mm diameter tamping foot device, fig. (5.4), built to the Harvard Miniature Compactor design. (134). This hand operated kneading compactor was used for compacting the 13 mm diameter samples and the 6 mm wide slices for the composite prisms, (Chapter 9, section 9.1.10) while the remaining samples were compacted using the automatic kneading compactor, fig. (5.5). This compactor was built along the lines suggested by Redwood[110] in his report on a study carried out at the University of Canterbury. This report was mainly on feasibility and costs, with no detailed working drawings. Unfortunately, in a prototype study of this nature where a design has been proposed without actually being built, many important factors were overlooked.

Very briefly, the compactor consists of a steel frame

5.5.1 (cont.)

fig. (5.6), designed for accommodating all the components and providing for a comfortable working table, while the overall measurements permit movement through standard doorways. The hydraulic system fig. (5.7) consists of a pump which supplies oil via a two-way solenoid valve A to the main ram, situated above the working table. Tamping is accomplished on the downward stroke of the main ram, and when the tamp is completed, oil is forced into the bottom of this ram, causing the foot to rise, the oil on its way actuating the turntable ram, which rotates the turntable by the required amount. The electronic logic circuitry fig. (5.8) controls the solenoid valves, times the dwell periods, and counts the number of tamps. It should be noted that the final pressure/time scale of the tamper foot is as shown in fig. (5.9). Owing to a delay in completing the electronics for the compactor, it was initially operated semi-automatically, thus enabling many preliminary tests to be carried out on soil-cement samples. Unfortunately, many problems were encountered in the building and operation of this machine, thus causing considerable loss of time on this project. The main problems encountered have been listed in Appendix (IV).

5.5.2 Calibration

Compaction to some known work effort can be specified by the Standard A.A.S.H.O. (Proctor), Modified A.A.S.H.O., or some other recognized dynamic test, so that any person using the correct equipment and compacting to any of these

5.5.2 (cont.)

standards can reproduce his results in any laboratory, on any material. Unfortunately, as yet, no such standard exists for kneading compactors, so a calibration technique had to be devised. The calibration adopted for equivalent Modified A.A.S.H.O. compaction in a Proctor mould was as follows:- A quantity of soil was made up to the appropriate O.M.C. and stored for 48 hours in the fog room. This soil was then divided in two, one half being stored in the fog room in a sealed plastic bag, while the other half was used to carry out a Modified A.A.S.H.O. dynamic compaction. The calculated amount of cement was mixed with the soil and quickly compacted in a Proctor mould. Very close control of layer thickness was maintained, with the thickness of each layer being recorded. Then the kneading compactor was used to compact the second half of the soil in the same mould as above, the cement being mixed in exactly the same proportions.

The same mixing time and weight of soil per layer were used for both dynamic and kneading compaction. Therefore, if the tamp pressure, dwell time and number of tamps per layer can be set so that the kneading compactor gives the same layer thickness as the modified A.A.S.H.O. compaction then a satisfactory calibration of the kneading compactor is obtained, but only for the material on which the calibration has been run. Therefore, the kneading compactor can be used so that a specific pressure, dwell time and number of tamps are applied to a certain amount of soil, using a foot of fixed area, and the result can only then be regarded as a particular standard

5.5.2 (cont.)

compaction associated with any kneading compactor. However, as any item of construction equipment is known to achieve a particular compaction on a particular material, it is this density which should be reproduced in the laboratory and not a particular standard of compaction. It is therefore suggested that the kneading compactor should be used to compact samples to a chosen dry density not necessarily related to any standard of compaction, thus eliminating the need for special calibrations for different soils.

5.5.3 Auxiliary Compactor Equipment

The full details of the auxiliary equipment can be found in Appendix (V). A different compactor foot; fig. (5.10) is required for each mould to be used on the compactor, cylindrical moulds require a triangular-shaped foot, fig. (5.11), designed to over 1/5 of the area of the cylindrical mould with each tamp. The beam moulds were all mounted on the auxiliary bed, as shown in fig. (5.12). Movement of the moulds along this bed was carried out manually by turning a winch drum wound with steel cable connected to both ends of the mould.

Sandy material and material wet of optimum moisture content cannot be compacted by the kneading compactor, as the compactor foot displaces the soil beneath it in slip circle failures and densification does not occur.

5.5.4 Suggested Modification of the Existing Kneading Compactor

In order to improve the range of the compactor and eliminate noises, the following suggestions are made. The turntable ram and solenoid AA fig. (5.7), should be removed

5.5.4 (cont.)

and replaced with a small electric motor. The main ram would function normally until the time of release of pressure, at which point solenoid valve B would open andforce oil into the bottom of the ram, at nearly full pressure, thus enabling a quick retreat of the tamper foot. The solenoid valve B would close as soon as the tamper foot had risen say 50 mm and solenoid valve A would open. Then an electrically operated clutch would be energised, causing the turntable to turn the required amount, while the tamper foot descends. The removal of the hydraulic turntable ram would remove some noise, permit the turntable to be situated in the centre of the compactor and provide a much wider range in the number of tamps per revolution of the turntable.

If the main electric motor, pump and all the solenoid valves could be removed from the main compactor and placed in a sound proof separate unit, this would greatly cut down the noise level and might eliminate stray pulses from the action of the solenoid valves which have caused malfunctions in the electronics. Connections from the separate unit could easily be made using flexible hydraulic pipes with quick-acting self-sealing couplings.

As the main ram has a diameter of 63.5 mm, it is not particularly suitable for compacting small samples, as a small oil pressure on the main ram causes a very large pressure under a small tamping foot. It is suggested that a 25mm diameter ram be installed alongside the large main ram and connections to the pumping unit made as an alternative to the main ram. The main ram should be situated in the centre of the machine

5.5.4 (cont.)

with the small ram to one side. Consequently, the turntable would need to be able to be moved from a position under the main ram to a similar position under the small ram. This, together with a longer main ram and a lower working table, would enable a much larger range of samples to be compacted. This is an unfortunate limitation of the present kneading compactor.

On the present compactor, no provision has been made for indicating the oil level, or for filling the reservoir, without taking off a section of the panelling. As the reservoir would be located with the separate pump unit in the redesigned kneading compactor, it would be easier to provide the necessary access.

CHAPTER SIX

LABORATORY TESTS ON SOIL-CEMENT SAMPLES

This chapter begins with a study of the standard tests for soil-cement, from which it becomes evident that modifications or additions to these tests are required. Some new tests are described, and these are incorporated in a suggested revised series of tests. The testing techniques are outlined, then the effect on the shrinkage, strength and creep of soil-cement with respect to variable parameters such as moulding moisture content, moulding density, etc., is discussed.

6.1 Standard Testing Techniques for Soil-Cement

Soil-cement, like any other construction material, requires some standard of acceptance to ensure that the quality of the product is satisfactory. In the United States of America, there are A.S.T.M. and A.A.S.H.O. standard laboratory tests, while in Great Britain a British Standard (BS 1924: 1967) specifies the standard tests to control the quality of the soil-cement produced.

New Zealand soil-cement practice in both laboratory and construction has been reviewed in Appendix (I), but the more important laboratory tests are those for unconfined compressive strength, durability, dynamic elastic modulus and C.B.R. In the past, in New Zealand, soil-cement acceptance has been based almost entirely on the unconfined compressive strength, with specified minimum strengths being required on all projects and a maximum strength also being set by some

6.1 (cont.)

authorities.

The selection of the design pavement thickness has been based mainly on CBR results, backed in most cases with Benkelman beam tests to control pavement deflections. Limited use has been made of elastic theory, but no allowance in design for internal stress build-up has been made. The construction thickness which had been used in nearly all pavements studied was the same as would have been allowed for conventional construction in similar material not stabilized. Most soil-cement pavements in New Zealand have been mixed in place, but some authorities have used plant mixed, paver laid material. Soil-cement for pavement construction in New Zealand has been compacted generally at optimum moisture content, but some authorities have compacted a few percent wet or dry of optimum moisture content.

In New Zealand there are at present no standards for testing stabilized soils, although a committee has been set up to prepare a suitable standard. The BS 1924 covers many of the simple tests and bases acceptance of a particular soil for stabilization on its unconfined compressive strength. On the other hand, the A.S.T.M. standards relating to stabilized soils (4),(5),(6) require a particular mix of soil and cement to pass the durability tests, namely the freeze-thaw and the wet-dry tests. In most parts of New Zealand, the freeze-thaw and the wet-dry tests are regarded as too severe for the local climatic conditions. The specimens normally used in New Zealand are made in the Proctor mould but, unfortunately, this does not

6.1 (cont.)

give the desired 2:1 length:diameter ratio. For fine-grained soils, this mould requires the preparation of large amounts of soil for testing, so the British Standard 102 x 51 mm mould seems to be more suitable. For medium grained soil the 204 mm long, 102 mm diameter mould is better than the Proctor mould.

In this project, the many properties of a soil-cement mix had to be studied, so the laboratory tests to be used had to be suitable. Therefore, existing standard tests were investigated and the following comments are made.

6.1.1 Preliminary Testing of Natural Soil

6.1.1.1 Grading

A particle size analysis is recommended, as well as a lump grading analysis. The lump grading analysis is carried out on a selection of sieves with openings ranging from the largest lump size to 0.074 mm. Sieving must be carried out with great care, to avoid breakdown of the lumps.

6.1.1.2 Classification

The usual procedure is to carry out the following tests: specific gravity, Atterberg limits (if applicable) and linear shrinkage.

6.1.1.3 Contamination of Soil with Organic Matter

The method described in BS 1924 : 1967, Test 18 for interference of cement hydration by organic matter, provides an easy test to indicate the likely suitability of a soil for stabilization.

6.1.1.4 Clay Analysis*

This was a specialist test which was carried out by Dr. Seed of the Geology Department, University of Canterbury.

6.1.1.5 Material Location

The location from which the particular soil was acquired should be adequately recorded to enable more material to be obtained if further tests are needed.

6.1.2 Moisture Content Determination

The BS 1924 test for moisture content determination fails to recognize the difference between a natural soil and a soil containing a stabilizer. If cement is being used to stabilize a particular soil, then the resulting hydration process uses moisture which becomes chemically bound and is not removed by heating to 105°C.

6.1.3 Compaction of Samples

The BS 1924 : 1967 specifies that for fine grained soils, unconfined compressive strength samples 102 mm long and 51 mm diameter be compacted statically in a hydraulic press. For larger samples of coarser grained materials, dynamic compaction is specified, although it is nowadays regarded as unrealistic, in that the strengths of compacted laboratory specimens do not agree with the strength of cores from the field. Kneading compaction has been suggested as an alternative by many research workers in soil mechanics, as being more representative of field compaction.

*See Acknowledgements.

6.1.3 (cont.)

From the limited amount of testing carried out in this project to compare dynamic and kneading compaction, it was found that the end products of both methods were surprisingly similar. The test consisted of removing cores from a particular roadway 80 days after compaction and breaking them in compression. Samples the same size as these cores were compacted using kneading and dynamic compaction and cured for 80 days in conditions similar to those experienced in the pavement. The resulting unconfined compressive strengths obtained from the laboratory samples were very close, and the strength of the dynamically compacted samples was equal to that of the field samples. Therefore, one might conclude that for soil-cement the compaction method is not as important as it is for natural soil compaction.

Other tests carried out clearly indicated that little difference existed between statically compacted and kneading compacted soil-cement samples. As static compaction is extremely easy and quick to perform, it would therefore appear to be the most logical method of compaction for routine testing, as suggested by BS 1924 : 1967.

6.1.4 Strength Tests

Both tensile strength and unconfined compressive strength have been used by many authorities for determining the suitability of soil-cement.

6.1.4.1 Unconfined Compression Test

This test is clearly specified in BS 1924 : 1967 and is probably the most used test for soil-cement. Unfortunately,

6.1.4.1 (cont.)

many sample sizes other than those specified in BS 1924 : 1967 have been used by laboratory workers. The 102 mm long, 51 mm diameter mould specified by BS 1924 : 1967 is a two-piece split mould, which has the disadvantage of producing, on the outer edge of the sample, small lines at the joints between the two halves of the mould. From these lines small cracks begin, and being diametrically opposite, they tend to initiate premature failure of the sample. This problem has been overcome by building a three-piece split mould of the given dimensions, as shown in fig. (6.1).

The unconfined compression samples are usually broken between flat parallel plattens, on which friction restrains the sample ends from expanding radially. Because the sample is restrained, the mode of failure is affected. Therefore, it was decided to place a rubber membrane, lubricated with silicone grease, on both plattens before inserting the sample. When direct sample to platten contact is eliminated, radial expansion of the sample in the transverse direction is uniform, and the familiar bulging that usually occurs at the centre of a sample is eliminated.

6.1.4.2 Tension Tests

The direct and indirect tension tests and the flexural test have been used to determine the tensile strength of soil-cement, but tensile strengths are not yet recognized as suitable pavement design criteria. Comments on both the direct and indirect tension tests have been presented in Appendix (VI).

6.1.4.2 (cont.)

The flexural test, often referred to as the modulus of rupture test, has been used by many research workers, as the applied load tends to represent the action of a wheel load on a pavement slab. Unfortunately, before the tensile strength can be calculated from the flexural strength, assumptions must be made regarding the elastic behaviour of the material. The modulus of elasticity can be determined electro-dynamically in a non-destructive test, but research workers have shown that statically determined elastic moduli are lower than the values obtained electro-dynamically. Also, the elastic modulus in tension has been found to be different from the elastic modulus in compression (Bofinger[13]).

From a comparison of the various tensile testing methods, the indirect tension test is now recommended for future soil-cement work.

6.1.5 Bearing Capacity

The California Bearing Ratio is a major design parameter in present roading design. Consequently, its use for soil-cement has been widespread. The method described by BS 1924 : 1967 mentions both soaked and unsoaked C.B.R. tests, but it does not specify how long after compacting the sample the soaking should begin. This point is very important and it, therefore, needs to be clearly defined. Possibly, a sample should be moist cured for seven days, then soaked for seven days before testing.

6.1.6 Durability Tests

In the United States of America, wet-dry and freeze-thaw tests are specified as routine tests for stabilized pavement design (A.S.T.M. tests : D 559-57 and D 560-57 or A.A.S.H.O. tests T 135-57 and T 136-57). By comparing the climatic conditions experienced in most parts of the United States of America with those in New Zealand, it would appear that the freeze-thaw and possibly the wet-dry tests are too severe to act as a sound base for soil-cement design in New Zealand. Only in isolated parts of New Zealand would a soil-cement pavement be subjected to freezing, while complete drying as carried out in the A.S.T.M. and A.A.S.H.O. tests should never occur once the seal coat is applied. Therefore, the use of a wetting and drying test seems unnecessary in the light of New Zealand climatic conditons. By obtaining strength results for soaked and unsoaked samples, it should be possible to obtain the strength reductions which might be expected on soaking. Consequently, the freeze-thaw and the wet-dry tests have been omitted from the list of suggested laboratory tests for soil-cement in New Zealand, but this does not exclude specific testing on soaked samples.

6.1.7 Fatigue Test

The fatigue properties of a cement stabilized pavement are extremely important if the pavement is to be designed with a given life expectancy. From research work carried out with repetitive loading, it is evident that fatigue of samples tends to reduce their life expectancy i.e., failure occurs at a stress

6.1.7 (cont.)

lower than the ultimate strength. No repeated load tests were carried out for this project, but the importance of such tests in any design procedure for cement stabilized pavements is fully realized.

The usual procedure for a fatigue test is to load and unload a small beam repeatedly until it fails. If the applied load is expressed as a percentage of the ultimate strength, then the number of load cycles required to cause failure can be plotted against this percentage for a range of applied loads, thus giving a fatigue curve.

6.2 Other Tests for Soil-Cement

In order to obtain a better understanding of the many properties of soil-cement, some new tests should be introduced to the standard laboratory program for soil-cement testing.

6.2.1 Shrinkage Test

As shrinkage is the main topic for study in this project, several different methods of shrinkage measurement were tried to find the most suitable method. Initially, specimen length was measured using a travelling microscope sighted on appropriate targets and the shrinkage strain was obtained by taking the difference between successive readings. This method was susceptible to many errors. The targets on which readings were being taken could not be manufactured precisely enough to ensure that subsequent sightings on that target corresponded with the original position. Any looseness in the measuring instrument

6.2.1 (cont.)

greatly increased the likely error in the readings of length change. The use of linear variable differential transformers (L.V.D.T.'s) was also investigated, but the large number of samples to be measured at any one time eliminated their use on the basis of cost.

After examining the above methods of length measurement the use of the following was decided. For large prisms a demec gauge reading between two demec points glued to the prism surface was used. The 102 mm long, 51 mm diameter samples were measured using the device shown in fig. (6.2), while the 13 mm diameter samples were measured using both this device and a dial gauge mounted above the vertically placed sample, such that the dial gauge anvil is pressed into a recess, as shown in fig. (6.3). This latter method proved exceedingly accurate and reliable; therefore, it could be recommended as the best method for obtaining shrinkages of small cylindrical samples.

6.2.2 Creep Test

A limited amount of work has been carried out elsewhere on the creep of soil-cement, mostly studying creep in compression, although Bofinger[16] did attempt to measure creep in tension. As a shrinking soil-cement pavement is in tension, it therefore follows that creep in tension must be determined and consequently used for design considerations.

The tension creep tester used in this project was basically simple, the sample being attached to one end of a lever arm and a load applied to the other end, fig. (6.4).

6.2.2 (cont.)

Movement vertically is measured by a dial gauge situated directly above the sample. Knife edges were used throughout to minimize friction and allowance was made for the force exerted by the dial gauge spring.

The compression creep testers used in this project were of two types; the first was loaded by the tension in a spring, while the second was loaded using a lever system and weights. The spring loaded tester had two distinct disadvantages; firstly, as the sample deformed, the tension in the spring was reduced and secondly, if the creep tester was used in the climatic room where the temperature varied throughout the day, the spring expanded or contracted to give variable loading conditions.

The direct loading compression tester fig (6.5), on the other hand, proved extremely reliable. Creep readings were obtained using the average of two dial gauge readings.

6.2.3 Stress in Restrained Samples

In order to study the build-up of stress in either a small prism or a road pavement of soil-cement, it was necessary to have a means of measuring this stress experimentally. Therefore, methods for measuring stress build-up in 76 mm x 76 mm x 286 mm prisms were investigated. As approximately 100 prisms were required to be tested at any one time, a simple restraining device had to be devised. A number of steel cradles were constructed with an open top and a 19 mm diameter hole in each end, as shown in fig. (5.1). On to each end of a 286 mm long sample were glued steel plates containing a ball and socket swivel,

6.2.3 (cont.)

shown in fig. (6.6). This swivel device was adopted as the best of several methods tried for applying pure tension at the specimen ends, without any bending moment. The main problem with the cradles was the high strength required in the swivel device to withstand the load resulting from the stress build-up within the sample. The glue used on the end plates was an epoxy resin Araldite GY 250 with hardners HY 850 and HY 830.

Connected to the swivels there were 16 mm diameter threaded bars, which protruded through the holes in the cradle ends. Nuts were placed on the outside ends of these threaded bars and tightened against the cradle ends using a extensometer straddling the length of the sample, fig. (6.7), such that the sample was held firmly, but not under stress. The cradled samples were then left either to crack under stress or be tested after prescribed periods of time in a tension testing machine. In this tension test, the load imposed by the sample on its cradle was transferred from the cradle to the testing machine. When the nut on the threaded rod could be turned by hand the testing machine then recorded the tension in the specimen. The stress build-up for a 76 mm x 76 mm x 286 mm loess soil-cement sample is shown in fig. (6.8), while fig. (6.9) shows a cracked soil-cement sample in its cradle.

A device shown in fig. (6.10) was built to measure stress build-up during moist curing in 76 mm x 76 mm x 286 mm prisms. The stress that developed in the soil-cement samples while they moist-cured was extremely small compared with the stress that

6.2.3 (cont.)

developed while drying; consequently, much more sensitive equipment was required to measure these small stresses. The apparatus consisted of a lever arm pivoted on a ball bearing so that, as a load could be applied to the sample, changes of length of the prism were indicated by the dial gauge mounted in its longitudinal axis. The prism was able to move horizontally on stainless steel rollers mounted between two flat brass plates. As it contracted, the movement was recorded by the dial gauge. Then a load was applied to the lever arm to bring the dial gauge back to its original position. This process was repeated daily, the added weight being recorded.

6.3 Laboratory Tests for Determining the Suitability of a Particular Soil-Cement

The existing standard laboratory test procedures for soil-cement are lacking in tests for measurement of such parameters as shrinkage and creep, and it was evident that a much broader experimental program was required. By developing a series of tests and obtaining the appropriate results, a better soil-cement mix can be designed.

6.3.1 Outline of Experimental Work Used in This Project

From early investigations of the shrinkage of soil-cement samples, it became evident that a number of other factors such as the moulding moisture content and the moulding density could influence the ultimate shrinkage. In view of this, the following variables were studied to determine their effect on ultimate shrinkage, unconfined compressive strength and tensile strength:

6.3.1 (cont.)

(a) moulding density

(b) moulding moisture content

(c) precure moisture content

(d) cement content

(e) delay in compaction after mixing

(f) mixing times, and

(g) pretreatment with lime, and combined addition of lime and cement to the loess soil.

In addition, a small number of creep tests were carried out on the sandy pumice soil-cement for these suitability tests. The results obtained and testing techniques have been briefly outlined in the paper by Dunlop et al[39].

The materials used were the modified loess and the sandy pumice with the characteristics described elsewhere in this thesis. The equipment and experimental techniques are described in Appendix VII.

The term "precure moisture content" is used to refer to the equilibrium moisture content at which the natural soil was stored for two weeks, before being mixed with the cement and the correct amount of water to give the desired moulding moisture content.

When tests for the effects of the precure moisture contents were carried out, the raw soil was stored at a range of precure moisture contents and mixed to a constant moulding moisture content before compaction. When reference has been made in this chapter to either density or moisture content of a soil-cement

6.3.1 (cont.)

mix, these are to be regarded as moulding density and moulding moisture contents respectively.

The resulting shrinkage and creep obtained from the tests have been expressed as strains after moist curing. The term "shrinkage" when used in the following discussion, is the ultimate shrinkage, unless otherwise specified.

The "moulding density" is the dry density including cement. Compaction was carried out to give a predetermined density, with constant moulding moisture content, unless otherwise specified. Thus, the "moulding moisture content" was the final moisture content at which the sample was compacted and cured.

For the modified loess, the Standard A.A.S.H.O. dry density was 1.999 t/m^3 at 11.4% moisture content, while the sandy pumice had a 100% A.A.S.H.O. dry density of 1.602 t/m^3 at 20.2% moisture content.

The detailed results from the various tests carried out are given in figs (6.11-6.57). Included with these figures are curves of best fit to the results, together with the 95% confidence limits. The latter limits give an indication of the scatter of results which can be seen to vary from figure to figure. A qualitative summary of the results is presented in Table (6.1).

6.3.2 Discussion of Results for Shrinkage

6.3.2.1 Moulding Density

For both materials tested, very similar curves of shrinkage vs. moulding density were obtained. These show a

6.3.2.1 (cont.)

very rapid increase in shrinkage with increases in density over the normal density range, as shown in figs (6.11) and (6.12). Accompanying this increase in shrinkage is a very marked gain in the strength of both soils with increase in density, as shown in figs. (6.13), (6.14), (6.15) and (6.16). This strength density is discussed later in section 6.3.4.1.

An increase in the density of a soil-cement sample means that a greater number of solid particles exist per unit volume, therefore there must be more wedge shapedvoids at the solid to solid contacts. As described in section 4.5, the adsorbed and capillary water existing in wedge shaped voids permits the development of attractive forces as drying occurs, with the adsorbed water being the main contributor to shrinkage. Therefore, the more solid to solid contacts present in a sample, the greater should be the shrinkage.

George[53] made a brief mention of the effect of density on soil-cement samples. He found that provided the moulding moisture content was reduced while the density was increased, then shrinkage was reduced, but if the moisture content was held constant and the density was increased, then shrinkage increased. In considering the moulding density for design purposes, the advantage in a gain in strength obtained by increased compaction will be more than offset by the disadvantage of the increase in shrinkage caused by this increase in density (figs (6.17) and (6.18)). Therefore, a low compaction should be aimed for in the design mix, thus keeping the shrinkage as low as possible, but a lower limit must be

6.3.2.1 (cont.)

set for the tensile strength if stability of the soil-cement is to be retained.

6.3.2.2 Moulding Moisture Content

From figs. (6.19) and (6.20) there are definite indications that, for variable moulding moisture contents in both the loess and sandy pumice soil-cement there is a maximum value for total shrinkage, and this maximum occurs on the dry side of O.M.C. (O.M.C. 11.4% for loess soil-cement and 20.2% for sandy pumice soil-cement). On the dry side of this maximum shrinkage point there is a rapid decrease in shrinkage with a decreasing moulding moisture content, while on the wet side of this point, a decrease in shrinkage with increasing moulding moisture content is again evident, but not as rapid.

Nakayama and Hardy[92] state that control of the moulding moisture is relatively ineffective for reducing shrinkage, in the light of their experimental work. They suggest that much of the excess moulding water is probably capillary water, which may be lost without causing shrinkage. The opposite has been found from the experimental work carried out for this thesis, which indicates that shrinkage is dependent to a considerable degree on moulding moisture content. Also, capillary water will always affect shrinkage, but in the case where a sample is moulded at a low moisture content, most of the water will exist in the adsorbed state and not in the capillary state; therefore, as seen in section 4.4, shrinkage must be greatly affected.

George[53] concludes that it is best to compact below

6.3.2.2 (cont.)

optimum moisture content and never above, as the moulding moisture content plays an important role in controlling shrinkage. He offers the following explanation. The more water that is provided, the more cement gel will be formed by the hydration process. As cement gel is responsible for a large part of the possible shrinkage, it is evident that increased moulding moisture content will cause increased shrinkage. He also states that the more water that is provided for evaporation, the greater will be the internal compressive stresses exerted on the solid particles during evaporation.

From the experimental work carried out for this thesis, George's observations would appear to be correct. If the density is held constant while the moisture content is changed, a number of observations can be made. Firstly, an increase in the moulding moisture content will increase the amount of adsorbed and/or capillary water available for evaporation (see Chapter 10); therefore shrinkage must increase. It is not only the cement gel which causes the increase in shrinkage as suggested by George, but the number of solid to solid contacts which have been developed within the cement gel. Secondly, (in the range below O.M.C.) when the moulding moisture content is increased, the soil particles will tend to compact more easily because of the increased lubrication; therefore, less disorientation of particles will result in mixtures containing more moisture. This will in turn tend to produce solid to solid contacts, which are more conducive to higher shrinkage in that the wedge-shaped voids so formed have a smaller

6.3.2.2 (cont.)

included angle. Once the amount of capillary water has reached a high level, shrinkage should remain constant as the moulding moisture is further increased. From the experimental results, it is observed that the shrinkage actually tends to drop off after reaching a peak.

Indications from the two materials studied in this project and from work carried out by George would favour the use of a very high or a very low moulding moisture content, but preferably on the dry side of optimum. The loess definitely requires compaction at a moisture content below optimum, but the sandy pumice could be compacted at optimum without causing excessive shrinkage.

6.3.2.3 Precure Moisture Content

The effect of varying the precure moisture content has received little attention from the many research workers in the field of soil-cement. When the precure moisture content is high, a high proportion of the total moisture in the soil-cement mix is contained as adsorbed moisture in the porous lumps of soil. On the other hand, if a large percentage of the total moisture was readily available for hydration because of a low precure moisture content, i.e. the water was not adsorbed in the porous lumps, it would seem to follow that the resulting hydration process would be more rapid than if only a small percentage of the total moisture were readily available. The effects of varying the precure moisture content, as recorded in this experimental program, are shown in figs. (6.25) and (6.26).

6.3.2.3 (cont.)

An increase in the precure moisture content has directly opposite effects on the shrinkage of the two materials studied, as can be seen in figs. (6.25) and (6.26). For a loess soil-cement containing lumps of natural soil, secondary cementation is greatly enhanced when the precure moisture content is high, because it is much easier for a liquid to penetrate a lump of damp soil than a lump of dry soil. When the precure moisture content is low, secondary cementation is greatly inhibited, with consequent rapid hydration of the cement with the greater quantity of added water. As the precure moisture content is increased, the secondary cementation process spreads further away from the cement grains, causing an increase in the stiffness of the soil lumps and thus reducing the shrinkage. This reduction of shrinkage with an increasing precure moisture content continues until the effect of self desiccation becomes prominent. If the precure moisture content is very close to the mixing moisture content, then the original cement grains will have to draw water from the soil lumps for the hydration process. Therefore, self desiccation occurs with a marked shrinking of the whole soil-cement sample. The sandy pumice soil-cement on the other hand, being very porous would take up water, yet not be greatly affected by secondary cementation, as the natural soil is relatively stable.

For the sandy pumice soil-cement compacted at low precure moisture content, most of the moulding moisture is readily available for hydration of the cement. On the other hand, at high precure moisture content the moisture readily available

6.3.2.3 (cont.)

for the hydration process is greatly reduced, and the cement must draw moisture from the sandy pumice soil lumps, thus greatly reducing the hydration rate. Therefore, it is evident that a low precure moisture content will induce rapid hydration, which tends to cause less shrinkage than the slow hydration process associated with higher precure moisture content. Possibly the gradual reduction in shrinkage for increasing precure moisture contents could be caused by secondary cementation.

6.3.2.4 Cement Content

For the sandy pumice soil-cement, there is a fairly rapid increase in shrinkage with increasing cement content until a maximum is reached, followed by a fall-off (fig. 33). If the sandy pumice soil is compacted without cement, there is no shrinkage, as can be expected, because only rigid solid particles are present in a sandy pumice soil.

For the loess soil-cement, the shrinkage starts off at a high value for zero cement content, then drops and passes through a minimum then rapidly increases again, fig. (6.31). These solid particles do not change in volume as moisture is removed from them, whereas for a natural soil containing clay lumps, the removal of moisture from within these lumps causes a volume decrease. Therefore, shrinkage of a natural loess soil on drying would be expected.

On mixing cement with either loess or sandy pumice to make soil-cement, the cement hydrates to form a gel which has a stabilizing effect on any natural clay lumps present in the mix; the cement gel also provides a main source of shrinkage.

6.3.2.4 (cont.)

Therefore, for a sandy pumice soil-cement, it can be assumed that the cement gel which must increase in quantity with an increase in the cement content, also causes an increase in shrinkage, as observed in fig. (6.32). With a soil containing clay, such as loess, the shrinkage which is high when no cement is present is inhibited by increasing the cement content until a minimum shrinkage point is reached where gel formation begins to over-ride the stabilizing effect on the natural soil. As the cement gel increases with increasing cement content, so does the potential shrinkage of the soil-cement increase as observed in fig. (6.31).

For mix design purposes, it is recommended that the following effects should be considered when specifying the quantity of cement to be added to any particular soil, and each soil must be considered separately. Where possible, for a sandy material, the cement content should be kept as low as practicable, while for a cohesive soil, a cement content near the minimum point on the cement content shrinkage curve should be used. Nevertheless, the tensile strength must be maintained at a reasonable level when reductions in cement contents are considered, as there comes a point at which the tensile strength is as important as the magnitude of the shrinkage. (figs. (6.17) and (6.18)).

6.3.2.5 Delay in Compaction

Delayed compaction always causes loss of density which in turn implies a reduction in shrinkage, figs (6.11) and (6.12).

6.3.2.5 (cont.)

For the loess soil-cement, fig. (6.37), there was an increase in shrinkage as delays in compaction increased to $1\frac{3}{4}$ hours after which decrease in shrinkage was observed. The shrinkage increase within the first $1\frac{3}{4}$ hours seems difficult to explain, but the later decrease in shrinkage could easily be predicted, in that delayed compaction causes a loss of density, with a consequent decrease in shrinkage. The sandy pumice soil-cement was not studied for shrinkage changes arising from variable delays in compaction, but both soil-cements studied for this project indicated a nearly linear relationship between loss in strength and delay in compaction, as shown in figs. (6.38), (6.39), (6.40) and (6.41).

6.3.2.6 Mixing Time

Mixing time had very little effect on the shrinkage of sandy pumic soil-cement fig. (6.42), although an increase in mixing time did appear to produce a slight strength loss. This strength loss would probably be caused by the breaking of the bonds being formed while mixing was occurring. Individual results of samples were found to be less scattered after excessive mixing.

6.3.2.7 Use of Lime on Loess

Treatment of a clayey material with hydrated lime before stabilizing with cement, or stabilizing entirely with hydrated lime may be worthwhile. As loess has a 22% clay content ($<2\mu$), it would seem reasonable to expect some benefit to be gained from treatment of the soil with lime. Unfortunately, the use

6.3.2.7 (cont.)

of lime-pretreatment fig. (6.47), and of lime in place of cement fig. (6.48), as a stabilizing material appeared to be detrimental in every way. Both tensile and unconfined compressive strengths were reduced by lime pretreatment. The lime possibly would have been more effective if the clay fraction was a montmorillonite and not an illite.

6.3.3 Other Factors Affecting Shrinkage

No attempt was made to investigate the effect on shrinkage of clay content, moist curing, curing conditions and the temperature while curing, but other research workers have reported on these points.

6.3.3.1 Clay Content

Nakayama and Hardy[92] and George[53] have obtained the effects on shrinkage of using variable clay fractions and different clay minerals. The clay structure lends itself to different shrinking and swelling characteristics, so the clay minerals can be listed in decreasing order of ability to shrink: montmorillonite, illite and kaolinite. George found that increasing the clay fraction of any particular mineral present caused an appreciable increase in shrinkage.

6.3.3.2 Moist Curing

Moist curing of soil-cement can produce unusual results; e.g. firstly, shrinkage of sandy material during moist curing is nearly zero, while shrinkage of clayey material can be quite significant, though it would not usually be more than 5% of

6.3.3.2 (cont.)

the total shrinkage. George[53] found that, in a sample containing a small percentage of clay sizes, the shrinkage increased after prolonged moist curing while, for material containing a large percentage of clay, the reverse was true.

6.3.3.3 Curing Conditions

Nakayama and Hardy[92] found that, if soil-cement samples were permitted to dry immediately after compaction, then any clay present would begin shrinking immediately. If the soil-cement contained no clay material or the soil-cement containing clay was given a specific period of time to moist cure, then immediate shrinkage was markedly delayed. The explanation given for the immediate shrinkage of a soil-cement containing clay was that the clay fraction offered little internal restraint and therefore must have participated in the shrinkage.

This conclusion reached by Nakayama and Hardy[92] is probably a sweeping statement, based on limited test results, though it would appear correct that a soil containing a high clay content would begin to shrink immediately drying is initiated. Two processes are involved: firstly, the hydrating cement attempts to remove moisture from the clay lumps so that a reduction in volume of this clay fraction occurs; secondly, evaporation is attempting to rob the cement grains of moisture, thus promoting shrinkage.

George[53] makes little comment about curing, except that for soil-cements containing small amounts of clay, greater total shrinkage occurred after prolonged moist curing than during immediate drying; the reverse was true for soil-cements

6.3.3.3 (cont.)

containing large amounts of clay. The suggested reason was that in low-clay mixes the greater shrinkage from prolonged moist curing may have been due to the higher proportion of gel and that on immediate drying less restraint to shrinkage was offered by the greater proportion of unhydrated cement particles. In a high-clay soil-cement mix on the other hand, if moist curing is prolonged, more and more lime is released by the cement and this reacts with more and more clay so the shrinkage of the clay soil is reduced. Unfortunately, George does not specify at which point the shrinkage is recorded from, i.e. whether the moist-curing shrinkage is included in the total shrinkage.

Nakayama and Hardy[92] also obtained similar results, though their scatter was very high. They considered that increased moist curing time will allow the formation of more gel, and since cement gel is the main cause of shrinkage, one could expect that shrinkage would increase. For a clay soil-cement, both the cement gel and the clay domains act as potential shrinkage mechanisms. As hydration proceeds, there is an increase in gel formation, but a reduction in untreated clay.

George also found that, for prolonged moist curing of a sandy soil-cement, there was an increase in shrinkage, compared with that after 28 days moist curing. On the other hand, for a clayey soil-cement, the reverse was true, and shrinkage was less after prolonged moist curing. As the amount of gel formed in both soil-cements would be similar, it must have been the clay fraction contained in the soil-cement which influenced the total moist cured shrinkage. In both soil-cements, gel formation

6.3.3.3 (cont.)

would increase with prolonged moist curing, but in the clayey soil-cement the shrinkage owing to the clay itself would decrease as more and more clay reacted with the cement.

Selection of the proper moist curing time for different soil-cements poses a complicated problem, but the experimental evidence indicates that an "adequate period" of moist curing is necessary for tensile strength to develop and any further moist curing is of little, if any, value. The "adequate period" of moist curing can best be obtained by plotting a moist curing tensile strength versus time curve, from which it is evident, by the changing gradient of the curve, at what time any further moist curing will be of negligible benefit. For most soil-cements four to seven days moist curing have been found to be adequate.

6.3.3.4 Effects of Mix Temperature on Shrinkage

George[53] carried out tests to determine the effect of mix temperatures on shrinkage. Samples mixed and compacted at elevated temperatures had a shortened setting time and produced an inferior soil-cement more susceptible to volume change. This was especially true for clayey materials. From the results, it may be observed that shrinkage does, in fact, increase with temperature for clayey soil-cements, but remains almost unchanged for low clay content soil-cements.

George found that provided hydration has ceased, increased drying temperatures will only reduce the time for total shrinkage to occur. Increased curing temperature should have the same effect as prolonged moist curing, i.e. decrease

6.3.3.4 (cont.)

in shrinkage for clayey soils and increase in shrinkage for low clay content materials.

6.3.4 Tensile and Unconfined Compressive Strength

6.3.4.1 Moulding Density

As shown in figs. (6.13, 6.14, 6.15 and 6.16) the strength of a soil-cement specimen increases with increasing moulding density. This is a similar relationship to that for unstabilized soils, where a reduction in void ratio increases the number of solid to solid contacts and consequently gives greater strengths. As mentioned in section 6.3.2.1, the density should be as high as possible in order to develop a high tensile strength, but shrinkage also increases with moulding density, so a high density is generally undesirable in soil-cement pavements.

6.3.4.2 Moulding Moisture Content

As the results in figs. (6.21, 6.22, 6.23 and 6.24) show, the moulding moisture content has different effects on cohesive and non-cohesive soil-cement.

A natural loess soil compacted at zero moisture content has a measurable strength, but if the sandy pumice soil is compacted dry it does not stand under its own weight. Consequently, the strength gain for a loess soil-cement with increasing moulding moisture content is much less than for a sandy pumice soil-cement. It is evident that as the moulding moisture content increases, so does the formation of cement gel, therefore the strength increases. When the moulding moisture content reaches a level at which the water required for complete hydration is available then

6.3.4.2 (cont.)

the use of any further water in the moulding process is unnecessary, and may even be detrimental to the strength.

6.3.4.3 Precure Moisture Content

The effect on strength of varying the precure moisture content is shown in figs. (6.27, 6.28, 6.29 and 6.30). It is noticed that all the curves show a decrease in strength as the precure moisture content approaches the moulding moisture content; this strength drop is more predominant for the sandy pumice soil-cement than for the loess soil-cement. It would appear that with more moisture readily available for the hydration process, the cement gel will form more quickly, and this in turn appears to cause a higher strength to develop.

6.3.4.4 Cement Content

As one would expect, an increase in cement content causes an increase in strength for both soil-cements studied, figs. (6.33, 6.34, 6.35 and 6.36). The sandy pumice soil has negligible strength before cement is added, while the loess soil has a measurable unstabilized strength, and a linear increase in strength with increasing cement content. Increasing the cement content permits an increase in the formation of cement gel, so it is evident that the strength must increase.

6.3.4.5 Delayed Compaction

As mentioned in section 6.3.2.5, the strength of both soil-cements tested decreases with increasing time before compaction, figs. (6.38, 6.39, 6.40 and 6.41). Once mixing of the soil, water and cement has commenced, the hydration process

6.3.4.5 (cont.)

proceeds rapidly, with the consequent development of primary stabilization, which causes bonds to develop in the soil-cement matrix. If compaction is attempted some time after first mixing, bonds formed by primary stabilization must be broken and the full strength of the material is never regained.

The exact effect of delays in compaction cannot be easily evaluated, but it appears that too great a delay would be extremely detrimental to the structural stability of the pavement slab. For most soil-cements a delay of no greater than 1 hour is acceptable.

6.3.4.6 The Effect of Drying a Soil-Cement Sample

When a soil-cement containing clay, such as loess soil-cement, is dried quickly after 7 days moist curing, the strength continues to increase until the sample is completely dry, as shown in fig. (6.53). On the other hand, when sandy pumice soil-cement is dried, it reaches a peak strength at 8.5% water content followed by a loss in strength as shown in fig. (6.54).

For the clayey soil-cement, very few incompressible particles exist in the clay matrix. Consequently, the main components of the soil-cement clay domains and cement gel, are both subject to volume change as drying occurs. By contrast in the sandy pumice soil-cement, only the cement gel changes in volume as drying occurs because the remaining components of the mix are incompressible solid particles. The contracting forces caused by drying are extremely large, therefore bond failure may occur around the solid particles causing a reduction

6.3.4.6 (cont.)

in strength at low moisture contents. This seems to indicate that a sandy pumice soil-cement must not be permitted to dry below half the moulding moisture content. By drying the sandy pumice soil-cement samples extremely slowly, this strength reduction can be slightly reduced, but cannot be eliminated.

6.3.5 Creep Tests Associated with the Suitability of a Soil-Cement

Almost as important as shrinkage in stabilized pavements is the effect of creep. Once shrinkage begins, stress build-up occurs within the base and, in turn, causes creep to take place. Unfortunately, the importance of creep in determining the suitability of a particular soil-cement was not appreciated earlier in this research work, and creep tests in tension were carried out only on the sandy pumice soil-cement. The first series of tests using 51 x 102 mm long samples was a complete failure, owing to the inaccurate method of measuring the specimen length. In later test series, such variables as moulding moisture content, moulding density and cement content were compared with the ability of the sandy pumice soil-cement to creep by using 13 mm diameter samples. Creep was found to increase with decreasing cement content (fig. 6.55), decreasing density (fig. 6.56) and decreasing moulding moisture content over the normal working range (fig. 6.57), but note that these curves cover only the initial period of drying. Also, not too much importance should be placed on the curves for creep versus moulding moisture content, because a sample compacted at a high moisture content loses water first from its capillary pores,

6.3.5 (cont.)

and little shrinkage takes place over the initial period of drying. If the creep of a sample made at an intermediate moisture content is compared with that of a sample which has been dried to that same moisture content after moulding at a higher moisture content, we see that the creep in the latter is only slightly less than in the former.

These creep results for variable cement contents and variable densities are as might be expected, in that creep strain is higher for both lower cement content and lower density. The results of creep for variable moulding moisture contents, as mentioned above, can lead to misconceptions in that, while the sample loses moisture from the capillary pores, creep is not as pronounced as when water is lost from the adsorbed state. Therefore, for a given moisture content reduction after curing, the samples moulded at a high moisture content indicate low creep compared with those moulded at a low moisture content, but after prolonged drying the reverse is true.

6.4 Proposed Design Mixes for Modified Loess and Sandy Pumice Soil-Cements

6.4.1 Design Mix for a Modified Loess Soil-Cement

By comparing the normally accepted design mix for a loess soil-cement with the design mix obtained from the results in section 6.3, (Table 6.2) it is evident that considerable discrepancy in the existing and proposed design mixes exists. In many loess soil-cement pavements the natural soil has been

6.4.1 (cont.)

mixed with water to give the optimum moisture content and then compacted at the maximum density. The cement content has normally been determined by carrying out unconfined compression tests, with a minimum strength being required before a soil-cement is acceptable.

For the loess soil-cement the proposed design mix shown in Table 6.2 was developed by considering the shrinkage and tensile strength curves with respect to the variables, moulding density, moulding moisture content, precure moisture content and cement content. For example, it is obvious from fig. 6.31 that the shrinkage can be considerably reduced by using a cement content of 4%, yet in fig. 6.33 it is evident that the tensile strength is not greatly reduced when the cement content is reduced from 8% to 4%. By using the proposed design mix compared with the normally accepted mix for a loess soil-cement shrinkage reduction of up to 60% can be made while a reduction in the tensile strength only amounts to 20%.

6.4.2 Design Mix for a Sandy Pumice Soil-Cement

By comparing the mix used for the sandy pumice soil-cement on Silverdale Road and that proposed from the tests carried out in section 6.3 (Table 6.3) it is evident that the mix being used is very close to the proposed mix except that the moulding density is too high. A reduction in the moulding density would definitely be advantageous in reducing shrinkage, but as shown in Chapter 9 the sandy pumice soil-cement does not develop high shrinkage stresses anyway.

CHAPTER SEVEN

EXAMINATION OF EXISTING THEORIES IN SOIL-CEMENT SHRINKAGE STRESSES

When this project began, only the initial work carried out by George[50] on cracking of soil-cement pavements was available on which to plan the initial program into shrinkage stresses. Other papers by George[51,52], Okada and Kawamura[98], Kawamura[72], Bofinger and Sullivan[17] and Pretorius and Monismith[108] became available in the course of this research project and the results obtained by these workers are discussed.

7.1 Review and Discussion of Existing Studies

7.1.1 Review of Papers by George

George[50] presented a simple method for predicting crack spacing and crack width; he assumed that drying across the slab section was uniform, and used ultimate shrinkage values which he determined experimentally. He examined a pavement which though cracked was continuing to shrink, presumably because of further drying. A shrinkage slab is restrained from moving by the frictional restraint of the sub-base and sub-grade, so that the movement of a contracting slab increases from zero at the midlength to a maximum near the free ends. As the slab must be in equilibrium, the total tensile force in the slab must equal the sum of the frictional restraint forces from the midlength of the slab to either free end. Assuming his soil-cement base to be perfectly elastic, he developed equations for predicting crack spacing and crack width.

In a later paper by George[51], creep was taken into account by adopting the Burger rheological model to represent

7.1.1 (cont.)

the creep of a cylindrical soil-cement sample which, after 7 days moist curing, was loaded to 50% of the 7 day ultimate compressive strength. Creep in tension was assumed to be the same as creep in compression. With reference to fig. (7.1), the strain ε_t for a constant stress σ can be expressed for the Burger Model by the following equation:

$$\varepsilon_t = \sigma\left[\frac{1}{E_m} + \frac{t}{\eta_m} + \frac{1}{E_k}\left(1-\exp(-t/\tau)\right)\right] \qquad \ldots\ldots (7.1)$$

By assuming a constant shrinkage rate, George was able to calculate the ratio of visco-elastic stress to elastic stress, and hence the true tensile stress which should develop in the soil-cement.

The following comments made by George appeared to be worth further consideration:

(a) Creep and shrinkage were found to be not independent of each other. Also, for any soil-cement mixture, creep was found to increase as the relative humidity decreased.

(b) The Burger model shows great promise in mechanical simulation of actual soil-cement behaviour.

(c) The shrinkage stress computed by visco-elastic theory was found to be 50% lower than that predicted by elastic theory.

(d) Rapid shrinkage favoured large stresses.

George[52] in his third paper, calculated shrinkage as a function of time by using the diffusion equation (100). Then with the aid of the Burger model to represent the creep characteristics of the soil-cement, he produced theoretical curves for shrinkage stresses within a small prism for different times.

7.1.1 (cont.)

Unfortunately, this work had already been carried out by Okada and Kawamura[98], as reviewed later in this chapter. However, the following conclusions from George's third paper are worthy of mention:

(1) The theoretical shrinkage stress was highly localized at the exposed surface.

(2) The tensile shrinkage stress at the exposed surface of a soil-cement slab attains a maximum value at an early age, then decreases rapidly.

(3) The maximum theoretical shrinkage stress was found to be much greater than the tensile strength of the soil-cement; consequently, a surface crack would form.

From a study of a model soil-cement base, George investigated shrinkage cracking with the following results:

(a) The "crack intensity" decreased (i.e. the crack spacing increased) with an increase in the thickness of the base, with increasing cement content and with increasing coefficient of subgrade friction.

(b) The "crack intensity" decreased with a decrease in the modulus of viscosity of the soil and with decreasing shrinkage rate.

(c) The "crack intensity" varied with the type and amount of clay-sized particles in the soil.

(d) Large aggregates, by virtue of their ability to intensify the stress in the shrinking matrix, increased crack intensity.

7.1.2 Comments on Papers Published by George

In the first of these three papers by George[50], he described a study carried out on a soil-cement pavement where non-uniform drying was not considered. Although non-uniform drying must occur under normal environmental conditions; if it is assumed that the stress distribution across the soil-cement base is uniform, then the equations presented in the paper are correct. In the second paper, (51) George brings in creep, which of course plays an important role in stress relief, but this interpretation of the creep results leave much to be desired. Firstly, by using large cylinderical samples for the creep tests, he has introduced an unknown parameter, because the effective rates of drying of the cylindrical samples and a road pavement are not related. Secondly, since creep is moisture content- and time-dependent, any increase or decrease in the rate of drying will alter the creep curve. George carried out the creep tests after the samples were moist cured for 7 days, which is not realistic in the field.

When a soil-cement pavement shrinks, tensile stresses develop which, in turn, cause creep in tension. As creep behaviour in tension has been shown to be different from that in compression (66), it would seem that tension creep tests should have been used. George states that the measured creep in compression increases as the relative humidity decreases, meaning that increased drying promotes increased creep. His statement that higher shrinkage promotes higher creep is not borne out by the results obtained in this project where high density samples show high shrinkage, but low creep.

The Burger model and its use for representation of creep in soil-cement has been examined only to a very limited extent

7.1.2 (cont.)

by George. For instance, different cements and soils, and different mixes of soil-cement, would each have a characteristic set of creep curves, but they should all follow the general pattern of the Burger model, if it were applicable. From the work carried out in this project using soil-cement specimens made from two different soils, it was evident that the Burger model did not follow accurately the experimental creep curves (obtained for this project), but that creep could be predicted approximately by this model provided the stress was maintained constant. It should be noted that George[51] only considered a stress on the creep specimens equal to 50% of their ultimate 7 day compressive strength, whereas higher or lower stresses will certainly produce different creep characteristics.

Also in George's analysis the shrinkage rate has been assumed linear, but it is shown in this thesis (Chapter 9) that this is not valid. The shrinkage vs. time curve will, in fact, depend on the soil used for the soil-cement, the curing conditions, and the drying procedure. Generally, the curve starts with a low rate of shrinkage, which increases, passes through a point of inflexion, and then decreases (Figs 7.2 and 7.3).

George was able to find agreement between experimentally observed crack widths and his theoretical results, although one could not say that his approach to the problem was reliable because many of his assumptions were unrealistic.

In his third paper (52), George was apparently unaware of the work which had been carried out by Okada and Kawamura[98], and which used the same techniques, but to a much fuller extent. The comments made by George[52] on his theoretical study of

7.1.2 (cont.)

shrinkage stresses must be regarded as suspect because of the nature of his initial experimental results. This study did consider non-uniform drying within a soil-cement base, but George allowed for drying from only the top face of the slab, which must surely be extremely severe, as this is not likely to be encountered in practice, where the top surface is invariably sealed with an impervious bituminous running coat. It could be argued that these severe conditions were imposed on the model samples in order to demonstrate the different mix characteristics, but unfortunately, such severe drying can distort the results to the extent that they are of no real value.

Most of the comments made by George on "crack intensity" could have been predicted from fundamental characteristics of a soil-cement, except for the test run which had inclusions of aggregate particles in the soil-cement mix. The fact that inclusions of aggregate were found to increase the intensity deserves consideration and possible further study.

7.1.3 Review of Paper by Okada and Kawamura[98]

Okada and Kawamura carried out the following study in Japan, using ideas presented initially by Carlson[20] and Pickett[100] for non-uniform drying of concrete beams. Non-uniform drying must lead to a non-uniform stress distribution, which in turn may cause a failure in the material, under severe conditions. Concrete, like soil-cement, is not homogeneous or isotropic and does not obey Hooke's law, except perhaps under instantaneous strains.

Provided one accepts the assumption of both Carlson and Pickett that shrinkage is proportional to the moisture content,

7.1.3 (cont.)

the diffusion equation for a sample such as that shown in fig. (7.4) is given by

$$k \frac{\partial^2 s}{\partial y 2} = \frac{\partial s}{\partial t} \qquad \text{..... (7.2)}$$

The solution of equation (7.2) is found by using the probability integral

$$\frac{s}{s_\infty} = \operatorname{erfc}\left[\frac{1-\frac{y}{b}}{2\sqrt{T}}\right] - \operatorname{erfc}\left[\frac{1-\frac{y}{b}}{2\sqrt{T}} + B\sqrt{T}\right] e^{B(1-\frac{y}{b})+B^2T} \qquad \text{.... (7.3)}$$

where s = free unrestrained unit linear shrinkage strain

s_∞ = value of s when $t = \infty$

t = time in days

k = diffusivity coefficient of shrinkage

f = surface factor

x, y = co-ordinates

l, b = the dimensions of the specimen (fig. (7.4))

$B = fb/k$

$T = kt/b^2$

$$\operatorname{erfc}(u) = \frac{2}{\sqrt{\pi}} \int_u^\infty e^{-u^2} du$$

Okada and Kawamura used the same arguments and assumptions as Pickett[100] except that the simplest shrinkage equation, eq. (7.3) was used throughout.

They assumed that the diffusivity and permeability parameters were constant over the range of time considered so these variables could be eliminated and calculations greatly simplified. Consequently, the validity of the diffusion equation for representing the shrinkage as a function of time could be checked. The first few experimentally-obtained average shrinkage points were used to obtain the diffusivity and permeability parameters.

7.1.3 (cont.)

If these parameters were then assumed to be constant, the remainder of the average shrinkage curve could be calculated and this in turn could be compared with the experimentally obtained results. The results presented in their paper show a good comparison between experimental and theoretical average shrinkage curves. The free unrestrained shrinkage was calculated using equation (7.3), and by combining this with the observed shrinkage of a soil-cement prism and experimental creep results, the drying shrinkage stresses were calculated for a number of samples. Unfortunately, no comparison between predicted and actual stresses has been recorded. Creep results were obtained from cylindrical samples under various compressive loads, and the ultimate compressive strength of the soil-cement at various times was also obtained using cylindrical samples. The creep curves were plotted as creep strain versus the ratio of the applied stress to the seven day ultimate compressive strength. This ratio was represented by

$$\varepsilon_{1_{t=t_o}} = f\left(\frac{\sigma}{\sigma_f}\right)_{t=t_o} \qquad \ldots\ldots (7.4)$$

where $\sigma = \sigma(t)$ = sustained stress

$\sigma_f = \sigma_f(t)$ = ultimate compressive strength

By differentiating equation (7.4) and assuming that small strain changes produce only small stress changes over a short time interval, the change in stress from $t = t_o$ to $t = t_1$ is given by:

$$(\Delta\sigma)_{t=t_o} = \left(\frac{d\xi}{df}\right)_{t=t_o} (\sigma f)_{t=t_o} (\Delta\varepsilon)_{t=t_o} + \left(\frac{\sigma}{\sigma f}\right)_{t=t_o} (\Delta\sigma f)_{t=t_o} \qquad \ldots\ldots (7.5)$$

7.1.3 (cont.)

where $\xi = \sigma/\sigma_f$,

$(\Delta\sigma)_{t=t_o}$; infinitesimal diff. of stress σ at $t = t_o$

$(\Delta\varepsilon)_{t=t_o}$ " " " strain ε at $t = t_o$

$(\Delta\sigma_f)_{t=t_o}$ " " " failure σ_f " $t = t_o$

The stress at $t = t_1$ is

$$\sigma_{t_1=t_o+\Delta t} = \sigma_{t=t_o} + (\Delta\sigma)_{t=t_o} \quad \ldots\ldots (7.6)$$

where $\Delta\sigma$; change in stress at $t = t_o$.

The details of an actual calculation of stress from the experimental results may be found in Appendix (VIII).

7.1.4 Comments on Okada and Kawamura's Paper

Okada and Kawamura have adapted the techniques proposed by Carlson[20] and Pickett[100] for concrete to predict shrinkage stresses in soil-cement. If one uses the diffusion equation to represent shrinkage, one must assume that the shrinkage of a soil-cement sample is proportional to its moisture content. This assumption would be satisfactory while the soil-cement sample is moist but, once appreciable drying has taken place, the error rapidly increases. By solving the general diffusion equation (7.2) and assuming that the diffusivity coefficient and the surface factor are constant, equation (7.3) is derived. However, because the diffusivity coefficient and surface factor have been assumed constant, both across the sample and with respect to time, large errors in calculating the resultant free shrinkage must occur. If the permeability and diffusivity parameters (called surface factor and diffusivity coefficient by Okada and Kawamura) are taken to vary with suction then, as shown in Chapter 8, the flow of moisture in soil-cement can

7.1.4 (cont.)

be adequately represented by using the diffusion equation.

The following comments can be made, on points brought forward by Okada and Kawamura:

(a) There appears to be some confusion in this paper over sample curing times and drying times. The strength vs. time curves start at the time when the sample was compacted and the strength at this point is recorded as zero, although most samples have an appreciable strength after compaction. Both the strength and the shrinkage samples appear to have been moist cured only one day; shrinkage has been obtained on the second day and presumably extrapolated back to zero time to obtain the shrinkage of a prism at one day after compaction. On the other hand, the creep samples have been moist cured for seven days before loading, and as the zero time for the creep curves must be taken from the point of loading, i.e. after seven days moist curing, it could be concluded that these creep curves are not applicable to the behaviour of the shrinking soil-cement prisms. A sample moist-cured for 7 days will have a much higher strength than a sample just compacted, and the creep will be less than in the true sample.

(b) In the creep tests carried out by Okada and Kawamura, the rate of drying, the moisture contained in the sample and the non-uniform stresses which develop when drying occurs, all greatly influence the measured creep. Therefore these factors need to be taken into account before an accurate shrinkage stress analysis can be made. On page 89 of their paper it is stated that 20, 40, 60 and 80% of the 7-day moist cured unconfined compressive strength was applied to the creep specimens before

7.1.4 (cont.)

they were allowed to dry in an environment with a relative humidity of 80% and a temperature of 20°C. On the other hand, on page 115, it is stated that the shrinkage prisms were moist cured for one day, waxed, pins inserted and then allowed to dry at a relative humidity of 50% and a temperature of 20°C. The strength samples were probably dried under these same conditions. For plotting the creep curves of ε_t vs. σ/σ_f, the applied stress (σ) has been divided by the seven day moist cure strength (σ_f). As time passed, the applied load was maintained constant although the strength of the sample continued to increase. Therefore the σ/σ_f ratio should have been varied with time. In their theoretical analysis, Okada and Kawamura have allowed for this, in that the strength has been taken as a variable with respect to time, but the ε_t vs. σ/σ_f curve which is used in the theoretical analysis is incorrectly plotted from experimental results as mentioned above. Even if the creep curves had been plotted with the corrected stress ratio, the different moist curing and drying conditions which were used for the tests would have produced large errors.

(c) It is evident that a problem exists in relating the creep of a cylindrical sample drying at an unknown rate, as used by Okada and Kawamura, to the creep that would occur in an actual soil-cement pavement, especially when creep was actually measured in compression instead of in tension.

7.1.5 Review of a Paper by Kawamura[72]

Kawamura suggested that shrinkage stresses could be predicted by using a mechanical model to represent the visco-elastic effects, instead of using the experimental method proposed by Okada and Kawamura in the previous section. Many

7.1.5 (cont.)

investigators have in the past indicated that stress-strain relationships in concrete and soil-cement can be considered as visco-elastic. Lee[80] has stated that stress and strain in any linear visco-elastic body can be dealt with as in an associated elastic body, if time can be removed by the Laplace transform. Kawamura was able to solve for strain changes in a linear visco-elastic body represented by the Burger model, by using the formulae for elastic beams or slabs presented by Pickett[100]. Shrinkage has been expressed by transforming equation (7.3) to the following:

$$S/S_\infty = \text{erfc}(\beta/2\sqrt{t}) - \text{erfc}[(\beta/2\sqrt{t}) + \alpha\sqrt{t}]e^{\alpha\beta+\alpha^2 t} \quad \ldots\ldots \quad (7.7)$$

where $\alpha = f/\sqrt{k}$, $\beta = [(1-(y/b))]\ (b/\sqrt{k})$

With respect to fig. (7.4), the condition of compatibility for a long narrow beam can be written as follows:

$$\partial^2 e_x/\partial y^2 = 0 \quad \ldots\ldots \quad (7.8)$$

The resultant strain in the direction of the length (e_x) is defined as the sum of the free unrestrained shrinkage (S) and the strain (ε_x) produced by stresses, as represented by:

$$e_x = S - \varepsilon_x \quad \ldots\ldots \quad (7.9)$$

When the stress (σ_x) and strain (ε_x) can be represented by a single direction component x, the following linear visco-elastic relation can be written:

$$P(\sigma_x) = Q(\varepsilon_x) \quad \ldots\ldots \quad (7.10)$$

where P and Q are linear differential operators of the form:

$$P = \sum_0^P P_r \frac{\partial r}{\partial_t r} \ , \quad Q = \sum_0^q q_r \frac{\partial r}{\partial_t r}$$

7.1.5 (cont.)

By taking the Laplace transform of equations (7.8), (7.9) and (7.10) and the expressions derived by Pickett[100], the following equations for shrinkage stresses have been obtained by Kawamura:

For complete longitudinal restraint

$$\frac{\sigma'_x}{S_\infty E_1} = \frac{S}{S_\infty} - (A(t)e^{\Phi_1 t} + B(t)e^{\Phi_2 t}) \qquad \ldots\ldots \quad (7.11)$$

where $A(t) = [\frac{\Phi_1}{\Phi_1 - \Phi_2}](\varphi_1 + \varphi_2 + \frac{\varphi_1 \varphi_3}{\Phi_1})(I\beta_1 - e^{\alpha\beta} I\alpha_1)$

$$B(t) = [\frac{-\Phi_2}{\Phi_1 - \Phi_2}](\varphi_1 + \varphi_2 + \frac{\varphi_1 \varphi_3}{\Phi_2})(I\beta_2 - e^{\alpha\beta} I\alpha_2)$$

$$I\alpha_1 = \int_0^t e^{(\alpha^2 - \Phi_1)\tau} \operatorname{erfc}(\alpha\sqrt{\tau} + \frac{\beta}{2\sqrt{\tau}})d\tau$$

$$I\alpha_2 = \int_0^t e^{(\alpha^2 - \Phi_2)\tau} \operatorname{erfc}(\alpha\sqrt{\tau} + \frac{\beta}{2\sqrt{\tau}})d\tau$$

$$I\beta_1 = \int_0^t e^{-\Phi_1 \tau} \operatorname{erfc}(\frac{\beta}{2\sqrt{\tau}})d\tau$$

$$I\beta_2 = \int_0^t e^{-\Phi_2 \tau} \operatorname{erfc}(\frac{\beta}{2\sqrt{\tau}})d\tau$$

For restraint against warping only

$$\frac{\sigma''_x}{E_1 S_\infty} = \frac{S}{S_\infty} - (\frac{S_{av}}{S_\infty})[A(t)e^{\Phi_1 t} + B(t)e^{\Phi_2 t}] + (1/B)[C(t)e^{\Phi_1 t} + D(t)e^{\Phi_2 t}]$$

where $C(t) = [\Phi_1/(\Phi_1 - \Phi_2)][\varphi_1 + \varphi_2 + (\varphi_1 \varphi_3/\Phi_1)][I'_{\alpha 1} - I'_{\beta 1} + (2\alpha/\sqrt{\pi})I_{R1}]$

$$D(t) = -[\Phi_2/(\Phi_1 - \Phi_2)][\varphi_1 + \varphi_2 + (\varphi_1 \varphi_3/\Phi_2)][I'_{\alpha 2} - I'_{\beta 2} + (2\alpha/\sqrt{\pi})I_{R2}]$$

$$I'_{\alpha 1} = \int_0^t e^{(\alpha^2 - \Phi_1)\tau} \operatorname{erfc}(\alpha\sqrt{\tau}\, d\tau$$

7.1.5(cont.)

$$I'_{\alpha 2} = \int_0^t e^{(\alpha^2-\Phi_2)\tau} \operatorname{erfc}(\alpha\sqrt{\tau})d\tau$$

$$I_{R1} = \int_0^t e^{-\Phi_1\tau} d\tau$$

$$I_{R2} = \int_0^t \sqrt{\tau}\ e^{-\Phi_2\tau} d\tau$$

For no external restraint

$$\frac{\sigma_x}{E_i S_\infty} = \frac{S}{S_\infty} - \frac{S_{av}}{S_\infty} - (A(t)e^{\Phi_1 t} + B(t)e^{\Phi_2 t}) + \frac{1}{B}(C(t)e^{\Phi_1 t} + D(t)e^{\Phi_2 t}) + (6-12\ y/b)\left[\frac{2b}{3l^2}\ \frac{V_{max}}{S_\infty} - \left(\frac{1}{2B} + \frac{1}{B^2}\right)(C(t)e^{\Phi_1 t} + D(t)e^{\Phi_2 t}) + \frac{\alpha^2}{B^2}(K_1 e^{\Phi_1 t} + K_2 e^{\Phi_2 t} + K_3 t + K_4)\right] \quad \ldots\ldots (7.13)$$

where $K_1 = \dfrac{(\varphi_1+\varphi_2)(\Phi_1+\Phi_1\Phi_3)}{\Phi_1^2(\Phi_1-\Phi_2)}$

$$K_2 = -\left(\frac{(\varphi_1+\varphi_2)(\Phi_2+\Phi_1\Phi_3)}{\Phi_2^2(\Phi_1-\Phi_2)}\right)$$

$$K_3 = \varphi_1 + \varphi_2$$

$$K_4 = \frac{(\varphi_1+\varphi_2)(1+\Phi_1+\Phi_2)}{\Phi_1\Phi_2}$$

In order to use the above equations to compute shrinkage stresses, the shrinkage diffusivity coefficient and the surface factor, together with the constants of the Burger Model, must be determined from shrinkage and creep tests.

Kawamura used the constants obtained by Hansen[59] for

7.1.5 (cont.)

representing the Burger Model, and used the diffusivity coefficient of shrinkage and the surface factor from Picketts's[100] paper and thus computed tensile stresses on the outside surface of a concrete beam. The details of the constants used and the stresses obtained are shown in Table 7.1.

7.1.6 Comments on Kawamura's Paper[72]

With the use of a visco-elastic model, Kawamura was able to produce an analysis for shrinkage stresses which eliminated the extensive use of experimental creep data. It is not certain if Kawamura used a computer program to solve all the equations, as mention was made only of solving by computer the equations involving integrals, but the problem is readily computerized once creep is represented by a visco-elastic model. Even though Kawamura studied the shrinkage stress build-up only in concrete, it would appear that a similar technique should also apply to soil-cement.

The theoretical development of a high tensile stress on the drying surface of a concrete sample within the first two days, followed by a rapid decrease in this stress as indicated in Table 7.1, agrees with experimental observations for concrete (Pickett[100]). However, the stresses developed throughout the remainder of the concrete sample are extremely low, compared with the observed experimental results for soil-cement in this project. For concrete samples, this slow stress build-up within the sample, other than on the drying edge, would appear to be approximately correct, but for soil-cement, where the permeability of the materials is higher, shrinkage is appreciable even at the sealed face.

7.1.6 (cont.)

In the light of the comments made above, and the obvious advantage of using a shrinkage stress analysis which is readily amendable to mathematical treatment, it appeared desirable that this method should be examined using data obtained for loess and sandy pumice soil-cement. By representing creep by a mechanical model, the errors which occur in obtaining experimental creep curves are eliminated.

7.1.7 Review of Papers by Bofinger and Bofinger & Sullivan

Bofinger[14] attempted to allow for shrinkage stresses in his pavement design, but as he did not take creep or non-uniform stress distribution into account, the results obtained were of limited value. Nevertheless, his attempt to allow for a combination of shrinkage, temperature and flexural stresses, emphasises the importance of considering combinations of all possible stresses.

The paper by Bofinger and Sullivan[17] which was concerned only with moist curing of soil-cement, presents evidence of the rapid gain in strength and shrinkage which occurs soon after compaction of a soil-cement. The authors maintain that shrinkage cracking occurs only in the first few hours, and any cracking thereafter is likely to be brought about by traffic loading. As this observation was made after studying only one material, which contained a considerable quantity of clay, it may not apply to the many soil-cements which contain little or no clay.

Also, Bofinger and Sullivan suggest that creep may relieve some of the stress build-up, but they make no attempt to measure this creep.

7.1.8 Comments on Bofinger and Sullivan's Paper[17]

Bofinger and Sullivan carried out investigations into the cracking of a soil-cement pavement while it was being moist cured. Their observation that rapid early shrinkage occurred must not be taken too seriously, as these tests were carried out on only one soil-cement mix. As shrinkage was being measured only while samples were being moist cured, a non-cohesive soil-cement would not shrink at all, while a highly cohesive soil-cement would show appreciable early shrinkage.

The measurement of shrinkage on a necked shaped tension briquette specimen, as recorded in the paper, appears suspect. There is a distinct possibility that non-uniform shrinkage strains would have occurred in the large ends compared with the narrow centre section. The authors predicted early cracking in their soil-cement bases but stated that, since it was not observed, it may have been concealed by the bitumen membrane. If this was so, then the bitumen must be dispensed with when sealing an experimental pavement for examining shrinkage cracking. Most certainly a transparent, low strength material would be required. Possibly a very thin coat of clear epoxy resin or one layer of heavy duty polythene would serve to seal the top face of an experimental pavement, yet provide only minimal increase in strength to the pavement cross section.

Their suggestion that heavy traffic be used to promote closely-spaced early cracking of a pavement is quite good, provided that the blocks of pavements so isolated are durable enough at their edges to withstand the continuing movements caused by traffic loading. Also, if these closely spaced cracks are formed, then the design should be for a flexible pavement.

7.1.8 (cont.)

If this method of promoting early cracking is used, then the seal coat should not be applied until the crack pattern is complete.

An interesting comment on their second test length of soil-cement was that, after four months, the moisture content had risen from 18% to 18.6%, yet a bitumen membrane sealed the top surface and the lower face was sealed with polythene. Possibly osmosis occurred through the single sheet of polythene. If the moisture content actually increased, then one may wonder how shrinkage could have taken place; in fact, expansion should have occurred. When a cohesive soil-cement, such as that used by Bofinger and Sullivan[17] is moist cured, self desiccation occurs whereby moisture is lost from the clay lumps to the hydrating cement grains, and this moisture can not be released by heating to 105°C. Therefore, if no outward loss or gain of moisture occurred, a reduction in moisture content should have been recorded after 4 months.

Stress relaxation through creep was mentioned by Bofinger and Sullivan, but was not taken into account, because they considered that creep was insignificant for samples moist cured for 7 days or more. Unfortunately, this statement is very misleading. If shrinkage takes place after 7 days moist curing then stress build-up within the soil-cement base must continue with resulting creep. Naturally the magnitude of this creep depends on the soil used to make the soil-cement, as non-cohesive soils will not shrink while moist curing, but cohesive soil will. Also creep within the first 7 days of moist curing is appreciable; therefore, allowance for this creep needs to be made.

7.1.9 Review of a Paper by Pretorius and Monismith[108]

Pretorius and Monismith used finite element techniques in an attempt to predict shrinkage cracking in a soil-cement pavement slab. Firstly, details of shrinkage, creep and strength were obtained experimentally for all layers of a test pavement. Shrinkage strains were measured using a dial gauge mounted on a stand above the vertically placed sample. The sample was 76 mm square and 457 mm long, with 6 mm diameter by 76 mm long stainless steel bolts moulded co-axially with the sample, 38 mm into each end. Both total shrinkage and shrinkage rate increased with decreasing relative humidity, and the total shrinkage increased also with prolonged moist curing. Pretorius and Monismith also suggested that the early rapid shrinkage was caused by suction forces resulting from loss of capillary water, while the later (slower) shrinkage was caused by the loss of surface-adsorbed and inter-layer water.

For concrete, Pretorius and Monismith had noted that (Illson[66]) the rate of creep in tension was greater than that in compression. Therefore they decided to measure creep in tension at two different relative humidities. From the creep curves so obtained, relaxation moduli were calculated.

The strength of soil-cement was measured using the unconfined compression test, the direct tension test and the modulus of rupture test. No simple failure criterion was found to exist, for the cases of uniaxial and biaxial stresses. Changes in humidity affected the strength such that lower relative humidities had the effect of contributing initially to an increase in strength and then to a marked reduction. Also, the strength was found to increase with the period of initial

7.1.9 (cont.)

moist curing. Flexural strengths of dried specimens were found to be independent of the relative humidities which caused the drying.

When using the finite element technique, as a relaxation method Pretorius and Monismith made the following assumptions:

(1) Linear visco-elasticity was applicable over the entire strength range to failure.

(2) Structural continuity existed between all layers.

(3) The results from experimental work were applicable.

(4) Every crack penetrated the asphaltic concrete to its full depth immediately and also to some depth into the subgrade.

(5) Temperatures in the asphaltic concrete were assumed to vary from 87°F to 50°F through its depth.

If the pavement slab is subject to uniform shrinkage with depth, then the developed stresses depend solely on the restraint offered by the other layers. This has been considered as the lower bound solution. It is very unlikely that the uniform shrinkage case will cause cracking, but the differential shrinkage situation will represent the critical case. Because of the complications arising from use of variable relative humidities, desiccation was assumed to occur at a rate such that the result was regarded as an upper bound solution. By estimating the range of stress between the upper and lower bound solutions, the likely stress was estimated.

7.1.10 Comment on Pretorius and Monismith's Paper[108]

The use of the finite element technique seems to be an ideal way of predicting shrinkage stresses in a soil-cement

7.1.10 (cont.)

base as it can make allowance for the various changes which take place within a pavement over a period of time. This method would have been used in this project if time had permitted, but many parameters had to be obtained experimentally before the finite element technique could be used successfully as will be demonstrated below.

For the measurement of shrinkage, Pretorius and Monismith dried a 76 mm square by 457 mm long sample over a period of time. Unfortunately, the shrinkage in a large sample with non-uniform drying will be much less than in a small individual element of soil-cement curing under the same conditions. Apparently, no moisture content determinations were made as their sample dried; therefore a moisture content: shrinkage relationship could not be obtained. Similar criticisms could also be made about the creep and strength tests described in their paper.

Pretorius and Monismith do recognize that different results were obtained by drying soil-cement samples in different environments while under test, but the way in which the results have been presented seems to indicate a lack of appreciation for the effects of humidity gradients within a drying sample. The assumptions they made are also open to criticism. A linear visco-elastic model was found by George[51] to be inadequate for representing soil-cement behaviour, so he used the Burger mechanical model instead. But in this thesis the Burger model has also been shown to be inadequate for predicting creep accurately, (Section 9.1.8) so the use of a linear visco-elastic model (in this paper) would appear to over-simplify the problem.

The statement that the penetration of cracks through the

7.1.10 (cont.)

asphaltic concrete and into the subgrade occurs instantaneously should be accepted with some reservations. The asphaltic concrete will greatly restrain the shrinkage of the soil-cement base and tend to prevent cracking, but if closer spaced cracks do occur they will often not penetrate through to the surface of the asphaltic concrete, as the asphaltic concrete will flow to take up the sudden strain release in the soil-cement base. It is also unlikely that a crack will penetrate into the subgrade, but it is likely that the base will slide on the subgrade interface. This occurrence has been found in a number of reported field observations, and has been observed by the writer.

The analysis of both a uniform shrinkage case and a differential shrinkage case does not necessarily give the lower and upper limits of the stress. Pretorius and Monismith state that "desiccation will probably start at the surface and migrate slowly towards the interior", yet the surface of the soil-cement base slab is sealed by the asphaltic concrete, so that any loss of moisture from the top of the slab will be negligible. Moisture loss which does occur will probably be sideways through the shoulders, or downwards into the subgrade. By assuming that a particular relative humidity distribution exists within a pavement, one tends to preset the response course which the pavement must follow. The only reasonable method of estimating the relative humidity distribution within a pavement is to use the environmental conditions in conjunction with the material flow parameters and the diffusion equation. Work carried out for this thesis shows that moisture flow within either a soil-cement sample or a pavement slab can be predicted adequately using the diffusion

7.1.10 (cont.)

equation. Of the theoretical results presented in this paper, one could not say that they represented an accurate picture of the true stresses, mainly because the assumptions on which the theories have been based have been incorrect.

7.2 Experimental Work Carried Out to Check the Validity of the Above Theories

7.2.1 Papers by George

In the first two studies by George[50,51], the problem of shrinkage cracking was outlined and an approximate method for predicting cracking was presented. The third study (George[52]) considered the problem of cracking in soil-cement bases in considerably more detail. No tests were carried out in this project specifically to test the ideas presented in these papers, but from the comments made in section 7.1.2, it is evident that many of the fundamental assumptions must be in error.

The use of rapid drying has been shown in this thesis to produce undesirable effects; therefore, by considering a soil-cement slab drying from the top face, it would appear that the results so obtained would be misleading. George concluded by saying that a low moulding moisture content and high density should be used for a good soil-cement. The use of the low moulding moisture content is in agreement with the results obtained in Chapter 6, but the use of a high density is not. It could be expected, as explained in section 6.2.2.1, that increasing the density would increase the shrinkage.

7.2.2 Paper by Okada and Kawamura[98]

As the shrinkage stress analysis proposed by Okada and Kawamura showed great promise, the relevant parameters were obtained for both a loess soil-cement and sandy pumicesoil-cement. This data was then used to predict shrinkage stresses using the method proposed by Okada and Kawamura. Outlined below are the problems which were experienced in obtaining the correct data and with them, a comparison of the theoretical and experimental shrinkage stresses.

For the initial test run in this project for the shrinkage stress analysis, the measured shrinkage was obtained using two-side-drying prisms for both the loess soil-cement and the sandy pumice soil-cement. These prisms were of similar dimensions (76 mm x 76 mm x 286 mm) to that used by Okada and Kawamura. The unconfined compressive strength, tensile strength and creep characteristics were all obtained using a 38 mm x 44 mm x 102 mm sample drying from one 44 mm x 102 mm side, instead of the cylindrical specimens used by Okada and Kawamura. The 38 mm wide sample drying from one side was introduced because it was realized that there was no way of relating the creep of a cylindrical sample to that of a rectangular prism and the 38 mm wide sample was designed to represent the same drying depth as that in a 76 mm x 76 mm x 286 mm two-side-drying prism. It was expected that, by allowing the creep sample to dry at the same rate as the 76 mm x 76 mm x 286 mm prism, the creep would be more representative of the actual situation.

Using the above obtained experimental data, the calculations for shrinkage stresses were carried out on a computer, using the method proposed by Okada and Kawamura, and a curve of theoretical

7.2.2 (cont.)

average shrinkage was plotted. When this curve was compared with the experimentally obtained results, a marked discrepancy was apparent (fig. 7.5).

The accuracy of equation (7.3) for the determination of shrinkages over a large time period was investigated and found to be applicable for the first day only, according to the limits set by Pickett[100]. In order to reduce the computation time, Pickett proposed the following equation, together with their limitations for predicting the average shrinkage.

If $T > 0.05$ use equations (7.14) and (7.15)

$$\frac{S_{av}}{S_\infty} = \frac{1}{b}\int_0^b \frac{S}{S_\infty}\,dy = 1 - \sum_1^\infty e^{-T\beta_n^2} H_n \qquad \ldots\ldots \quad (7.14)$$

$$\frac{2b\,V_{max}}{3l^2 S_\infty} = \frac{1}{b^2}\int_0^b \frac{S}{S_\infty}\,y\,dy - \frac{S_{av}}{2S_\infty}$$

$$= \sum_1^\infty e^{-T\beta_n^2} G_n \qquad \ldots\ldots \quad (7.15)$$

where $H_n = \dfrac{2B^2}{\beta_n^2(B^2+B+\beta_n^2)}$

$$G_n = \left(\frac{1}{\cos\beta_n} - \frac{B}{2} - 1\right)\frac{F_n}{\beta_n^2}$$

$T = kt/b^2$

V_{max} = maximum deflection at $\frac{l}{2}$,

l = length of the prism.

Note that in order to solve equations (7.14) and (7.15) β_n needs to be obtained where

$$\beta_n \tan\beta_n = B = \frac{fb}{k} \qquad \ldots\ldots \quad (7.16)$$

7.2.2 (cont.)

A special subprogram had to be used to evaluate equation (7.16) because of the frequent use made of the values of β_n.

If $T < 0.05$ and $B > 5.0$ use equations

$$\frac{S_{av}}{S_\infty} = \frac{1}{B}\left[e^{B^2T}\varphi(B\sqrt{T})-1 + \frac{2B\sqrt{T}}{\sqrt{\pi}}\right] \qquad \text{..... (7.17)}$$

$$\frac{2bV_{max}}{3l^2S_\infty} = \left[\frac{1}{2B} + \frac{1}{B^2}\right]\left[e^{B^2T}\varphi(B\sqrt{T})-1 + \frac{2B\sqrt{T}}{\sqrt{\pi}}\right]-T \qquad \text{..... (7.18)}$$

where $\varphi = \frac{2}{\sqrt{\pi}} \int_x^\infty e^{-x^2} dx$

If $T < 0.05$ and $B < 5.0$ use equations:

$$\frac{S_{av}}{S_\infty} = BT\left[1- \frac{4}{3\sqrt{\pi}} B\sqrt{T} + \frac{1}{2}(B\sqrt{T})^2 - \frac{8}{15\sqrt{\pi}} (B\sqrt{T})^3+\right] \qquad \text{..... (7.19)}$$

$$\frac{2bV_{max}}{3l^2S_\infty} = \left[\frac{BT}{2} -T\left(1 + \frac{B}{2}\right)\left(\frac{4}{3\sqrt{\pi}} B\sqrt{T} - \frac{1}{2} (B\sqrt{T})^2+ \right.\right.$$

$$\left.\left. \frac{8}{15\sqrt{\pi}} (B\sqrt{T})^3\right)...\right] \qquad \text{..... (7.20)}$$

Using these limits and their respective equations the theoretical average shrinkage curve was calculated, but again it failed to correspond with the experimentally obtained curve (fig. 7.5). At this stage it was decided to introduce a diffusivity co-efficient which varied with respect to time, as this eliminated the worst assumption made by Okada and Kawamura. An examination of the existing method of evaluating the diffusivity co-efficient indicated that, if a material being tested had high shrinking properties, as does soil-cement, then Okada and Kawamura's method of evaluating and assuming constant the diffusivity co-efficient is totally inadequate. On the other hand, if a slow shrinking material, such as concrete, was being tested

7.2.2 (cont.)

then a constant diffusivity coefficient would not greatly affect the results of the shrinkage stress analysis. The only method at present available for obtaining the initial values of diffusivity co-efficient and surface factor is by using equation (7.3) and rearranging it into the form

$$\sqrt{k}\ x_1 t(1-0.752\sqrt{t}\ x_1 + 0.5t\ x_1^2 - 0.301t\sqrt{t}\ x_1^3 = b\frac{S_{av}}{S_\infty} \quad \ldots\ldots \quad (7.21)$$

where S_{av} is the average shrinkage of a sample such that $y/b = 0.50$ and $x_1 = f/\sqrt{k}$. By solving for x_1, both the diffusivity co-efficient and surface factor can be obtained. Just how accurate these values are remains to be seen because, as mentioned above, high shrinking materials such as loess soil-cement tend to cause problems, so that the limits set for the applicability of equation (7.3) as proposed by Pickett are not met when solving for loess soil-cement samples. By assuming that '$B = \frac{fb}{k}$', which can be obtained by evaluating equation (7.19) for the first two days, is a constant with respect to time then the theoretical and experimental average shrinkage curves can be matched by varying the diffusivity coefficient. The resulting diffusivity coefficients have been plotted against time (fig. 7.6). This method of obtaining variable diffusivity co-efficients can be subject to criticism on the grounds that equations (7.14), (7.17) and (7.19) were obtained from equation (7.2) by assuming that the diffusivity co-efficient was constant. Unfortunately, unless the diffusivity co-efficient is assumed constant, these equations cannot be derived.

As mentioned above, '$B = \frac{fb}{k}$' must be assumed constant

7.2.2 (cont.)

before variable diffusivity co-efficients can be calculated for use in equations (7.14), (7.17) and (7.19). Curves which have been obtained for unstabilized soils, for the relationship of permeability and diffusivity (equivalent to the surface factor and the diffusivity co-efficients for this analysis) to suction, have been shown by Richards[116] to be nearly parallel over a considerable suction range. Therefore as 'B' is the ratio of the surface factor to the diffusivity co-efficient, then 'B' must remain nearly constant .

When these variable diffusivity co-efficients are applied to the cross-section of a sample at any particular time, errors will again be evident, in that the drying face of the prism will be much drier, and will therefore have a lower diffusivity coefficient than the sealed side. Allowance was later made for this by matching the moisture content at a particular point on the cross-section of the prism with the moisture content of the average shrinkage vs. moisture content curve, and in this way the unrestrained shrinkage at any point on the cross section of the prism could be obtained with some degree of confidence. Using a series of these unrestrained shrinkages, the computer program then calculated the stresses at five points on the prism cross-section, as detailed in Appendix VIII and Fig. (7.7).

Again the calculated shrinkage stresses were completely in error when compared with the experimentally-obtained stresses. The use of experimentally-obtained creep curves unfortunately presents many problems and likely errors, but any alternative which has been suggested by research workers in this field seems to fail to produce the desired results. As commented on in

7.2.2 (cont.)

section 7.1.4, Okada and Kawamura plotted their creep curves using the seven day moist cured unconfined compressive strength as base, whereas in the actual creep tests, the strength must be continually increasing. If the creep curves of ε_t vs. σ/σ_f, were replotted with increasing strength (fig. 7.8), the curves moved closer to the vertical axis, so that as $t \rightarrow \infty$, $\frac{d\varepsilon}{df} \rightarrow 0$. In the early stages of drying, the error caused by plotting the creep curves with a constant strength was quite small, but the error increased until at 41 days the tensile stress on the sample surface, as indicated by Okada and Kawamura's method for restrained samples, was 22% lower than calculated by the increasing strength method for unrestrained samples. One might question the fact that the $\sigma/\sigma f$ ratio comes very close to the vertical portion of the ε_t vs. $\sigma/\sigma f$ replotted curves, while for the restrained samples, the $\sigma/\sigma f$ ratio does not even intersect the ε_t vs $\sigma/\sigma f$ curves after the first few days. The only explanation that can be offered is that the creep curves were obtained on samples which had been moist cured for 7 days and would, therefore, be stiffer than 1 day moist cured samples. Also, their creep results were obtained on large samples drying in a relative humidity of 80%, while their shrinkage prisms were dried at a relative humidity of 50%. Increased drying increases the creep, therefore it is evident that the recorded creep in the paper by Okada and Kawamura would be much lower than that which would actually have taken place in the soil-cement prisms.

After correcting the creep curves, using equation (7.14) instead of the less accurate equation (7.19) for predicting the

7.2.2 (cont.)

free unrestrained shrinkage, and using a variable diffusivity co-efficient, it was still evident that something was drastically wrong with either the hypothesis or the experimental data, because the stresses predicted for a fully restrained prism did not agree with those obtained experimentally from the samples restrained in the steel cradles. At this stage, it was decided to construct prisms half as wide as the 76 x 76 x 286 mm shrinkage prisms, and to allow them to dry from only one side, in the hope that the new results would be more applicable to the hypothesis. Of course, the two samples should ultimately predict the same stresses in a fully restrained sample, but the observed shrinkages would be different. It was this decision to examine a one-side-drying sample which brought to light a completely new problem without helping to solve the old one. When the length of the sample was measured with a 203 mm Demec gauge on a series of gauge points spaced across the sample from the drying face to the sealed face, it was found that the sample first curved concave towards the drying face, then straightened and curved concave towards the sealed face. The observed shrinkages for a loess prism are shown in fig. (7.9), while the deflected shapes of the drying face are shown in fig. (7.10). This so-called "strain reversal" will be discussed at greater length in a later section (section 9.3).

From the measured shrinkages for the one-side-drying sample, calculations for shrinkage stresses were again carried out, but again these results did not indicate the behaviour of a fully restrained sample, nor did they predict the resultant

7.2.2 (cont.)

average stress induced in it. At this stage, the hypothesis as it stands was set aside.

7.2.3 Paper by Kawamura[72]

Before calculating the shrinkage stresses in loess and sandy pumice soil-cement prisms, the equations presented by Kawamura were derived from his initial conditions in order to check their validity. When it was established that his equations were in fact correct, they were incorporated in a computer program which was designed to evaluate the shrinkage stresses as obtained by Kawamura.

The results obtained from the computer program did not correspond with those presented by Kawamura as shown in fig. (7.11). As analytical methods were required to solve Kawamura's equations in the computer program it was decided that perhaps the particular method used in this project was inaccurate. Consequently, three different subroutines were developed to solve Kawamura's equations, but the results obtained by them all were identical yet completely different from Kawamura's results. The values of the free unrestrained shrinkages obtained for this analysis using the diffusion equation, (upon which the shrinkage stress predictions are dependent) were confirmed as correct when compared with the tables presented by Pickett[100]. The only conclusion is that Kawamura's calculations are incorrect.

Nevertheless, shrinkage stress predictions were carried out using the above computer program. Only the average stress build-up within the loess and sandy pumice soil-cement prisms (figs. (6.8) and (7.12)) had been obtained experimentally;

7.2.3 (cont.)

therefore any comparison between theoretical and experimental results necessarily involved the average stress across the sample rather than the individual stresses at different points within the prism. Firstly, shrinkage stresses were predicted for the loess soil-cement using a computer program based entirely on Kawamura's equations, and these are plotted as the lower curve in fig. (7.11) for the force in the sample. The program was then modified to permit variable diffusivity co-efficients to be used, and again the average force in the sample was calculated; this is also plotted in fig. (7.11). Then the diffusivity co-efficient, as originally calculated for the first shrinkage stress analysis, was multiplied by 3.0 and 4.0, with the results shown in fig. (7.11).

It is evident by comparing all the curves in fig. (7.11) that the original equations as proposed by Kawamura were totally inadequate for predicting shrinkage stresses in a restrained soil-cement sample. Even the analysis using a modified diffusivity co-efficient did not predict either the corrected rate or the magnitude of stress build-up, but it was a considerable improvement on the original analysis. When the original constant diffusivity co-efficient was multiplied by 4.0, a good match of experimental and theoretical curves was achieved. Unfortunately, this method of obtaining a theoretical stress curve similar to the experimental one is completely artificial, with no grounds to justify a multiplication factor of 4.0. Therefore, a new method of shrinkage stress analysis should be developed.

7.2.4 Paper by Bofinger and Sullivan[17]

No specific tests were carried out to prove or disprove any of the work carried out by Bofinger and Sullivan, as the work in this thesis is concerned mainly with volume changes associated with drying. Nevertheless, volume change during the period of moist curing is of great interest, as this curing period may prove to be cricital for cracking.

One may query the conclusions reached in this paper, in the light that only one soil-cement mix was studied. The use of a full size soil-cement base, which can be cured under desired conditions, has many advantages, but many of the results presented should be treated with suspicion, because of the unexplained phenomena which were mentioned in section 7.1.8.

7.2.5 Paper by Pretorius and Monismith[108]

Again no specific testing was carried out to investigate any of the proposals put forward in this paper, but many of the comments made in section 7.1.10 were based on experimental results obtained in the routine testing for this thesis. Probably the most important point is that a hypothesis is only as good as the initial data on which it is based. In this particular case, the initial data is definitely suspect, although the theoretical approach is basically a sound one. Further work using the finite element technique is definitely warranted.

7.3 Summary

The two main problems associated with the above studies on shrinkage stresses in soil-cement pavements have been either over-simplification of the stress analysis or incorrect interpretation of the initial parameters. Nevertheless, the studies

7.3 (cont.)

carried out by Okada and Kawamura[98] and Kawamura[72] provide a sound base on which a new hypothesis for shrinkage stress analysis can be built. On the other hand, Pretorius and Monismith[108] have used the finite element technique satisfactorily, but have failed to correctly evaluate their initial conditions. The finite element technique should be ideal for predicting stresses within a soil-cement slab, but the understanding of drying processes of a soil-cement and its creep under stress has not yet been sufficiently developed to enable the finite element technique to be used to best advantage.

CHAPTER EIGHT

MOISTURE FLOW IN SOIL-CEMENT

The moisture content is without doubt the most important parameter for comparing the characteristics of soil-cements, yet little investigation of the connection has been made by other research workers. There are two ways in which the moisture contained in a pervious material can be expressed. In the first method, the measurement is of the mass of moisture retained in a material, while in the second method the measurement is of the energy of retention of the moisture retained in the material. As the mass of moisture retained within a sample is easily measured, it has in the past been almost the only measure of moisture content in engineering investigations; the mass of moisture is usually expressed as a percentage of the dry mass of the material. Unfortunately, moisture contents defined in this way tend to be extremely variable over small distances in a supposedly uniform continuous medium, and they rarely provide information on the likely flow patterns of the moisture. In the second way of expressing the moisture content, normally referred to as "the suction", the negative pressure with which the moisture is retained in a soil is balanced against the water vapour pressure in the soil's environment.

Before one can attempt to predict the flow of moisture in a soil-cement, one must have both a suitable mathematical model to represent this flow and appropriate flow parameters for the particular soil-cement. As these flow parameters are energy functions, it is obvious that the moisture contained in

a soil-cement must be expressed in compatible terms before it can be used in the mathematical model representing moisture flow. Fortunately, moisture content can be related uniquely to suction in any soil, and the relationship between them may be readily obtained for any particular material. Thus, once the moisture content of a material has been obtained, then the corresponding suction can be found, and vice versa. This enables the continuing use of moisture content determinations in both the laboratory and the field, and eliminates the need for regular and time-consuming suction determinations.

For natural soils, research workers have shown that the diffusion equation, which is analogous to heat transfer in a body, adequately predicts moisture flow in these soils provided the moisture content of the soil is expressed through the energy-dependent variable suction, and provided suitable flow parameters are obtainable. The suction-moisture content relationship and the moisture flow parameters must be obtained by experimentation.

8.1 Determination of the Suction versus Moisture Content Relationship

The moisture content expressed as a percentage of the dry mass is not readily amendable to mathematical analysis, unless the moisture contained in a sample is measured in terms of its suction. In very dry soils, the suction may exceed 70,000 kPa, while in soils which are in equilibrium with a free water surface, the suction will be close to zero.

Schofield[126] introduced the pF scale, which expressed the suction as the common logarithm of the height in cm of a water column which the suction would support. The relation

8.1 (cont.)

between pF and relative humidity is shown in fig. (8.1).

The available techniques for determining the suction of a natural soil and the working range of each technique are listed in Table (8.1). Croney et al[30] have described most of the conventional methods used for determining suction, but more recently the development of psychrometric apparatus (Ref. 115) to measure suction has brought about a marked change in testing techniques. The psychrometer consists of a wet and dry bulb thermometer placed in an atmosphere in humidity equilibrium with the soil. Evaporation of water takes place from the wet bulb at a rate dependent on the ambient humidity. The temperature of the wet bulb then drops until the heat loss owing to evaporation equals the heat gain by radiation convection and conduction from the surroundings. The temperature difference, i.e. the wet bulb depression, has been shown to be linearly related to the humidity and hence to the total suction. Unfortunately, the psychrometric apparatus appeared difficult to set up and expensive to build, so it was not considered further, but in retrospect it would have eliminated many of the problems which were encountered when conventional equipment was being used. Because of the lack of time and money, the vacuum desiccator and pressure membrane methods were adopted to cover the range of pF from 1.0 to 7.0. The vacuum desiccator method covers the range pF 4.5 - 7.0, while the pressure membrane method covers the range pF 1.0 - 4.5. The solute concentrations for the loess and sandy pumice soil-cements were very small, so the separate portions of the suction moisture content curve obtained from the vacuum desiccator and the pressure membrane methods

8.1 (cont.)

coincided, to give a continuous curve. The vacuum desiccator method measures the total suction, including any solute suction, but the pressure membrane method measures soil suction only, and ignores any solute suction.

The equipment used for determining the suction versus moisture content curve is described in Appendix IX, together with the test procedures. The suction versus moisture content curves for loess soil-cement and sandy pumice soil-cement are shown in figs. (8.2) and (8.3) respectively, while the suction versus moisture content relationships for the natural sandy pumice and Horotiu subgrade are shown in figs. (8.4) and (8.5) respectively.

8.1.1 Vacuum Desiccator Method

The principle of the vacuum desiccator method is that a sample is placed in a controlled humidity environment, so that moisture exchange between sample and environment takes place until equilibrium is reached. The humidity of the environment above an aqueous solution of sulphuric acid is related to the concentration of the acid. Different concentrations of sulphuric acid are used for successive tests. The vacuum desiccator equipment is normally simple to use, but a number of problems were encountered in this study. Firstly, the equilibrium time of 4 days, as recommended by Croney et al[30], was too short for samples in the lower suction range. It was found that in the lower humidity range two weeks were required for clayey soil-cement to come to equilibrium. It is therefore recommended that for a sample of 4 gm or less, the equilibrium point should always be checked before the sample

8.1.1 (cont.)

is exposed to the next humidity. Secondly, a problem was encountered in the use of rubber connectors between the desiccators and the main vacuum line (fig. 8.6). Tubing clips on rubber tubing were used to isolate the desiccators from the main vacuum line, but the tubing tended to become permanently deformed by the tubing clip. This deformation was aided by the vacuum in the line so that the rubber connector remained sealed when the clip was released. A ground glass stop-cock is recommended for future use.

8.1.2 Pressure Membrane Method

The pressure membrane cell works on the following principle: water is forced from the soil sample by gas pressure of up to 1500 kPa applied to one face, while the opposite face remains in contact with a pervious membrane. This membrane is similar to plastic sausage skin; it allows water to pass, but prevents the passage of gas. Provided the membrane material is maintained wet and its pore size is sufficiently small to prevent the collapse of the water menisci in the pores at the gas pressure used, it is suitable for pressure membrane cells. Full details of the cell and of the test procedure are given in Appendix IX.

In using these cells, a number of problems were encountered. The initial design was based on the pressure membrane cell of Aitchison et al[2], where the body of the cell was made of perspex (fig. 8.7). The perspex body has the advantage that one can see the accumulation of diffused gas as it collects around the porous stone above the membrane. Unfortunately, it is difficult to make a satisfactory pressure connection to perspex, so the

8.1.2 (cont.)

bottom half of the cell, to which the gas pressure is applied, should have been made of brass. The gas pressure was provided by a nitrogen cylinder, and the pressure on each cell was topped up each day to compensate for loss of gas by diffusion through the membrane. The method of building up the pressure each day was time consuming, and led to loss of accuracy in determining the equilibrium moisture content. A recommendation, which may warrant consideration in any future work with pressure membrane cells, would be the use of either a pressure regulator or a pressure compensator. The compensator could consist of a cylinder containing a piston, loaded by a dead weight. The appropriate weight would exert the desired pressure, and any loss of gas through the membrane would be compensated for by the vertical displacement of the piston in the cylinder.

As no manufactured membrane material was locally available, different makes of sausage skins were tried for membrane material, but proved useless as the sausage skin would break down even under low gas pressure. Eventually a special high grade visking membrane was imported from the United States. This visking membrane proved fully satisfactory.

Provision is necessary for flushing out the top of the cell to remove any diffused gas, as the membrane must be kept wet at all times to prevent gas passing through it. The flushing device finally adopted is illustrated in fig. (8.8(a)).

When using high pressures, a good sample-to-membrane contact is required, as an appreciable part of the total moisture transfer is in the vapour phase. This greatly increases the time required to reach equilibrium and also increases the

8.1.2 (cont.)

susceptibility of the test to temperature changes. By surrounding the cells with polystyrene foam beads and running the test in a constant temperature room with control of $\pm$ 0.5°C, it was possible to keep temperature effects within acceptable limits.

8.2 Determination of the Permeability

Before the diffusion equation can be used to predict moisture flow in unsaturated soil-cement, the permeability and diffusivity parameters of the material must be obtained. The diffusivity parameter is defined as the product of the permeability and the slope of the moisture content-suction curve.

Attempts to determine the permeability of a soil in the laboratory have brought forward many complicating factors. Gardner[48] was the first to use the results obtained from outflow data in which he plotted the flow in cusecs against time to obtain an outflow curve. Gardner used the pressure membrane cell to produce the outflow curve, but unfortunately did not allow for the impedance offered by the membrane itself. Later research workers such as Miller and Elrick[86], Rijtema[119] and Richards & Richards[118] have attempted to calculate membrane impedance.

Kunze and Kirkham[78] took extreme care during the early stages of obtaining their outflow data, and were able to account for the total boundary impedance during their test. The use of data from the initial portion of the outflow curve would necessarily be more reliable as air duffusion would affect the later outflow data. Kunze and Kirkham for their method of determining permeability, had to find the ultimate outflow Q_∞ by experiment. For clayey soils this would take many months.

Richards[116] suggested that the method used by Kunze and Kirkham be modified by obtaining Q_∞ from early outflow data

8.2 (cont.)

and the theoretical outflow curve. This value of Q_∞ may only be approximate, but the time involved in measuring Q_∞ and the likely errors owing to vapour loss from the apparatus warrants the use of this modified method. Details of the method used in this project are given in Appendix X.

8.2.1 Theory for Permeability Test

The relevant theory required to apply Richards' method is reproduced below.

The equation defining the outflow at any time t is:

$$\frac{Qt}{Q_\infty} = 1-2\sum_{n=1}^{\infty} \frac{h^2 l^2}{\alpha_n^2[hl(hl+1)+\alpha_n^2]} e^{\frac{-D\alpha_n^2 t}{l^2}} \quad \ldots\ldots \quad (8.1)$$

where Qt = outflow at time t

Q_∞ = ultimate outflow at $t = \infty$

hl = ratio: impedance of sample/impedance of membrane or plate

l = length of sample

α_n = solutions of ($hl = \alpha' \tan \alpha'$)

D = diffusivity

Equation (8.1) can be plotted as log $(\frac{Qt}{Q_\infty})$ versus log $(\alpha_1^2 \frac{Dt}{l^2})$ giving a family of curves for varying values of 'a' $(= \frac{1}{hl})$ fig. (8.9), where $(\alpha_1^2 \frac{Dt}{l^2})$ is the dimensionless reduced time τ. By plotting log Qt versus log t as an overlay of the experimental data and by matching the curve with those in fig. (8.9), an estimate can be made of 'a' and 't_{RP} ($\tau = 1.0$).' Special emphasis should be place on the matching of the initial outflow data and the tail. From 'a', α_1^2 can be determined, therefore $D = \frac{1.01^2}{\alpha_1^2 t_{RP}}$

8.2.1 (cont.)

and the permeability

$$K = D\frac{\partial\theta}{\partial P} = \frac{DQ_\infty}{V\Delta P} \qquad \ldots\ldots \quad (8.2)$$

where $\partial\theta$ = volumetric water content

∂P = pressure of suction increment

V = volume of sample

Q_∞ is determined from the difference in the scales of the experimental results, compared with the theoretical curves.

8.2.2 Apparatus

Initially the permeability cells used were similar to the pressure membrane cells used for the suction determinations (fig. 8.7), and were similar to those used by Aitchison et al[2]. However, many problems were encountered in the use of this particular design, and the cell was progressively modified, as shown in fig. (8.8). The following points deserve mention:-

(1) After flushing the cell, water in the small diameter reading tube tended to cling to the inside of the tube and different quantities of water were left clinging to the tube after successive flushes with the same volume of water. This was overcome by using a wetting agent in the flushing water, which broke down the surface tension so that globules of water did not cling to the sides of the glass reading tube.

(2) To flush the porous stone adequately to remove all air bubbles, it was found necessary to displace approximately 20 ml of water, but as a 3 mm internal diameter tube was considered necessary for measuring the very small changes in the water outflow, this meant that a 2.86 m high tube was necessary to accommodate the displaced water. This long tube was eliminated

8.2.2 (cont.)

by enlarging the top of the normal 300 mm length of 3 mm diameter tube.

(3) A small gap was left between the stone and the sides of the perspex cell to facilitate the accumulation of air bubbles and their easy access to the reading tube.

(4) The flushing device had to be modified many times before it functioned satisfactorily. In its early form, a rubber bulb with a capacity of over 20 ml was used for flushing the cells. Through the centre of this bulb was passed a glass tube with a number of small holes in the section containing the bulb, fig. (8.10). Above the bulb was a stop-cock to allow for adjustment of the reference mark. It was discovered, after a considerable time, that air bubbles being moved by flushing tended to travel up the flushing tube and become trapped inside the rubber bulb where they could not be seen. Therefore, one could never be certain if the correct volume of water was being measured.

The next modification placed the rubber bulb on a separate branch tube, fig. (8.8(b)), so that the air was never able to reach the rubber bulb. This again did not prove entirely satisfactory, as the rubber bulb appeared to alter its volume with time, so it was decided to build the third version, shown in fig. (8.8(c)). In this version, the rubber bulb operates entirely in air, with the set volume of water always below the bottom stop-cock. The two stop-cocks were found necessary to control the flushing and the reference water level. This final permeability cell proved extremely successful when the perspex base was replaced by a brass base with a flexible connection to

8.2.2 (cont.)

the manometer board. A high pressure gas hose was used as the flexible coupling, thus allowing the cell to be turned upside down to avoid resaturation of the sample when the pressure is released from the cell, before the cell is dismantled. The manometer was connected permanently to the permeability cell, as shown in fig. (8.11), but again the problem of pressure loss over a period of time required periodic attention. The use of a compensating device, as described in section 8.1.2 for pressure membrane cells would be justified. Also suggested by Richards, the incoming nitrogen was passed through a humidifier before coming in contact with the sample in the permeability cell, thus preventing loss of moisture from the sample to the nitrogen.

8.2.3 Results

Any results obtained using pressures greater than 140 kPa proved worthless, because of the rapid rate at which nitrogen diffused through the membrane. Below this pressure it was found that the results could be obtained with a reasonable degree of confidence, provided a set procedure was followed. It was found in this project that the following points should be considered before adopting a test procedure. As the outflow immediately after applying the pressure increment is appreciable, many readings should be taken within the first half hour. To be certain that no flushing errors occur within this time, the cell should be flushed just before the pressure increment is applied. As water continues to flow down the inside of the reading tube over a period of time, it is necessary to apply correction factors to all the readings obtained within the first half hour,

8.2.3 (cont.)

as flushing cannot be done during this period. By obtaining a curve of the change in meniscus height with respect to the time after flushing, using a perspex disc in place of the usual sample, only the flow down the inside of the tube is recorded. The readings obtained in an actual test are then reduced using this curve to produce true readings of the loss of moisture from the sample over a period of time.

Over the 2 day period adopted for obtaining readings for each pressure increment, evaporation from the enlarged chamber at the top of the reading tube presents a source of error. This is overcome by stretching a damp cloth, connected to a jar of water, over the mouth of the chamber.

As the specimens were held for only two days at each pressure increment, the ultimate outflow Q_∞ could not be determined experimentally. Instead, Q_∞ was estimated using Richards' method, with particular attention paid to the initial portion of the outflow curve and the tail. In the experimental work carried out, there was no difficulty experienced in using Richardsmethod to obtain Q_∞. Permeability determinations were made on loess soil-cement and sandy pumice soil-cement samples as well as on samples of the natural sandy pumice and of the subgrade from Silverdale Road in Hamilton. Unfortunately, the results obtained from the soil-cement samples were scattered and appeared to be too low. This was probably owing to further hydration of the cement which would have occurred when the moisture content of the samples was being raised to saturation. The natural sandy pumice and subgrade material produced good results, as shown in fig. (8.12) and fig. (8.13).

8.2.4 Field Diffusivity Parameters

A comparison of diffusivity parameters obtained in situ and in the laboratory, as presented by Richards[116], indicates the possible error which can result from using laboratory obtained results to predict moisture flow in the field. The discrepancy between field and laboratory results should be small for soil-cement, unless cracking has occurred. In natural clay soils, large cracks may exist in the field, but these are avoided when obtaining small samples for laboratory tests. Therefore, the laboratory-obtained diffusivity parameters are representative of only small sections of soil, and these may be separated by cracks, along which water migration is facilitated. This brings forward the point that diffusivity parameters would be better if they were obtained in the field, as suggested by Richards[116] using observed field suctions at different times.

8.3 Inverse Differential Water Function

The inverse differential water function $\frac{\partial h}{\partial \theta}$ (h) is the gradient of the suction-volumetric water content curve at any suction, and it was evaluated using the suction-moisture content curve, with moisture contents expressed in volumetric terms or from the outflow data obtained from the permeability cells. For both the natural sandy pumice and the Horotiu subgrade, the inverse differential water functions were obtained from outflow data, with the resulting curves shown in figs. (8.14) and (8.15).

On the other hand, the inverse differential water functions for both the loess and sandy pumice soil-cement samples were obtained from the suction versus moisture content curves (figs. (8.17) and (8.16)) because it was felt that the permeability

8.3 (cont.)

determinations, and consequently the outflow curves, were unreliable, as explained in section 8.2.

8.4 Measurement of Moisture in Soil-Cement

8.4.1 Moisture Content Profiles in Laboratory Samples

For any theoretical prediction of moisture flow in soil-cement samples to be acceptable, it must give good agreement with experimentally obtained results on samples whose size and boundary conditions correspond to the mathematical model. Ideally, nondestructive determination of moisture contents is required, using either psychrometric probes or gamma rays. It was found that the psychrometric equipment, though reliable, would have been costly to build, and would have required a great deal of time to perfect the appropriate techniques, and the gamma ray method has been found unreliable for accurate research. As the moisture content of a sample was required at many positions within a sample at different ages, the only course open was to make many identical samples and at different times, to break each sample into small portions, find the moisture content of each, and so determine the moisture gradients. The samples needed to be broken and not cut or sawn, to avoid the generation of heat, and a guillotine, fig. (8.18), was built which would break the samples at any desired position. The fracture obtained was found to be extremely clean provided blunt cutting edges were used.

Soil-cement samples were dried under different conditions and moisture content profiles were obtained for different drying times under each condition. The testing program covered the

8.4.1 (cont.)

following sample sizes and conditions: sandy pumice soil-cement and loess soil-cement samples 76 mm x 38 mm x 286 mm drying from one 76 x 286 mm face, and 76 mm x 76 mm x 286 mm samples drying from two opposite faces. Also, a number of road cross-sections were modelled in loess soil-cement, 152 mm deep and 600 mm long. These were placed in completely sealed glass containers with sand on the bottom and side, as shown in fig. (8.19).

8.4.2 Measurement of Suction in the Field

No field suction determinations were made for this project, but a brief outline of an accepted technique seems worthy of mention. For determination of the field diffusivity parameter, suctions at different times must be recorded, using gypsum block moisture meters. Basically, these consist of a pair of electrodes embedded in a porous block, whose water content (and hence electrical resistance) is determined by the pore size distribution in the element, the external suction and the previous moisture history. Ordinary dental gypsum plaster is used as the porous medium.

With a suitable mix of gypsum plaster, a block can be made with a pore size distribution which will determine suctions in the range pF 2.5 - 4.5. The blocks deteriorate with time, but are reliable when new. Other types of blocks such as nylon do not deteriorate, but they are less sensitive to moisture changes.

8.5 Mathematical Modelling of Moisture Flow

8.5.1 General Theory

The theory of moisture flow in soils is extremely complex, but assumptions may be made to simplify the mathematics. The flow of water in saturated soil under a potential gradient may be expressed in terms of the diffusion equation. In civil engineering, the simplest form of its use is for the representation of consolidation in one direction using

$$\frac{\partial u}{\partial t} = C_v \frac{\partial^2 u}{\partial z^2} \qquad \ldots\ldots \quad (8.3)$$

where u = excess pore pressure

and C_v = coefficient of consolidation.

In contrast to this special case of consolidation, the general circumstances of transfer of water in soils may involve two-dimensional or three-dimensional flow in a two- or three-phase medium (soil solids, water, air) owing to potential gradients arising either from natural causes or from engineering effects e.g. environmental conditions and weights of buildings respectively.

By generalising Darcy's law, the following equation can be obtained for flow in three dimensions.

$$V_x = -K_x \frac{\partial \psi}{\partial x}, V_y = -K_y \frac{\partial \psi}{\partial y}, V_z = -K_z \frac{\partial \psi}{\partial z}$$

where K_x, K_y, K_z are the permeabilities in the x, y, z directions and V_x, V_y, V_z are the macro flow velocities in the x, y, z directions, Klute[77], used the law of conservation of mass to deduce the equation for isothermal liquid phase flow:

$$\frac{\partial \theta}{\partial t} = \nabla(K \nabla \psi) \qquad \ldots\ldots \quad (8.4)$$

8.5.1 (cont.)

where θ = volumetric water content

$$\nabla = \left(\frac{\partial^2}{\partial x^2} + \frac{\partial^2}{\partial y^2} + \frac{\partial^2}{\partial z^2}\right)$$

ψ = $h + z$ = total potential

h = suction

z = height above datum

As h and K are single value functions of θ

$$\frac{\partial \theta}{\partial t} = \nabla(D\nabla\theta) + \frac{\partial K}{\partial z} \qquad \text{.....} \quad (8.5)$$

where $D = K \frac{\partial(-h)}{\partial z}$ ..... (8.6)

The poly-phase equation can similarly be derived, but the constants and variables required in the equation cannot be obtained from existing experimental techniques.

Consider the equation in terms of diffusion of potential

$$\frac{\partial \theta}{\partial \psi}\frac{\partial \psi}{\partial t} = D(K\nabla\psi) \qquad \text{.....} \quad (8.7)$$

where $K = K(\psi)$.

Substituting for ψ, the diffusion equation is obtained:

$$\frac{\partial h}{\partial t} = \frac{\partial h}{\partial \theta} \nabla(K\nabla(z-h)) \qquad \text{.....} \quad (8.8)$$

Any technique for measuring flow parameters must involve the vapour and adsorbed phase terms; therefore, equation (8.8) may be adopted with a fair degree of confidence. This equation is non-linear and can therefore probably best be solved by using a finite difference method.

Limitations and accuracy of equation (8.8) can be listed as below.

8.5.1 (cont.)

(1) If the flow parameters cannot be measured accurately, the equation is worthless.

(2) Sharp suction gradients cannot be dealt with acceptably.

(3) If soils contain large amounts of soluble salts these affect the suction.

(4) The diffusion equation is temperature dependent because of changes in humidity with temperature.

(5) No allowance is made for non-homogenous or non-isotropic soils.

(6) The equation does not model the hysteresis which is observed when a soil is cycled between wet and dry.

Of the above limitations, the adequate prediction of the flow parameters would be the most important. Sharp suction gradients are only likely to occur if a pavement is flooded, and since most soils contain low solute concentrations, resulting errors in suction determinations from this cause are small. Changing temperatures will effect moisture migration, but this is related more to changing temperatures throughout the day and is not a long term effect. The difference between vertical and horizontal flow parameters can be allowed for in the analysis, so that non-isotropic and non-homogenous conditions are reasonably well covered and therefore not a serious limitation on equation (8.8). In most incidences of moisture change within a road pavement, equilibrium is normally reached by either moisture loss or moisture gain without cycling changes, therefore hysteresis is not a major problem.

8.5.2 Numerical Analysis of the Diffusion Equation

In order to solve equation (8.8), only three parameters are required, namely the suction (h), the permeability (K(h)) and the inverse differential water function ($\frac{\partial h}{\partial \theta}(h)$). Both K(h) and $\frac{\partial h}{\partial \theta}(h)$ are dependent on time; therefore, they are not single-valued functions of the suction h. Using the forward difference technique, equation (8.8) can be expressed for two-dimensional flow in a finite difference form:

$$\Delta h_5 \simeq \frac{\Delta t}{(\Delta l)^2} C_5[\bar{K}_1(h_1 - \Delta l - h_5) + \bar{K}_2(h_2 - h_5)$$

$$+ \bar{K}_3(h_3 + \Delta l - h_5) + \bar{K}_4(h_4 - h_5)] \qquad \ldots\ldots \quad (8.9)$$

where $\bar{K}_1$ = mean permeability for h_1, etc.

h_5 is the suction at the point considered

C_5 is the $\frac{\partial h}{\partial \theta}$ at the point considered.

h_1, h_2, h_3 and h_4 are suctions at adjacent points of the mesh respectively above, right, left and below point 5, as shown in fig. (8.20). The following stability criterion is needed so that control of time and length increments will provide meaningful results in equation (8.9).

$$\frac{\bar{K}\Delta t}{(\Delta l)^2} C_5 < 0.5 \qquad \ldots\ldots \quad (8.10)$$

The main problem when applying equation (8.9) is to determine the flow parameter and to define the boundary conditions accurately.

The suction-moisture content relationship can be adequately determined by the methods described in section 8.1, from which the results obtained may be regarded as reliable. The only other

8.5.2 (cont.)

method for obtaining permeabilities is by using the moisture content profiles for different drying times within a soil-cement sample. Richards[116] suggested that the diffusion equation could be expressed in the finite difference form, where the permeability and diffusivity do not vary significantly over the spacing of the points 1-5, so that

$$\Delta h_5 = \frac{D\Delta t}{(\Delta l)^2} (\bar{h}_1 + \bar{h}_2 + \bar{h}_3 + \bar{h}_4 - 4\bar{h}_5) \quad \ldots\ldots \quad (8.11)$$

where h_5 is the suction of the reference point 5

D is the diffusivity at h_5

t is time

Δl is the spacing of points 1-5

$\bar{h}_5$ is the mean suction at point 5

$\bar{h}_1$-$\bar{h}_4$ are mean suctions at points 1-4 at distances Δl from point 5 along the two axes (fig. 8.20).

Equation (8.11) can be rewritten as follows to give the diffusivity:

$$D = \frac{\Delta h_5 (\Delta l)^2}{\Delta t (\bar{h}_1 + \bar{h}_2 + \bar{h}_3 + \bar{h}_4 - 4\bar{h}_5)} \quad \ldots\ldots \quad (8.12)$$

By considering the flow in a given period of time past a point where there is a particular suction, a suction versus diffusivity curve can be constructed. This method was used in this thesis for obtaining the diffusivity versus suction curves for loess soil-cement and sandy pumice soil-cement (figs. (8.21) and (8.22)), but owing to the variability of the experimental results, it was soon evident that at least 100 diffusivity points for different suctions were required before a reasonable curve could be constructed. The variability of the experimental results is

8.5.2 (cont.)

not caused by faulty laboratory techniques, but rather that the soil properties are very sensitive to small changes.

8.5.3 Comparison of Theoretical and Experimental Results

In order to test the two-dimensional finite difference form of the diffusion equation for representing moisture flow in soil-cement samples, a number of prisms were dried under controlled conditions of evaporation and air humidity, and records were kept of moisture content with respect to time as they dried. A computer program was then prepared, to solve the above equation and so to predict the moisture content profiles within each particular prism studied using the known flow parameters of the soil-cement and the known air humidity and evaporation rate.

The evaporation rate from a free water surface was determined by using a perspex box, which had the same dimensions as the 76 x 286 mm drying side of a soil-cement prism. This was partly filled with water and placed in the same environment in which the samples were dried. Water loss from inside the perspex box was found by weighing, and was recorded with respect to time after conversion to an evaporation rate expressed in cm/sec. The theoretical moisture content profiles for loess soil-cement prisms are shown in figs. (8.23) and (8.24) and for sandy pumice soil-cement prisms in figs. (8.29) and (8.30).

8.5.3.1 Moisture Flow in Small Soil-Cement Samples

By experimentally determining the moisture content profiles across 286 mm x 76 mm x 38 mm soil-cement prisms and 286 mm x 76 mm x 76 mm soil-cement prisms after they had been exposed to

8.5.3.1 (cont.)

known environmental conditions, a basis was made for comparison with theoretically-obtained moisture content profiles. These experimentally obtained moisture content profiles were used in the shrinkage stress analysis (section 9.2.1). It was found that experimental moisture content profiles must be extremely reliable to be usable in the shrinkage stress analysis.

8.5.3.1.1 Loess Soil-Cement Prisms

The loess soil-cement prisms, with a drying face width of 76mm were dried in the curing room at a temperature of $27\frac{1}{2}^{o}C$ for 12 hours of the day and $0^{o}C$ for the other 12 hours. Details of the curing room can be found in Appendix III while the appropriate environmental conditions are given in Table (8.2). A large loess soil-cement sample with a drying depth of 304 mm was permitted to dry in the constant temperature room at $20^{o}C$ and relative humidity of 58%. This large soil-cement sample was restrained between bulkheads in order to permit shrinkage stresses to develop, and the age at which the first crack developed and the moisture content profile at this time were also recorded. This moisture content profile was plotted in the direction of the moisture flow. Later these results were compared with the theoretically obtained moisture content profile, as shown in fig. (8.25).

Examination of the moisture content profiles for the 38 mm wide and 76 mm wide samples (figs. (8.26), (8.27)), shows that the theoretical moisture flow program is capable of predicting moisture flow in small samples of soil-cement, with considerable accuracy.

8.5.3.1.1 (cont.)

From these results, it would seem that, for a loess soil-cement, the diffusion equation is adequate for predicting moisture flow at least to within reasonable experimental error. One may question the use of the experimental moisture content profiles obtained from the small soil-cement prisms to estimate the permeability function of the loess soil-cement, but if the use of this permeability function is extended to larger samples, it is evident that accurate predictions of moisture content profiles can be achieved. Naturally, the best way to test the permeability function obtained from small prisms would be to use it to predict moisture flow in a full size soil-cement road base, and to compare those results with experimentally recorded moisture content data. Unfortunately, time did not permit the building of a full size soil-cement base, but a model road cross-section as discussed in section 8.5.3.2 was the largest sample built. This loess soil-cement cross section had a drying width of 608 mm and a drying depth of 152 mm (fig. 8.19), so that moisture flow was occurring in two dimensions only. As shown in fig. (8.28), the experimental and theoretical results for this model cross-section show good agreement, indicating that the permeability functions determined from the 76 mm wide prism are applicable for larger samples.

The advantages of using a small sample to determine the permeability function are as follow:

(a) Moisture flow in both the adsorbed state and the vapour phase is accounted for.

(b) The permeabilities are determined perpendicular to and parallel to compaction planes in a soil-cement with material properties identical to those of a full sized soil-cement base (fig. 8.33).

8.5.3.1.1 (cont.)

(c) Simple tests are used for finding the permeability of soil-cement whereas the conventional method for determining the permeability of a soil is lengthy and much more complicated.

8.5.3.1.2 Sandy Pumice Soil-Cement Prisms

The prisms of sandy pumice soil-cement were dried in an atmosphere of nitrogen in a large sealed perspex box, which was kept in the constant temperature room at 20°C. The nitrogen surrounding the soil-cement prisms was dehumidified by sodium hydroxide flakes in trays placed in the perspex boxes. These trays were washed out and refilled each day, followed by a complete flushing of the perspex box with dry nitrogen. The environmental conditions inside the perspex box are given in Table (8.2).

No large sandy pumice soil-cement samples were built for determining the moisture content profiles because of the limited time available, and because of the success which was achieved in theoretical representation of the moisture flow in the large loess soil-cement samples. For the small sandy pumice prisms, a comparison of the theoretical and experimental results is given in fig. (8.31) for the 38 mm wide specimen and fig. (8.32) for the 76 mm wide sample. Again the theoretical moisture content profiles figs. (8.29) and (8.30), closely represented the moisture content profiles from experiments, except in the later stages of drying; after 20 days there was a discrepancy between the results in both the 38 mm and the 76 mm sandy pumice soil-cement specimens, especially near the sealed edge of the samples. As mentioned in section 9.2.2, an error in the plotting of the

8.5.3.1.2 (cont.)

experimental moisture content profiles is quite likely to cause some discrepancy, but it is more than likely that the main source of error is in the permeability versus suction curve. At low suctions, any error in this curve does not greatly influence the resulting moisture flow, but in regions of high suction a small error in the permeability results in moisture flow predictions which are slightly in error. As the permeability in the high suction range is considerably smaller in magnitude than the permeability in the low suction range fig. (8.22) , it is evident that any error in a low permeability will influence the moisture flow characteristics more in the regions of high suction than in regions of lower suction. This source of error is likely to account entirely for the discrepancy between experimental and theoretical moisture content profiles presented in this thesis.

The rate at which a soil-cement sample dries is dependent on the evaporation rate at the drying face of the sample and on the inverse differential water function. This evaporation rate was determined by measuring the loss of water from a free water surface, as mentioned in section 8.5.3. As the rate at which the evaporation was set in the theoretical prediction compared very closely with the evaporation rate for the experimentally obtained moisture contents on the drying face, it is evident that the value of the inverse differential water function used in the theoretical analysis, must be correct.

No properly-laid pavement is likely to dry out rapidly or completely; therefore, only small suction changes are ever likely to occur. As the theoretically predicted moisture

8.5.3.1.2 (cont.)

contents appeared to be extremely reliable in the lower suction range and under small suction changes, it is evident that the diffusion equation as used for the small prisms should be quite satisfactory for predicting moisture changes in a soil-cement base. Further, from a comparison of the theoretically and experimentally obtained moisture content profiles for both loess soil-cement and sandy pumice soil-cement, it can be seen that the diffusion equation can be used successfully on soil-cement made from two widely different soils. This suggests that the diffusion equation can be applied to soil-cement made from other types of soil intermediate between these two extremes. The loess soil-cement samples were moulded at a lower moisture content than the sandy pumice soil-cement samples, so drying times for the two sets of samples were different, the sandy pumice samples taking considerably longer to dry than the loess soil-cement samples. No sample from either soil type was dried completely, as it was felt this would be unrealistic in the light of normal environmental conditions which would exist in the field. Over approximately the first half of the drying, close agreement between theoretical and experimental results was evident for both soil-cements. However, in the later drying stages, the loess soil-cement tended to dry more slowly near the sealed face than was predicted by the theoretical approach, the reverse being true for the sandy pumice soil-cement. It seems that the presently-determined permeability functions are slightly incorrect in the region of higher suctions, the loess permeability function being too high and the sandy pumice permeability function too low.

8.5.3.1.2 (cont.)

Errors such as this are inevitable when using the experimental results obtained from small soil-cement samples to obtain the permeability function, especially in the later stages of drying, where moisture changes are small and occur almost entirely in the vapour phase. The only apparent way to improve this method for obtaining the permeability function would be to improve both the drying techniques for soil-cement prisms, as suggested in Chapter 9, and the method for measuring the moisture content profiles with respect to time. The drying techniques can easily be improved, but accurate measurements of the moisture content profiles is not so easy. By using psychrometric equipment, accurate determination of moisture content profiles might be possible, but the presence of a number of probes in a soil-cement prism, and their effect on the moisture flow, would need to be carefully considered.

8.5.3.2 Moisture Flow in a Loess Soil-Cement Model Road

In order to test the mathematical model for predicting the movement of moisture in soil-cement samples much larger than the small prisms considered above, a model cross-section of soil-cement pavement slab 152 mm deep and 610 mm long was placed in a completely sealed glass container and surrounded by sand on the bottom and one edge, as shown in fig. (8.19). This model simulated the cross-section of an actual pavement slab cut along its centre line and the sand represented the subgrade. All complicating factors such as water table and surface evaporation were eliminated in order that the theoretical prediction of the movement of moisture should be as simple as

8.5.3.2 (cont.)

possible.

The subgrade sand had a suction of 10^7mm of water, i.e. pF = 6, and the soil-cement model cross-section was compacted at the same moisture content as for the smaller prisms described in section 8.5.3.1, so that the permeability function would be the same for both. Conditions and material properties applying to the experimental samples were then used in the mathematical model to predict the moisture content profiles at one-day intervals of drying. A comparison of the experimental and theoretical results obtained after 40 days' drying is shown in fig. (8.28), this being the average from two identical samples. Unfortunately, sharp suction gradients exist at the sand/soil-cement boundary, and these distort the relaxation field in the computer solution.

The forward difference technique used to represent the diffusion equation became unstable in areas of sharp suction gradient or when the stability criterion, equation (8.10), was violated. Where sharp suction gradients occur, the following modifications were found necessary to allow moisture movements to be predicted by numerical methods.

(1) The element length was adjusted to align points in the mathematical model on the soil-cement sand boundary.

(2) If the initial soil-cement suction was used as the initial suction at the soil-cement/sand boundary, it was found that a large suction gradient occurred in the highly permeable sand, and this created instability in the system. If, on the other hand, the initial suction at the soil-cement/sand boundary

8.5.3.2 (cont.)

were taken as the initial suction of the sand, then the soil-cement, with a much lower permeability than the sand, reacted more slowly to the sharp suction gradient and was therefore able to buffer the initial rapid moisture changes, and the system remained stable.

(3) At the soil-cement/sand boundary, special attention had to be paid to the material in which the forward point was situated, so as to relate the appropriate inverse differential water function at the forward point to the permeability function for the remaining points in that material. This meant that special equations were required to represent the materials at the soil-cement/sand boundary.

After carrying out these modifications to Richards' moisture flow program which is described in Appendix XI, satisfactory results were obtained, as shown in fig. (8.28), even with the presence of large suction gradients. A situation with such large suction gradients as experienced in this model would be extremely unlikely to occur in the field, except perhaps in the case of flooding, where a saturation front would be moving through the material and therefore the conditions modelled would be much more severe than are likely in practice. Note that large suction gradients are only a mathematical problem and not physical.

8.6 Predicting the Likely Moisture Flows Under a Road Pavement

The loss of moisture by evaporation from a soil-cement pavement, either through the top face before a seal coat has been applied, or from the shoulders, greatly influences the development of shrinkage stresses in the base. Also any change

8.6 (cont.)

in the water table level causes movement of moisture either into or out of the soil-cement base, and this in turn influences the expansion and contraction of the base. In order to predict the long-term performance of a soil-cement base, it is necessary that any moisture movements in the base can be predicted theoretically.

Richards carried out a study of moisture movement under a pavement surfacing by using the diffusion equation to predict moisture flow in the pavement slab in both vertical and horizontal directions. This study, which is briefly outlined in Appendix XI, indicated that, for the particular site chosen by Richards, his theoretical predictions closely resembled those observed in the field. However, before any such theoretical moisture flow predictions can be attempted, a considerable amount of information is required:

(1) The moisture content at which each layer of the pavement is placed must be known.

(2) The moisture content versus suction, and the permeability versus suction relationships must be obtained experimentally.

(3) As moisture flow in a pavement may occur in either or both the saturated and unsaturated states, any permeability prediction involves moisture flow in both these states.

(4) A changing water table quite often plays a major role in influencing the moisture profile, while the environmental conditions such as rainfall, humidity and evaporation govern moisture movement near the surface.

8.6 (cont.)

(5) The constituents of a pavement are extremely important in that the type of shoulder material will determine the rate at which evaporation from the pavement will occur.

(6) The seal coat will either permit or prevent evaporation, while the moisture contents at which the sub-base and subgrade are placed will influence the equilibrium of the pavement layers.

(7) The presence of vegetation, drains, hills and depressions will also cause moisture movement, although their effects are rather unpredictable and can be neglected in preliminary studies.

Once information about all these points has been collected, it should be possible to use a computer program similar to that used by Richards[114] to predict moisture movement. Unlike the Australian conditions used by Richards, many parts of New Zealand quite often have a high water table, therefore the lower boundary of any computer program for predicting the moisture profiles will most certainly be influenced by seasonal changes in the height of the water table.

8.6.1 Richards' Moisture Flow Program

A copy of Richards' computer program was run on the IBM 360/44 computer at the University of Canterbury, using the data presented by Richards for the Horsham road site in Australia. This took twenty-two minutes to simulate the moisture conditions after fifty-two weeks at ten runs per week, and indicated a much slower running time than experienced by Richards using a CDC 3200/3600 computer, in which 100 weeks took nine minutes.

8.6.1 (cont.)

In an attempt to improve Richards computer program, modifications were made so that the most recently-calculated data was used to update the permeability values. Unfortunately, little was gained by upgrading the data, and this was at the expense of large amounts of computer time. Consequently, this method was discontinued.

By reducing the permeability arrays in Richards' computer program, a great deal of storage was saved. In the case of the horizontal permeabilities, the value calculated at any step was required only in the next step and it could thereafter be removed from storage. On the other hand, the vertical permeabilities must be stored in a one-dimensional array, sufficient to cover all points across the section.

Richards[114] has not mentioned any sensitivity analysis which he may have carried out on his moisture flow program. Consequently, a number of trials were carried out on the program to test the sensitivity of the method to changes in evaporation, permeability, cycle time, and layer properties. Firstly, the evaporation rate was doubled, which resulted in the top of the shoulder rapidly drying out, while only a small change in suction was recorded at the second element below the shoulder surface. Below this second element no change in suction was recorded. This probably means that the permeability of the shoulder and its surrounding material was so low that the system was unable to cope with an unrealistically high evaporation rate. Possibly this also indicates an internal check built into the method, such that both the evaporation and the permeabilities of the material must be in the correct ranges for the particular

8.6.1 (cont.)

field situation. Otherwise, this situation will result in a rapid suction rise in the zone exposed to evaporation without any effect on the material under it. Similarly, if the permeability used was low by a factor of ten, then again rapid drying would occur at the surface only. On the other hand, if the permeability was high by a factor of ten, then instability was found to occur at the lower right corner of the model.

As the moisture changes in Richards' study pavement occurred quite slowly, it was apparent that the number of cycles required per week could possibly be reduced. By running the program at one cycle per week, a very slight difference in suctions resulted compared with those presented by Richards for ten cycles per week. For between two and ten cycles per week, identical results were obtained, so the program for the IBM 360/44 was set to run at 2 cycles per week, which resulted in a considerable time saving.

When using Richards' computer program, if fictitious properties were substituted for the actual layer properties, suction changes of the expected magnitude did occur. This indicated that the technique used by Richards was sufficiently sensitive to property changes, and that it should be adequate for predicting moisture changes at road sites.

Richards' use of the natural suction profile in the subgrade soil to set up the initial suctions at the road site seems unusual, because each layer of a pavement would be compacted at a suction not related to that of the natural soil profile. The initial suctions in the pavement slab should be obtained for his program from the moisture contents at which the

8.6.1 (cont.)

pavement layers were constructed, and the natural suction profile of the subgrade should be used only for determining the initial suctions below the pavement construction and outside the shoulder.

The humidity of the soil may be related to the suction by the well-known thermodynamic relation

$$h = \frac{RT_a}{Mg} \log_e \frac{H}{100} \qquad \text{.....} \quad (8.13)$$

where h = suction

R = gas constant

T_a = the absolute temperature

M the molecular weight of water, and

H the relative humidity.

It must be remembered that variations in temperature will change the soil humidity (equation (8.13)). Richards[114] has assumed the temperature remains constant at 20°C, while in fact it varies greatly from this especially near the surface. Possibly by using an average temperature of 20°C the long term effect will be negligible, but over one summer or winter period an appreciable error is inevitable.

The evaporation from the shoulder of a road has been expressed by Richards[114] as

$$e_{shoulder} = E_{sat} \left(\frac{H-H_a}{100-H_a}\right) - I \qquad \text{.....} \quad (8.14)$$

where E_{sat} = evaporation from a free water surface

H and H_a are the relative humidities for soil, moisture and atmosphere respectively.

I = infiltration.

8.6.1 (cont.)

Unfortunately Richards has used

$$e_{shoulder} = E_{sat}(H-H_a)-I$$

in his computer program, but the air humidity was always less than 80% at his Horsham road site, then the value of $(100-H_a)$ would be relatively large compared with the 1.0 implied by the approximation. Consequently, the true evaporation would have been much larger than was implied by his method.

Richards has stated that when the general difference equation used for representing moisture flow (equation (8.9)), is applied to the boundary between two soil layers, it is only approximate and may in some cases distort suction gradients across the boundary. Nowhere in his paper is there mention of how to deal with this boundary problem, and his computer program indicates that equation (8.9) has been applied across soil boundaries regardless of its implications.

When preparing a road site for simulation by finite difference model, the decision on whether to place the node points on the two soil interfaces or straddling them poses a real problem. After making a computer run with different layers of materials, it was evident that special equations were required to represent the soil elements adjacent to the soil interface. As Richards' computer program stands, the suction at point 'X' fig. (8.34) would be represented as follows: at this point the inverse differential water function refers to the soil with $K_1 = 2$. All the permeabilities except in the J-1 direction will refer to the layer in which $K_1 = 2$. On the other hand, the permeability in the J-1 direction refers to the soil in which $K_1 = 3$ and should therefore not be multiplied by the inverse differential water

8.6.1 (cont.)

function for the $K_1 = 2$ layer. Consequently, special equations are needed to overcome this problem at boundaries between different materials.

8.6.2 Predicted Moisture Flow in an Existing Road

As time for this project was limited, it was not possible to build a full-scale road pavement for the study of moisture movement and shrinkage cracking; therefore an existing road was adopted for study. This pavement is situated in Hamilton City and forms part of Silverdale Road.

8.6.2.1 Details of Silverdale Road

The cross-section of Silverdale Road is shown in fig. (8.35). The base is constructed of cement-stabilized sandy pumice, while the sub-base is unstabilized sandy pumice material. The subgrade changes four times in the section under study, but over most of its length it consists of Horotiu sandy loam. The details of the materials used in the road may be found in Table (8.3). The environmental conditions for the road site were obtained from a nearby agricultural research station and are shown in fig. (8.36).

As mentioned, the subgrade changed four times along the length of Silverdale Road. It would seem reasonable to assume that a changing subgrade could greatly affect the shrinkage of the soil-cement base, so as this study was carried out after Silverdale Road had cracked, it meant that the crack patterns could be measured for the portions of the road founded on different subgrades. The analysis was confined to the two main subgrades, Horotiu sandy loam and Te Kowhai clay loam. Crack spacing over the length of road which was founded on Te Kowhai clay loam

8.6.2.1 (cont.)

subgrade averaged 5.65 m, while crack spacing over the Horotiu sandy loam subgrade was found to average 2.98 m. The road section considered was level, and other conditions over the length of the road were very similar.

8.6.2.2 Results from Silverdale Road

A computer program Appendix XV was developed to predict the likely moisture changes which would have taken place after the pavement was constructed, and the array used for representing Silverdale Road is shown in fig. (8.34). The flow parameters used in this program have been described in section 8.1, 8.2 and 8.3, while the environmental conditions are referenced in section 8.6.2.1.

In coding up the physical dimensions of Silverdale Road for the computer program, a mesh size of 130 mm was adopted, and allowance was made for a base, sub-base and subgrade. For the internal boundaries between pavement layers, special equations were needed to represent adequately the moisture flow across them, as mentioned in section 8.6.1. Laboratory tests carried out for this project showed the seal coat to be impermeable, but the shoulder, on the other hand, was susceptible to evaporation and atmospheric humidity, and to run-on and run-off of water from rainfall. The evaporation, humidity and rainfall were represented by 4th order equations, as shown in fig. (8.36), and the temperature was assumed constant at 20°C for the purpose of determining the humidity of the soil at any time. The lower boundary of the model was set below the lowest level recorded for the water table, so that once the position of the water table

8.6.2.2 (cont.)

was established, suctions at all mesh positions below this level (fig. (8.37)) would be set to pF = 1.0. As the subgrade was a sandy material, it was highly likely that the water table would influence the soil above it up to and including the zone influenced by climatic changes. For the purpose of this program, climatic changes were assumed to influence the top 104 mm of soil. At the left boundary of the model, the initial suctions were evaluated by assuming that the water table set the suction values up to the level of climatic influence. At this level, an expression similar to that used by Richards for his natural suction profile was applied to the section just below the climatic influence zone, because there was insufficient suction information available for the natural soil profile from Silverdale Road. The right-hand boundary of the model is located at the centre line of the road, and (assuming no transverse subsurface drainage), may be considered as a mirror line reflecting the other half of the road. Below the pavement slab, the water table again set the suctions up to the climatic influence line and thereafter the following equation was used:

$$\Delta h_5 = \frac{\Delta t}{(\Delta l)^2} C_5 [\bar{K}_1 (h_1 - \Delta l - h_5)$$

$$+ \bar{K}_3 (h_3 + \Delta l - h_5) + \bar{K}_4 (2h_4 - 2h_5)] \qquad \ldots\ldots \quad (8.15)$$

Using this model and the boundary conditions set out above, the computer program was used to predict the moisture changes which were likely to have occurred throughout 1965, under Silverdale Road. The soil-cement pavement was at its driest state on the 6 July with the suction profiles shown in fig. (8.38). After this time water infiltration through the shoulders increased the suctions under the pavement.

CHAPTER NINE

PROPOSED METHOD FOR SHRINKAGE STRESS PREDICTION

Of published research on shrinkage stress prediction, only the work of Okada and Kawamura[98] and Kawamura[72] appeared worth pursuing. The relevant information was obtained for both loess soil-cement and sandy pumice soil-cement in order to check the accuracy of the methods suggested by Okada and Kawamura and by Kawamura. These methods did not give correct results and it is likely that they failed because the authors ignored the effect of the moisture content parameter on shrinkage, creep and strength changes. However, both methods do give an adequate base from which to develop a new method for soil-cement behaviour.

Because the rate of drying of a sample depends on its size, it is evident that shrinkages obtained from small samples will be greater than the shrinkages obtained from large samples for the same period of drying. Therefore, any experimental data used in an equation to predict shrinkage stresses must depend not solely on time, but also on a parameter which is the same in a small test sample as in a large prism for which shrinkage stresses can be predicted.

The only parameter considered adequate to fit this condition is the moisture contained in a particular element of soil-cement at any one time, be this parameter the actual moisture content expressed as a percentage of the dry mass, or the suction representing the energy of retention of the

water in the soil-cement. To enable the moisture content of a soil-cement sample to be obtained by prediction, a careful examination of the flow of moisture through natural soil was made as described in Chapter 8.

It is evident that both moisture content and time may influence shrinkage, creep and strength changes, therefore these parameters must first be investigated before any shrinkage stress prediction method is proposed.

9.1 Additional Experimental Results

Before the formulation of a new method for shrinkage stress prediction could be completed, a number of additional experiments were required to clear up uncertainties resulting from uncontrolled variables. In this section, a brief outline of these experiments is presented, together with the results which they provided; details of the experiments can be found in Appendix XII.

9.1.1 Effect of Carbonation

Carbonation is the reaction between free lime in concrete or soil-cement and atmospheric carbon dioxide. It was found by Verbeck[138] to play an important role in changing the shrinkage characteristics of concrete, especially near the surface. At 100% relative humidity, carbon dioxide did not readily diffuse into the pores of the concrete, because they were saturated with water, and carbon dioxide had to dissolve in this water before it diffused inwards. At low humidities, only small quantities of free water were available, so carbonation did not occur easily, but at intermediate relative humidities, the shrinkage was greatly increased by carbonation. The tests also

9.1.1 (cont.)

indicated that sample size had very little effect on shrinkage in a carbon dioxide free atmosphere, but in an atmosphere containing carbon dioxide, shrinkage was greatly affected by sample size. Verbeck's drying shrinkage curves in carbon dioxide-free air were interesting, in that they showed that provided the sample was restrained against deflecting, its size did not affect the shrinkage at a predetermined relative humidity. This meant that, as assumed in this thesis, drying did not affect the ultimate shrinkage, although the shrinkage was controlled by loss or gain of moisture. Unfortunately, Verbeck recorded only an average shrinkage for all the samples, instead of recording shrinkages across a one-side drying prism, which would have provided much more information on differential shrinkages, and the effect on shrinkage of atmospheric carbonation at the drying face could have been obtained. As a result, it was decided to investigate the effect of carbonation on soil-cement.

The equipment used is shown in fig. (5.2). Equal flows of air at room temperature were passed over identical samples, but one flow had the carbon dioxide removed from it first. The results obtained for the loess soil-cement samples indicated less shrinkage on the drying face for the sample drying in air containing carbon dioxide, while over the remainder of the thickness the shrinkage was the same for both samples. For the sandy pumice soil-cement samples, the shrinkage values at corresponding points were identical.

This indicated that the shrinkage of a porous sandy material would not be affected by carbonation, while that of a

9.1.1 (cont.)

fine-grained soil-cement would be slightly affected on the drying surface only. Qualitative chemical analyses of specimens exposed to atmospheric carbon dioxide showed only a slightly higher concentration of the carbonate ion at the drying face for both types of soil-cement.

9.1.2 Calcium Ion Migration

It was thought that the water movement taking place during drying might carry soluble calcium ions towards the drying face. Qualitative chemical analyses for the presence of calcium ions showed no enrichment of the drying face of either the loess or the sandy pumice soil-cement.

9.1.3 Moisture Movement Under Load

Movement of moisture in a sample under load proved difficult to measure, because water moved internally from a point under stress to a point of lower stress; thus, the sample retained the same overall moisture content (although some of the absorbed water had moved within the sample.)

From numerous tests, it was discovered that a sample under stress dried at a faster rate than an identical unstressed sample, and this occurred under both tensile and compressive stresses. Also, the greater the imposed stress, the faster the sample dried. This finding further complicated the prediction of moisture movement using the diffusion equation, since if a sample was dried while restrained in such a way as to induce shrinkage stresses, these stresses would then increase the drying rate.

9.1.4 Moisture Content Determination

Moisture content determinations on soil-cement are difficult to standardise, because of cement hydration. When a moist soil-cement sample is placed in an oven to dry at the usual temperature of 105°C, hydration of the cement is greatly accelerated by the raised temperature. Provided sufficient water is present, the effect of the higher temperature is to cause more rapid combination of water with the cement, and this chemically-bound moisture is not driven off by heating to 105°C. Normal oven drying is rapid with the sample being placed in the oven at 105°C and dried to constant mass. In an alternative slow drying method, a sample is permitted to dry in an environment at 20°C and relative humidity of 53% for at least one week before oven drying at 105°C. From tests carried out for this project, it was found that the moisture content obtained by the slow drying method was up to 3½% higher than that obtained by the rapid drying method.

Once the humidity of the samples dropped below 90%, the difference between the two methods was negligible. Therefore, if true records of the moisture contents of samples are to be obtained, it is recommended that the samples should first be air-dried for a week at room temperature and then oven-dried at 105°C. Unfortunately, this discrepancy was not discovered until late in this research project, and small errors have resulted, but corrections have since been made to allow for the discrepancies.

9.1.5 Hydration

The stage at which hydration either ceases or produces

9.1.5 (cont.)

only minor further changes is of some interest, since drying combined with continuing hydration would produce additional complications in the shrinkage stress analysis. However, from the tests carried out (Appendix XII), it is evident that hydration continues at a reducing rate as a soil-cement sample is moist cured; after 7 days moist curing 90% of the total hydration has taken place. Also, it is found that once drying is initiated and not halted, hydration of the cement does not appear to continue, although this observation may not apply to an actual soil-cement pavement, where the curing conditions are not necessarily the same as in the laboratory. The usual curing conditions in the field involve water curing for up to seven days, then a seal coat is provided. During the period of watering, it is very unlikely that moisture loss will occur from the surface of the pavement slab, in fact it is quite possible that the pavement slab will absorb extra water, in which case the hydration rate will increase. By the time drying is permitted, it can safely be assumed that nearly 100% of the hydration will have taken place. Also, if the pavement temperature is above normal, as can easily occur on a hot summer day, hydration will proceed faster.

9.1.6 Surface Temperature Effects

The temperature below a bitumen seal, even in New Zealand, may rise to 60°C on a hot summer day (104). On account of this, it was thought that evaporation might occur through the partially permeable bitumen seal. Many samples were cut from the test road in Hamilton, and these were heated to the above surface

9.1.6 (cont.)

temperature at the rate normally experienced on a hot summer day, and it was found that very little evaporation occurred through the seal, though moisture migration from the hot upper regions of the soil-cement base to the cooler regions below, was found to be appreciable. A brief outline of the tests carried out and the results obtained follows.

A number of sandy pumice soil-cement base sections were prepared with a bitumen seal coat and tested for moisture evaporation and moisture migration. After establishing a surface temperature vs. time curve, fig. (9.1), to which the pavement in the field was likely to be subjected, a number of these soil-cement base sections were tested by heating at a rate defined by this prescribed curve, and then quickly broken into sections to obtain the moisture contents at different depths. Thermocouples were placed in the seal coat to measure the temperature for heating control and others at different depths in the soil-cement base to record the temperature profile.

As shown in fig. (9.2), moisture migration under a temperature gradient in a soil-cement base needs to be fully studied before the performance of a particular pavement can be described in mathematical terms. Also, as mentioned in section 9.1.4, temperature affects the curing of soil-cement, so that the strength - age relationship is also altered by a rise in temperature. Fortunately, high temperatures only occur in the early afternoon on exceptionally hot days, and most of the time the temperature is near the yearly average in the stabilized sandy pumice base, and is less than the normal laboratory curing temperature. Therefore in laboratory samples the overall curing

9.1.6 (cont.)

rate is higher than in the field, and consequently it is conservative.

The greatest effect on strength, creep and shrinkage is from the loss of moisture by evaporation at the top of the stabilized base and from the gain of moisture at the bottom, from the subgrade beneath. As the rise and fall of temperature occurs daily, the stabilized sandy pumice is cycled daily between shrinkage and expansion, which could tend to weaken the soil-cement base. The full details of the test carried out and the results obtained are presented in Appendix XIII .

9.1.7 Shrinkage Tests

Measured shrinkage is greater in thin samples than in thick ones because of the non-uniform moisture profile which occurs in large samples. In all samples, the outside edge dries rapidly, but in thick samples it is prevented by the core of the sample from shrinking freely. The core of the sample is compressed slightly, and the outside edge remains in tension. This, in turn, causes creep at the drying face, with a consequent reduction in shrinkage-induced stress. It should be noted that the shrinkage recorded is only the shortening of the sample as a whole and it gives no indication of what the free unrestrained shrinkage would be. Also, the ultimate shrinkage is greatly underestimated in a large sample, because any shrinkage stress causes creep which in turn means a reduction in the recorded ultimate shrinkage. Consequently, the use of samples with the smallest diameter physically possible provides the

9.1.7 (cont.)

closest approximation to the true curve for free unrestrained shrinkage vs. moisture content. The unique shrinkage vs. moisture content curves obtained in this project using 13 mm diameter samples are shown in fig. (9.3) for the loess soil-cement and fig. (9.4) for the sandy pumice soil-cement. The details of the curve shapes will be discussed in Chapter 10.

9.1.8 Creep Tests

After carrying out creep tests to try to reproduce the results of Okada and Kawamura[98], it was decided that their 44.5 mm wide, 38 mm deep sample was too large to allow uniform drying within the sample. Thereafter, 13 mm diameter samples were used for all remaining creep tests in both tension and compression. The compression creep samples were 26 mm long, and the tension samples were 102 mm long. The samples were tested enclosed in perspex boxes, fig. (6.4), to prevent non-uniform drying along the length of the sample.

It was also found that the perspex boxes could be used to vary the rate of drying, by restricting their inlet and outlet. This variation of the drying rate was necessary in later tests where the drying rate was compared with the rate of creep.

From the initial tests with the 13 mm diameter samples creep strains were recorded at different stresses and at various times of drying, but there appeared to be something lacking in these results, in that the moisture present or the drying rate, or perhaps both, should have been taken into account in plotting the creep curves. By carrying out numerous creep tests using

9.1.8 (cont.)

different compressive and tensile stresses while the samples dried at varying rates, it was established that the drying rate greatly influenced the creep of a soil-cement sample. The drying rate was expressed as the time-rate of change of moisture content:

$$\frac{\dfrac{\text{original MC} - \text{MC}^{(t)}}{\text{original MC}}}{\Delta t}$$

For loess soil-cement the effect on creep in tension of varying the drying rate after 1, 3, 5 and 7 days drying is shown in figs. (9.5), (9.6), (9.7) and (9.8) respectively. The curves for creep in compression were similar.

A better representation of creep was obtained when the ratio: applied stress/moisture content was introduced, and all the available results were plotted on one graph, as shown in fig. (9.9).

In an attempt to investigate variable loading rates for variable drying rates, another series of creep tests was carried out. Unfortunately, the interpretation of results became impossible, so further testing along these lines was abandoned.

In order to understand the behaviour of soil-cement prisms (a) completely unrestrained and drying from one side and (b) internally restrained against deflecting and drying from two sides, an understanding of the changing strains within a prism appeared essential. When a change in the deflection of a soil-cement prism occurs from concave to convex, then strain reversal must occur. One can observe from the creep hysteresis curves, fig. (9.10), that a reduction in load causes little change in strain compared

9.1.8 (cont.)

with the change in strain which occurs on loading a sample.

From the many creep tests on soil-cement carried out for this project, the following points should be noted:-

(1) As indicated in section 9.1.3, an imposed stress on a soil-cement sample can influence the drying rate, though only by a small amount. As moisture must be removed by evaporation, rate of moisture loss under stress depends on the ratio surface area to volume, so that as small a sample as possible should be used, e.g. 13 mm diameter, as used in this project.

(2) Creep of soil-cement is much greater for a drying sample than for a sample remaining in either the wet or dry state. The same also applies to concrete, but when a concrete specimen is completely dry, no creep is recorded (Neville[95]), yet for completely dry soil-cement samples made from both loess and sandy pumice it was found in this project that some creep did occur. Two possible explanations for this could be that, (a) on removing the soil-cement sample from the oven at 105°C and waxing it, a very small amount of moisture was absorbed from the atmosphere into the soil-cement voids, (b) there is a faint possibility that moisture which is bound in the cement gel is withdrawn by the suction of the oven dry clay particles and therefore available to lubricate particles.

(3) For concrete, Davis and Travell[32] observed that the faster a sample was dried, the faster it crept and the ultimate creep was also higher. By observing fig. (9.8), one can also see that the drying rate has a direct bearing on the creep rate for a soil-cement, but the effect on the ultimate

9.1.8 (cont.)

creep would be dependent on the particular soil-cement mix.

(4) As a road pavement is subject to changes in both temperature and humidity, it was decided to carry out tests for creep and shrinkage on soil-cement samples which were cured in a climate room cycling between a maximum relative humidity of 95% at 0°C and a minimum relative humidity of 58% at 26½°C. The results obtained for both creep and shrinkage, when the relative humidity was alternated between 95% and 58%, were similar to those which would have been expected had the creep and shrinkage tests been carried out at some intermediate relative humidity closer to the lower limit. Hansen[60] found for concrete that, by alternating the humidity between two limits, creep was represented by a curve between the two limits, as for soil-cement.

(5) A limited number of loading tests for soil-cement were carried out in a curing environment in which the samples were subjected to alternating cycles of wetting and drying. When the results obtained were compared with those for unloaded samples curing under identical conditions, it was found that greater deformation occurred in a loaded sample compared with an unloaded sample. L'Hermite[81] observed similar results for concrete.

(6) One of the main criticisms of the seepage theory is that, if a concrete sample is dried, loaded in compression, and then soaked, creep occurs more rapidly. This observed phenomena is directly in contrast with that proposed by the seepage theory; therefore, a test as described above was carried out for soil-cement and the results were similar to those obtained for concrete. To obtain information on the action of wetting a loaded dry sample, tension creep tests were carried out on identical samples in the

9.1.8 (cont.)

unloaded and loaded states. After a prescribed time of soaking, both samples were removed from the water and a moisture content determination was made on each. While free water remained around a sample, readings on the dial gauge mounted above the sample indicated expansion of that sample. It was found that the loaded samples did not expand as much as the unloaded samples, yet the difference in moisture content between them was negligible. This bears out Neville's[95] comment (for concrete) that for shrinkage to occur, large quantities of moisture have to be removed from a sample, while creep can occur with little or no loss of moisture. Further, a rapid strength loss occurs on resaturation of a sample, of soil-cement or concrete. This means that for a constant stress the stress/strength ratio greatly increases with increase in the degree of saturation. Therefore, creep must also rapidly increase with degree of saturation, and this has been observed experimentally.

(7) The effect of variable temperature on creep and shrinkage was not studied in this thesis, but Neville[95] has presented results for concrete which indicate that creep increases with increasing temperature, though the magnitude of the change is very small.

(8) Creep recovery, i.e. viscous elastic rebound, occurs in soil-cement after unloading, and it appears to depend on the amount of creep which has occurred up to the time of unloading and the proportion of the load removed. Similar observations have been recorded by Neville[95] for concrete.

(9) There is a possibility of micro-cracking occurring in a soil-cement sample under tensile stress. Neville[95] states

9.1.8 (cont.)

that the start of micro-cracking in poor quality concrete is in the range of 0.3 - 0.4 of the applied stress/strength ratio. It is likely that this range of stress/strength ratio also applies to soil-cement, for it was observed in this project that if the stress to strength ratio for the tension creep tests was greater than 0.4, then failure of the sample always took place within the seven days' test period. With stress to strength ratios of 0.6 and greater, most samples failed immediately the stress was applied. No doubt surface defects in a few samples could have caused premature failure, but since bending moments in the soil-cement tension creep samples were not allowed to develop, most of the failures would be in pure tension only.

In order to predict the shrinkage stresses within a soil-cement prism, it is necessary first to predict the creep which will occur as internal stresses develop. The first attempt to predict the internal stress release in a shrinkage soil-cement prism used experimentally-obtained creep curves, but the stresses predicted did not correspond with those obtained experimentally, so a number of rheological models were investigated in order to obtain a better representation of the creep in soil-cement prisms. Also, when experimental creep results were used, the shrinkage stress analysis could not be done on a computer. A Maxwell model, consisting of a Hookean spring and a Newtonian dashpot in series, was adopted to represent creep, mainly because of its simplicity, but also because it was possible to vary the viscosity coefficient.

The creep strain was plotted against time for a constant

9.1.8 (cont.)

stress and variable drying rates, and from this plot values of the viscoelastic coefficients were calculated. The plotting and calculations were repeated for a range of constant stresses, and finally all the viscoelastic coefficients were plotted with respect to their appropriate time-rate change of moisture content as shown in fig. (9.11) for loess soil-cement and fig. (9.12) for sandy pumice soil-cement.

9.1.9 Strength Tests

Because the shrinkage and creep tests were conducted on 13 mm diameter specimens, the strength tests also had to be carried out using the same small samples. Unfortunately, the results obtained from these strength tests were not highly satisfactory. Firstly, the small cross-sectional area compared with the relatively large surface area of the samples tends to cause premature failure through any surface imperfection. This was confirmed by examining the strengths obtained for the 51 mm diameter and 13 mm diameter soil-cement samples after 7 days' moist curing, where it was found by experimentation that a 16% increase in the strength of the 13 mm diameter sample was required to establish relativity with the 51 mm diameter sample. Consequently, all the strength results obtained from the 13 mm diameter samples were increased by 16%.

Secondly, testing of such small samples presented many problems which could only be overcome by developing suitable techniques. The direct tension test was known to be extremely difficult to carry out accurately, so the indirect tension test (section 6.1.4.2) was employed throughout. No loading

9.1.9 (cont.)

strips were used, as the machine plattens tended to provide more consistent results for these small samples. The tensile strength curves for both loess soil-cement and sandy pumice soil-cement are shown in figs. (9.13) and (9.14).

9.1.10 Composite Prisms

In a further attempt to understand the behaviour of soil-cement samples, as well as to explain the phenomenon, a series of three composite prisms were built. It was reasoned that if a prism was built up from thin slices anchored together only at the ends, then deflection of the composite prism would take place as the composite effect of a series of homogenous prisms, but when required the end anchorages could be broken off, so allowing each slice to expand or contract, according to the stress in it.

Manufacturing these prisms presented a number of problems. They were made from six 13 mm wide slices held together by two steel caps glued across the ends of all six slices. Even though the slices were held in close contact, they were able to move relative to one another, and the whole composite prism was waxed, except on the drying side. Originally, plastic sheet with plenty of small holes in it was to have been placed between slices to help sliding of one slice over the next, but it was found that the moulded face of each slice of soil-cement made a good sliding surface. The moisture flow did not seem to be greatly affected by the discontinuity between the slices, so the slice-to-slice contact must have been extremely good.

9.1.10 (cont.)

Three composite prisms were made and the shrinkage was recorded up to the time the ends were removed. The steel ends were broken from the composite prisms at different ages, and in each case strain release occurred in each of the six slices. The sign of the stress which must have existed in each particular slice was given by the direction of the strain release, so that a previously compressed slice would expand on release and vice versa. The magnitude of the stresses could not be obtained from these experimental results, but an estimate of the stress profiles was made (fig. (9.15)) for each of the three composite prisms.

9.2 Shrinkage Stresses in Small Soil-Cement Prisms

As explained in Chapter 7, the published methods for predicting shrinkage stresses in soil-cement were tested, and it was obvious that Okada and Kawamura's[98] method was the only acceptable one. Consequently, experimental parameters appropriate for that method were obtained for both loess soil-cement and sandy pumice soil-cement, but the stresses so predicted still did not correspond with the experimentally recorded stresses, so it was obvious that some new method of predicting shrinkage stresses was necessary.

As the moisture content of any element of soil-cement in a sample greatly influences the shrinkage process, it was decided that, as far as possible, all parameters required for stress analysis should be related to the moisture content.

An experimental study was made to find whether strength, elastic modulus and free unrestrained shrinkage were at all time-dependent, but it was found that all these three parameters

9.2 (cont.)

were dependent only on the moisture within the soil-cement. This statement applies almost equally to the conditions in either a soil-cement prism or a pavement slab. On the other hand, it was found that creep was dependent on both moisture content and drying time.

9.2.1 Theory for New Shrinkage Stress Prediction Method

Consider three cases of restraint for a soil-cement prism.

Case (I). Fully restrained at both ends from bending and shrinkage in the longitudinal direction.

Case (II). Restrained against deflection in the transverse direction.

Case (III). Completely unrestrained.

Provided the free unrestrained shrinkage strain 'S' (defined as the unit linear deformation that would occur if each infinitesimal element were unrestrained) is obtainable at any time, stress determinations should be able to be made. Unless the distribution of the free unrestrained shrinkage happens to be compatible with the conditions of continuity in the sample, stresses are produced that modify the deformation to made them compatible. The resultant unit deformation in the x direction (fig. 7.4)) 'e_x' is defined as the algebraic sum of the free unrestrained shrinkage strain 'S' and the strain produced by stresses. In other words, it is the measured deformation of a soil-cement prism as it shrinks.

There are six partial differential equations required for a complete mathematical statement of the conditions of compatibility, but Pickett[100] has pointed out that only one

9.2.1 (cont.)

equation

$$\frac{\partial^2 e_x}{\partial y^2} = 0 \qquad \ldots\ldots \quad (9.1)$$

is required for long narrow beams and slabs if the stresses are considered to be independent of the longitudinal coordinate x. In narrow, thin slabs when the stress in the y direction is zero, σ_z is negligible. Therefore

$$e_x = \varepsilon_s - S \qquad \ldots\ldots \quad (9.2)$$

where ε_s = strain produced by stresses. If it is assumed that soil-cement is adequately represented by the Maxwell Model shown in fig. (9.16), then if $S = S(t)$, and $e_x = e_x(t)$

ε_s = total strain = $\varepsilon_1 + \varepsilon_2$.

For Case (I), fully restrained

$$e_x(t) = 0$$

from equation (9.2) $\varepsilon_s = S(t)$ ..... (9.3)

$\therefore S(t) = \varepsilon_1 + \varepsilon_2$

$$\bar{S} = \bar{\varepsilon}_1 + \bar{\varepsilon}_2$$

From fig. (9.16) $\sigma = E(t)\,\varepsilon_1 = \eta(t)\bar{\varepsilon}_2 = \eta(t)(\bar{S} - \bar{\varepsilon}_1)$

$\therefore \bar{\varepsilon}_1 - \bar{S} = -\frac{E(t)}{\eta(t)}\varepsilon_1$

$$\bar{\varepsilon}_1 = \bar{S} - \frac{E(t)}{\eta(t)}\varepsilon_1$$

$$\bar{\varepsilon}_1 = f(\varepsilon_1, t) = \bar{S}(t) - \frac{E(t)}{\eta(t)}\varepsilon_1 \qquad \ldots\ldots \quad (9.5)$$

$\varepsilon_1 = 0$ at $t = 0$

$\varepsilon_1^k = \varepsilon_1(k\Delta t)$

An approximate solution of equation (9.5) is:

9.2.1 (cont.)

$$\frac{\varepsilon_1^{k+1} - \varepsilon_1^{k}}{\Delta t} = \bar{S}(k\Delta t) - \frac{E(k\Delta t)}{\eta(k\Delta t)} \varepsilon_1^{k}$$

$$\therefore \varepsilon_1^{k+1} = \varepsilon_1^{k} + \Delta t[\bar{S}(k\Delta t) - \frac{E(k\Delta t)}{\eta(k\Delta t)} \varepsilon_1^{k}]$$

$$= \varepsilon_1^{k} + \Delta t[S_k - \frac{E_k}{\eta k} \varepsilon_k^{1}] \qquad \ldots\ldots \quad (9.6)$$

where $\bar{S}_k = \frac{S_{k+1} - S_{k-1}}{2\Delta t}$ ..... (9.7)

η_k is dependent on moisture content and time.

E_k is dependent on moisture content.

At k + 1

$$\sigma_{k+1} = E_{k+1} \varepsilon_1^{k+1} \qquad \ldots\ldots \quad (9.8)$$

For Case II, partly restrained,

$e_x(t) = S_{av}(t)$ = average measured shrinkage of a drying soil-cement sample

$\therefore$ Equation (9.2) becomes

$$\varepsilon_s = S(t) - S_{av}(t) \qquad \ldots\ldots \quad (9.9)$$

For Case III, unrestrained,

To prevent deflecting the moment M' per unit width of beam is

$$M' = \int_o^b \sigma'_x \, y dy \qquad \ldots\ldots \quad (9.10)$$

where σ'_x is the stress in a prism restrained from deflecting

$$\sigma'_x = E(t) \left[S' - \frac{1}{b} \int_o^b S' dy \right] \qquad \ldots\ldots \quad (9.11)$$

where $S' = S(t)$

By substituting Equation (9.11) in (9.10):

$$M = \int_o^b E(t)[S' - \frac{1}{b} \int_o^b S' dy] y dy \qquad \ldots\ldots \quad (9.12)$$

If $E(t) = n E_{b=o}$

9.2.1 (cont.)

where the elastic modulus at the sealed surface $E_{b=o}$ is taken as the reference elastic modulus.

From equation (9.12)

$$M' = E_{b=o}\left[\int_{-y_c}^{b-y_c} n\, S'y\,dy - \frac{b}{2}\int_{-y_c}^{b-y_c} S'\,dy\right] \quad \ldots\ldots \quad (9.13)$$

where y_c is the distance from the sealed surface to the neutral axis. Now the stress σ_x'' in each fibre will be proportional to the strain

$$\therefore \quad \sigma_x'' = \varepsilon_s E(t) = \frac{E(t)}{y_p}\, y' \quad \ldots\ldots \quad (9.14)$$

where y_p = curvature

y' = distance of fibre from the neutral axis. For no external restraint there is no moment in the slab, so the moment in equation (9.13) must be removed by super-imposing an equal and opposite moment $-M'$.

From equation (9.10) $M' = \int_{-y_c}^{b-y_c} \sigma_x''\, y\,dy$

$$= \frac{1}{y_p}\int_{-y_c}^{b-y_c} E(t)y^2\,dy$$

$$\therefore \quad \frac{1}{y_p} = \frac{M'}{\int_{-y_c}^{b-y_c} E(t)y^2\,dy}$$

$$\frac{1}{y_p} = \frac{M'}{(EI)_1} \quad \ldots\ldots \quad (9.15)$$

where $(EI)_1 = \int_{-y_c}^{b-y_c} E(t)y^2\,dy$

By adopting a transformed section, using the elastic modulus at the sealed surface as a reference, the curvature can be computed, and the stress resulting from a moment $-M'$ is obtained by substituting equation (9.15) in equation (9.14).

9.2.1 (cont.)

$$\sigma''_x = \frac{M'_y E(t)}{(EI)_1}$$

$$= \frac{E(t)(y-y_c)}{(EI)_1} [E_{b=o} \left[\int_{-y_c}^{b-y_c} n\, S'ydy - \frac{b}{2}\int_{-y_c}^{b-y_c} S'dy\right]$$

$$\text{i.e. } \sigma''_x = \frac{E(t)(y-y_c)}{IT}\left[\int_{-y_c}^{b-y_c} n\, S'ydy - \frac{b}{2}\int_{-y_c}^{b-y_c} S'dy\right] \quad \ldots\ldots \quad (9.16)$$

where IT = transformed moment of inertia.

$$\therefore \quad \varepsilon_t = S(t) - S_{av}(t) + \left(\frac{y-y_c}{IT}\right)\left[\int_{-y_c}^{b-y_c} nS'ydy - \frac{b}{2}\int_{-y_c}^{b-y_c} S'dy\right] \ldots \quad (9.17)$$

9.2.2 Moisture Content vs. Time Curves

As the moisture content parameter plays a major role in controlling the theoretical development of shrinkage stresses in soil-cement prisms, it was decided that moisture content profiles, after different periods of drying, should be measured experimentally for prisms restrained as for Cases I, II and III in section 9.2.1 above. This not only ensured a correct base on which to build the shrinkage theory, but also provided the experimental moisture content profiles to check the accuracy of the computer program for moisture flow. In the final stages of this project, the moisture flow program was directly linked with the shrinkage stress program to dispense with this extra stage. The prisms used for Cases I and II samples were 76 mm wide, 76 mm deep and 286 mm long, with two opposite sides of the prisms open to permit drying, while all other surfaces of

9.2.2 (cont.)

each sample were sealed with wax. The completely unrestrained sample was 38 mm wide, 76 mm deep and 286 mm long, with only one side open to drying, the remainder of the sample being sealed, as shown in (fig. 7.4).

Comments on measuring the moisture contents experimentally have been given in section 8.4.3.1. In making remarks about the accuracy of these moisture content profiles, no confidence limits have been provided, but the following techniques were developed for moisture content determinations. Twelve identical prisms drying under the same conditions were used, and two sections through each drying prism were removed at specified times. Sections from the 38 mm wide prism were broken into 3 equal portions, A, B and C, fig. (9.17), from the drying face to the sealed face, and from the two sections an average moisture content was obtained for each of the three portions. When plotting the moisture content profiles, the moisture contents from the three portions were designated as representing the moisture content not at the centre of each portion, but at the centroid of a trapezium abcd shown in fig. (9.18). The use of the centroid of this trapezium may not appear very significant, but when a drying gradient exists, the centroid of the trapezium drops well below the centre of the corresponding portion.

It was found that the rate of drying was not always uniform along the length of a prism so a moisture content determination was made from two sections, one an end, and one a centre portion of the prism. By using the average results from twelve prisms, a fair degree of confidence can be placed

9.2.2 (cont.)

in the final moisture content profiles.

9.2.3 Tensile Strength

The seemingly simple tensile test unfortunately has presented many problems which require attention before meaningful results are obtained. As mentioned in section 9.1.9, 13 mm diameter samples were tested in indirect tension and the resulting strengths were corrected to allow for any surface defects. For future tensile strength testing, the following procedure is recommended. The moisture content parameter has been found to influence the tensile strength so much that the only other important parameter, time, has been ignored without any loss of accuracy in tensile strength results.

In order to measure the tensile strength accurately at any moisture content, a small sample which had been dried slowly before testing appeared to be the only solution to the problem. However, as mentioned earlier these small samples with large surface area to volume ratios produced very scattered results. If large samples with a cross-section at least 200 mm square were allowed to dry very slowly before testing in direct tension, then more consistent results should be obtained. In this case the moisture content to be related to the tensile strength would need to be the average moisture content across the whole cross-section of the sample. Provided the drying rate is slow, the difference in moisture content between the centre and the drying surface of the sample should not be greater than 10%. Another possible improvement would be to seal the samples after varying periods of drying and allow the internal moisture to come to

9.2.3 (cont.)

equilibrium before testing in direct tension.

9.2.4 Measured Shrinkage Strains

In order to measure the shrinkage of prisms unrestrained or restrained against deflecting, cases III and II, section 9.2.1, demec points were positioned across the prisms as shown in fig. (7.7).

It was at first difficult to ensure that equal drying took place at opposite faces of the two-side drying prisms, but with improved drying techniques the measured shrinkages at any time across the two-side drying prisms were equal, as shown in figs. (9.19) and (9.20). Improved drying was brought about by eliminating the samples from contact with a direct air flow within the drying container.

For the completely unrestrained soil-cement prisms, the measured shrinkage distribution across the prisms was nearly linear with time, as shown in figs. (7.9) and (9.21).

9.2.5 Elastic Modulus

The elastic tension and compression moduli for specimens at specific moisture contents was obtained by rapidly loading the specimens and measuring their deflection. Samples 13 mm in diameter were used in the testing program, and the elastic modulus in tension was obtained from the direct tension test. This was done on both loess soil-cement and sandy pumice soil-cement.

Because the elastic moduli in tension and compression were nearly equal, only one stress-strain curve was used for each of the materials, for shrinkage stress prediction. As the

9.2.5 (cont.)

stress-strain curves for any particular soil-cement at a constant moisture content were nearly linear for 90% of the loading range, the elastic modulus was taken as the secant modulus at the elastic limit. The resulting elastic modulus vs. moisture content curves for loess and sandy pumice soil-cement are shown in fig. (9.22) and fig. (9.23) respectively.

9.2.6 Free Unrestrained Shrinkage

As explained in section 9.1.7, the free unrestrained shrinkage for a drying soil-cement has been obtained experimentally instead of by using previously suggested theoretical methods. By drying six 13 mm diameter samples slowly, measuring at regular intervals their shrinkage and weight loss, and averaging the six results, a sufficiently reliable curve was obtained for shrinkage vs. moisture content. The curves for loess soil-cement and sandy pumice soil-cement are shown in fig. (9.3) and fig. (9.4) respectively, where it may be noted that the 95% confidence limits indicate only small variations from the curve of best fit.

9.2.7 Creep Characteristics

As mentioned in section 9.1.8, no adequate parameters were found for defining creep. From the many creep tests carried out on soil-cement, it was evident that both the time under stress and the moisture present in a sample influenced the visco-elastic coefficient of the Maxwell Model. When the visco-elastic coefficients were plotted against the respective moisture contents, there was a large scatter of results. A study of the results showed that an allowance should be made for the drying

9.2.7 (cont.)

rate. When the viscoelastic coefficients were plotted against their respective time-rates of change in moisture content $(\frac{\Delta MC}{\Delta t})$ the more meaningful curves shown in figs. (9.11) and (9.12) were obtained.

The adoption of the Maxwell Model has greatly simplified the representation of the creep mechanism. It is assumed in the use of the Maxwell Model that no creep occurs while a soil-cement sample is moist curing; the moist curing creep has been found by experiment to account for only 5% of the total creep, so this assumption is within experimental accuracy.

Many research workers have commented on the comparison of creep in tension with creep in compression, but no definite answers have yet come forward. Creep in tension is the main mechanism involved in a drying soil-cement pavement, so creep in compression did not receive the same attention in this project as creep in tension, but it was found that creep in tension was the same as creep in compression for low stresses. Once the tensile stresses became greater than 40% of the ultimate tensile strength, then creep in tension increased morerapidly than creep under the same magnitude of compressive stress, as shown in fig. (9.24). This seems feasible, because at tensile stresses greater than 40% of the tensile strength, the soil-cement bonds are severely strained. However, if a stress of the same magnitude was applied in compression to a soil-cement sample, the effect on the bonds would be negligible, owing to the much higher compressive strength of a soil-cement.

9.3 Comparison of the Calculated Shrinkage Stresses Compared With the Experimental Results

Both the loess soil-cement and the sandy pumice soil-cement prisms were used to compare the observed experimental results with the theoretical results obtained from the new hypothesis. It was not possible to measure the actual stresses at any particular point in the section of a drying soil-cement prism, but the average stress across the whole prism and its deflected shape were measured experimentally. Consequently, the predicted results have been compared with these experimental curves.

9.3.1 Results from Loess Soil-Cement Prisms

A number of prisms, of different widths, were used to obtain moisture content profiles and drying shrinkage strains with respect to time, but because of scatter in other series of tests, only the results for the 38 mm wide prisms have been used in the theoretical prediction. Figs. (9.25), (9.26) and (9.27) indicate the theoretical shrinkage stresses obtained for the three different cases of restraint, Cases I, II and III, section 9.2.1, for the 38 mm wide prism. The stresses for the completely restrained prism, Case I, have been compared with the tensile strength (fig. (7.12)), where it can be seen that after $6\frac{1}{2}$ days drying, longitudinal cracking must occur internally between the centre and the sealed face of the prism. Probably the most interesting point is that this cracking is internal, and not on the drying face as predicted by Kawamura[72] for concrete. From the loess soil-cement prisms fully restrained in the steel cradles, it was found that failure occurred at seven days' drying,

9.3.1 (cont.)

so the predicted failure at 6½ days is very close, when the accumulation of errors is taken into account. The predicted time of failure is not totally theoretical, as the analysis is based on a number of experimental curves.

From figs. (9.3) and (9.4) it can be seen that the free unrestrained shrinkages are within ± 4%, while the viscoelastic coefficients used in the Maxwell Model are within ± 10%, (figs. (9.11) and (9.12). The elastic modulus vs. moisture content curves (figs. (9.22) and (9.23)) are within ± 2%. It is not easy to predict the likely overall error in the shrinkage stresses, but by carrying out a sensitivity analysis with small variations in the initial parameters the following results were obtained. A variation of 4% in the free unrestrained shrinkage caused a 3% change in the predicted shrinkage stresses, while a 2% variation in the elastic modulus caused a 2% change in the predicted shrinkage stresses. By varying the viscoelastic coefficients by 10%, the change in predicted shrinkage stresses were 3%. Therefore it can be observed that the overall effect of errors in the initial parameters will not unduly affect the final predicted shrinkage stresses. On the other hand, an error of ± 10% could be expected from the experimentally obtained failure of a soil-cement prism, so that an error of ½ day or 7½% in the time of sample failure is well within experimental tolerance. From fig. (6.18), the theoretical and experimental curves for the average force developed in a completely restrained loess soil-cement prism also appear to be well within experimental error.

The predicted curvature of the completely unrestrained loess

9.3.1 (cont.)

soil-cement prism, Case III, section 9.2.1, is close to the observed curvature, with the 'strain reversal' point coming at 5½ days' drying time, compared with the predicted time of 5 days, (fig. (9.28)). The initial deflected shape of the loess soil-cement prism, up to the time of 'strain reversal', corresponds very closely with the theoretical results, but past this point the two curves diverge quite markedly.

9.3.2 Results from Sandy Pumice Soil-Cement Prisms

For the sandy pumice soil-cement, the 38 mm wide prisms have similar characteristics to the loess soil-cement prisms of the same size, but the shrinkage stresses are much lower. Therefore, as shown in fig. (7.12), failure of a fully restrained sandy pumice prism can never occur under drying shrinkage induced stresses. The difference between the predicted average force in the prism and the measured average force is well within experimental error, especially when one considers the small forces being recorded. The shrinkage stress distributions for the fully restrained sandy pumice soil-cement prism are shown in fig. (9.29).

The prisms of both cases II and III, section 9.2.1, both indicate a complete change of stress during drying, from tension to compression on the drying face and the opposite on the sealed face, as shown in figs. (9.30) and (9.31). The predicted 'strain reversal' time for the sandy pumice soil-cement is later than the experimentally observed reversal time (fig. (9.32)) ; the shrinkage curves correspond closely over the early drying period, but a marked separation of the theoretical and experimental

9.3.2 (cont.)

curves occurs in the later stages of drying.

9.3.3 Comments on the Results from Loess Soil-Cement and Sandy Pumice Soil-Cement

In general, for both materials the stress predictions obtained using the proposed method were very close to the measured results, although in the later stages of drying, the Case III prisms of both materials tested tended to deflect more than predicted theoretically. There are several possible explanations for this discrepancy, but it is likely that the allowance made for creep in the theoretical prediction is the main source of error. As mentioned in section 9.1.8, many experimental creep curves were obtained, but the results were not considered to be entirely satisfactory.

Consider the case of a 38 mm wide soil-cement prism drying from one side. Each successive element of soil-cement from the open face towards the sealed face has different characteristics once drying has started. The moisture content, the rate of moisture loss and the induced stress in every element vary with time, and it is impossible to represent all these different changes with the information obtained from one creep test.

From the work carried out for this thesis, it is seen that creep behaviour must be represented by some sort of rheological model which permits variations in both the elastic modulus and the visco-elastic coefficients. The elastic modulus was found to be independent of time, but was directly related to the moisture content. The length of time a soil-cement sample has been moist-cured has some effect on the elastic modulus, but

9.3.3 (cont.)

experimental work carried out for this thesis indicated a maximum change of 5% in the elastic modulus when moist curing was prolonged. On the other hand, the visco-elastic coefficients appear to depend on the time since moulding, the moisture content, and the rate of change of moisture content.

For a rheological model with variable elastic moduli and visco-elastic coefficients to be usable, it must be composed of simple elements to simplify analysis. The Burger Model can be made to represent the creep of a particular soil-cement mix under a constant stress, but if the stress is varied then the coefficients must vary, and it is then impossible to determine all the coefficients required.

For this reason, the simpler Maxwell Model shown in fig. (9.16) was adopted, although it does not accurately represent the deformation change which occurs in soil-cement when a load is suddenly removed; the recoverable deformation indicated is a little larger than actually occurs, because of plastic behaviour of the soil-cement. As can be seen in fig. (9.16), the strain release as the load is gradually reduced is much less than the original deformation, and this is important when the deflection of a one-side drying soil-cement prism is being predicted.

When using the Maxwell Model in this thesis, the visco-elastic coefficient for a particular soil-cement element was evaluated by using the time-rate of change in moisture content. Then from the experimentally obtained creep curves (figs. (9.11) and (9.12)) , the appropriate visco-elastic coefficient was read off.

The time-rate of change in moisture content is not related to the actual moisture contained in a sample, but it was soon

9.3.3 (cont.)

apparent that if the actual moisture content was introduced by multiplying the two factors together, a confused state developed. This can be seen by comparing two soil-cement elements, one drying rapidly, so that the time-rate of change in moisture content is high, consequently after a period of time the moisture content will be low, and the other drying slowly so that the time-rate of change in moisture content is low, consequently after the same time period the moisture content is relatively high. If these factors are combined by multiplication, then the product of these moisture contents and the corresponding time-rates of change could be numerically equal for the two cases, yet from the experimental work carried out in this project the visco-elastic properties are markedly different. Other ways of combining these factors have not been investigated.

The Maxwell Model does not adequately represent the release of strain in soil-cement when the stress is reduced, and there is difficulty in evaluating the visco-elastic coefficients as they vary with changing moisture content and time. As a result, a quite appreciable error can be expected in the stress prediction.

9.4 Summary and Discussion of Proposed Method for Shrinkage Stress Prediction

If shrinkage stresses can be accurately predicted in a soil-cement prism, the prediction can be extended to a soil-cement pavement slab. The basic parameters controlling the behaviour of a soil-cement pavement slab are creep, moisture flow, strength development and shrinkage, and once these are understood and evaluated, they can then be inserted in the shrinkage stress

9.4 (cont.)

equations to predict the behaviour of a pavement slab. The prediction proposed in this chapter depends on the experimentally-determined curves for free unrestrained shrinkage versus moisture content, elastic modulus versus moisture content, moisture content profiles for different periods of drying, and visco-elastic coefficients from the Maxwell Model.

The predicted curve for free unrestrained shrinkage versus moisture content obtained from 13 mm diameter samples closely approximates the predicted curve for free unrestrained shrinkage versus moisture content for a sample of infinitesimal diameter. As mentioned in section 7.2.2, when the free unrestrained shrinkages were predicted directly from a form of the diffusion equation and plotted with respect to the drying time, it was found that the results did not agree with experimental findings. Consequently, for this project the free unrestrained shrinkages were obtained experimentally, and they have been used successfully in conjunction with the predicted moisture content of any element of soil-cement at a particular time. 13 mm diameter soil-cement samples were used to reduce non-uniform drying when measuring the free unrestrained shrinkages, but other errors such as surface irregularities would tend to cause a small scatter in the results. It can be seen in figs. (9.3) and (9.4) that the error in the curves is not more than 4%.

After examining the results obtained in Chapter 8, the error in the determinations of the moisture contents in a soil-cement at any time can safely be assumed to be not more than $\pm$ 2%. The Maxwell Model proposed for the new shrinkage stress prediction is accurate enough for this purpose, but the representation of

9.4 (cont.)

creep adopted for soil-cement cannot be regarded as entirely satisfactory, owing to the problems encountered in evaluating the visco-elastic coefficients. In order to improve this aspect of the stress analysis further, it is necessary to extend the research to examine methods of representing creep under variable loading conditions and variable drying rates.

Not withstanding the inaccuracies which still exist in the representation of creep, the proposed method for shrinkage stress prediction has provided a very reliable representation of the mode of behaviour and of the shrinkage stresses which develop when a soil-cement prism dries. It should, therefore, be possible to extend this method of prediction to a soil-cement pavement slab, provided the moisture conditions can be predicted throughout the pavement. This is done in Chapter 11 for a sandy pumice soil-cement pavement slab.

CHAPTER TEN

A FURTHER LOOK AT THE POSSIBLE STRUCTURE OF SOIL-CEMENT

In Chapter Four, section 4.5, a possible structure for soil-cement was proposed, based on readings of previous research. This thesis does not primarily aim to develop and prove a form for the structure of soil-cement, but nevertheless a basic understanding of the form of this structure should help in explaining some of the physical phenomena which occur as a soil-cement pavement shrinks. By using the proposed structure to account for results obtained from many of the experimental tests carried out for this project, the correctness of the proposed structure can be ascertained.

10.1 A Brief Outline of the Proposed Structure

The proposed structure of soil-cement can be summarized as follows:-

On the microscopic scale, cement gel and domains of clay particles have been assumed to be similar in their laminar arrangement and at each contact between laminae, a wedge-shaped void is created. Primary physico-chemical bonds are present at the apex of each wedge-shaped void, while large range secondary van der Waal forces act over the remaining areas of the solid surface. When a wedge-shaped void is saturated, moisture exists both in adsorbed layers on the solid surfaces and as capillary water. As drying occurs, some capillary water is removed, causing first a meniscus to form as shown in fig. (3.3)

10.1 (cont.)

and second, a reduction in the radius of this meniscus. As the radius is reduced, the attractive forces exerted by capillarity on the solid surfaces of the wedge-shaped void increase, so that contraction occurs. Drying also causes a reduction in the thickness of the adsorbed water layer, and this in turn increases the effect of the van der Waal forces and the primary forces at the apex, and the wedge-shaped voids tend to close, causing shrinkage. The above process is reversed when a soil-cement is resaturated and expansion occurs.

10.2 Shrinkage and the Proposed Structure

From the discussion in Chapter Six on the effect on shrinkage of such parameters as moulding density, moulding moisture content, cement content, precure moisture content, delayed compaction and mixing time, it is apparent that the new structure would hold good. Shrinkage can be accounted for by assuming that contraction of wedge-shaped voids in the soil-cement is caused by tension arising from a decrease in the radius of each capillary water meniscus, and by reduction in the thickness of the adsorbed water layers as evaporation occurs. For instance, the measured shrinkage of any soil-cement is greatly increased when the moulding density is increased, provided all other moulding conditions are held the same. More wedge-shaped voids must exist in a heavily compacted specimen than in a lightly compacted one, therefore a greater number of locations exist at which potential shrinkage can occur. Also when the compactive effort becomes very great, there is considerable orientation of the laminate particles in the direction perpendicular to that of the compactive effort. The

10.2 (cont.)

more wedge-shaped voids that are orientated perpendicularly to the direction of compaction, the greater must be the shrinkage in this direction. Therefore, it could be expected that the total shrinkage should increase with increasing density. This was observed for both loess soil-cement and sandy pumice soil-cement, as shown in figs. (6.11) and (6.12), where it can be seen that the relationship is nearly asymptotic. Likewise, by examining the effects on shrinkage (as described in Chapter Six) of changing the remaining parameters, i.e. moulding moisture content, cement content, precure moisture content, delay in compaction and mixing time, it can be concluded that the proposed structure for soil-cement is feasible.

A similar conclusion can be reached by examining the effects of the above parameters on both the unconfined compression and the tensile strength of soil-cement samples. A full discussion of all the processes involved can be found in Chapter Six.

Figures (9.3) and (9.4) show the free unrestrained shrinkage-moisture content curves for loess soil-cement and for sandy pumice soil-cement. A study of these shows that the rate of shrinkage increases slowly as the sample loses moisture from the "as moulded" state. At a moisture content of 7.75% (fig. 9.3) for the loess soil-cement and a moisture content of 11.00% (fig. 9.4) for the sandy pumice soil-cement, the shrinkage rate becomes constant, and as more moisture is lost from the sample, the shrinkage rate gradually decreases. When evaporation occurs from a fully saturated sample, initially only capillary water is lost, then as the quantity of capillary water decreases, the

10.2 (cont.)

adsorbed water starts to be removed. While only capillary water is evaporating, the shrinkage rate is slow, but when the adsorbed water starts to be removed, the shrinkage rate increases until, when most of the adsorbed water has gone, the shrinkage rate decreases again. This predicted occurrence of shrinkage is in line with the experimental curves obtained for loess soil-cement (fig. (9.3)) and sandy pumice soil-cement (fig. (9.4)).

10.3 Creep and the Proposed Structure

Only a small number of tests was carried out on sandy pumice soil-cement to measure creep in tension, with respect to variation in moulding conditions, but the results obtained provide a useful field for discussion.

10.3.1 Moulding Density

Consider first the effect on creep in tension of varying the moulding density of soil-cement, fig. (6.56). It is evident that the creep is less in more dense samples than in less dense ones. If an explanation similar to that presented for shrinkage was offered to explain the occurrence of creep, then a state of contradiction would arise. In other words, by increasing the density and therefore the number of wedge-shaped voids, one would expect that the creep potential of a sample should also increase in a way similar to that for shrinkage. But as shown in fig. (6.56), the initial creep of the two samples is quite different, though for the remainder of their length the curves are almost parallel. The stiffness of a soil-cement specimen greatly influences its initial deformation under stress. A dense soil-cement specimen contains more wedge shaped voids, and is stiffer than a lightly compacted sample, but under stress the deformation is controlled more by the (cont. p.204)

10.3.1 (cont.)

stiffness than by the extra wedge-shaped voids present. Thus the creep of a dense sample is not greatly different from the creep of a highly compacted sample.

10.3.2 Moulding Moisture Content

The variation of creep with different moulding moisture contents for the sandy pumice soil-cement is shown in fig. (6.57). Unfortunately, none of the creep tests was continued until deformation had ceased, but nevertheless, certain conclusions can be drawn from the results. Firstly, it is evident from the curve with a moulding moisture content of 11.6% that after evaporation begins the time-rate of creep increases briefly then reduces. It seems that only capillary water is lost from the sandy pumice samples until the moisture content reaches 9.5%. It is apparent that at this moisture content (after 80 hours drying for the 11.6% sample and after 150 hours drying for the 14.7% sample in these tests) the time-rate of creep increases for both the 11.6% and 14.7% samples. So it can be assumed that the removal of adsorbed water has a greater influence on creep than the removal of capillary water.

The second conclusion which can be drawn from the results is that the greater the moulding moisture content, the greater is the total creep. When considering this, one must remember that the moulding moisture is that which is actually built into the soil-cement and does not include water which is permitted to enter after the structural form has developed. Therefore the higher the moulding moisture content, the more moisture there is available for evaporation, which in turn means higher potential shrinkage and creep.

10.3.3 Cement Content

Fig. (6.55) shows that the higher the cement content, the lower the creep. A similar conclusion to that presented for the effect of varying density on creep can be applied to the effects of variable cement contents. Increasing the cement content of a soil-cement sample causes a larger volume of cement gel to be formed, but the structural unit must be more rigid than for samples with lower cement contents. Thus, for a soil-cement sample with a high cement content, the instantaneous deformation under stress, and the creep, must be lower than for a sample with a low cement content.

10.3.4 Other Tests

Concrete researchers have shown that a concrete specimen does not creep if completely dry, but they also mention that it is extremely difficult to seal a dried specimen without permitting moisture to enter. Similarly, in this project soil-cement samples tested in tension after oven drying and sealing with wax, have been found to creep, but it is likely that these samples had absorbed a small amount of moisture from the air before the seal coat was applied. Obviously creep will occur in soil-cement when only a trace of moisture is present.

When a soil-cement sample is loaded either in compression or tension, it is found that the evaporation rate is greater than that which occurs for an unloaded sample drying under identical environmental conditions. Neville[95] commented that for concrete the presence of a stress and the process of creep do not influence the rate of evaporation, but as he suggests, it is possible that his work had been attempted using insensitive weighing equipment and large samples.

10.3.4 (cont.)

Consider the action of a compressive load on a wedge-shaped void fig. (3.4) in a soil-cement sample. According to the proposed structure for soil-cement, water must be squeezed from the apex of the wedge so that the structure is in an inflated state with elevated pore-water pressure. When this inflated state is near the drying surface of a sample, the local evaporation rate must be higher because of this ready supply of water. On the other hand, in a large diameter soil-cement sample under external stress the surface area to volume ratio is low, so that few of the wedge-shaped voids in the inflated state are near the drying surface. Therefore, the effect of external stress on the evaporation rate should be less in a large diameter sample than in a small one.

The time-rate of creep of soil-cement is much greater when the sample is either losing or gaining water than when it is maintained at some constant moisture content within the possible range. Nevertheless, it has been shown by Ruetz[123] that moisture flow through a sample of cement paste, with no change in the moisture content, did not influence the time-rate of creep. As explained in section 4.5, the proposed soil-cement structure can easily account for creep of a drying sample, but it is more difficult to explain the rapid creep which occurs on re-wetting of a sample. As a sample is re-wetted, water enters the wedge-shaped voids very quickly, the primary forces acting at the apices and the van der Waal forces are rapidly reduced so that expansion of the loaded sample occurs in all directions. The rate of expansion in different directions depends on the principal orientation of the wedge-shaped voids

10.3.4 (cont.)

and this in turn depends on the compaction characteristics. The presence of a load on the sample affects only the later stages of re-wetting, as explained in section 9.1.3, so considerable quantities of water must penetrate the loaded wedge-shaped voids, and in doing so must greatly reduce the strength of the soil-cement. This in turn implies a great increase in the ratio: stress caused by the external load on the original dry sample/wet strength. This means that creep must occur.

In another test two identical soil-cement samples were dried, then one of these specimens was loaded in compression before both were saturated. Both samples expanded rapidly, but the one under a compressive stress of 44.6 kN/m^2 produced an overall expansion of 29 μm, compared with an expansion of 32 μm for the unloaded sample. However, after equilibrium was established, the moisture content of the loaded sample was found to be 2.5% greater than that of the unloaded one. This appears to be contrary to the behaviour of the proposed structure in section 4.5, in which an applied stress would tend to squeeze moisture from the wedge-shaped voids, but it must be remembered that only the wedge-shaped voids which are predominantly perpendicular to the direction of the applied load tend to close, while the remainder expand slightly. When a sample is under a compressive stress, the number of expanding wedge-shaped voids in the direction parallel to the applied load is much greater than the number of closing wedge-shaped voids orientated perpendicular to this applied load. Therefore, more moisture should be taken in by the expanding wedge-shaped voids than is

10.3.4 (cont.)

expelled from the closing ones, and the specimen should gain in moisture content.

Another interesting compression creep result was obtained for both loess and sandy pumice soil-cements in the course of routine testing. The test involved the loading of one of two identical soil-cement samples, and permitting both to dry under the same conditions. Once creep and shrinkage had ceased, the loaded sample was unloaded and left until creep recovery had ceased. On re-wetting both specimens to their original moisture content, it was found that the previously loaded creep sample expanded more than the unloaded sample.

Ruetz[123] found that the same phenomena occurred in concrete samples, but to a greater extent. His explanation was that, because a large swelling strain occurred during re-wetting in the direction parallel to the previously applied compressive stress, it indicated rebound from a correspondingly large shrinkage strain, so shrinkage strains which occur during drying must be orientated in the direction of any compressive stress which is applied during drying.

Perhaps Ruetz' speculation that orientation of shrinkage strains occur under load is a little misleading. Consider the condition where both a creep sample and a shrinkage sample have been dried from their moulded condition until they are both at a point of time just prior to re-wetting. At this point the creep specimen which has also been subjected to shrinkage is compressed in the direction of the applied stress and slightly dilated in the transverse direction. By comparison, the shrinkage specimen will be contracted to a limited extent in all three

10.3.4 (cont.)

directions. When the stress is released from the creep sample, the rebound which occurs has been shown in fig. (9.10) to be approximately 20% of the original deformation. This indicates that many more bonds must have been formed by the close contact of solid particles in a creep sample, compared with a shrinkage sample. On resaturation of the unloaded creep sample and the shrinkage sample, it is evident that both samples will rapidly take up water, but the creep sample which exists in a highly compressed state, will be markedly affected by the breaking of the bonds formed by solid-to-solid contact when the water enters the sample. Therefore, the creep sample should expand more than the shrinkage sample.

10.4 Molecular Sieve Device

Mills[87] and other research workers have gained a better understanding of the swelling and strength characteristics of cement gel by saturating their cement paste with liquids having different sized molecules. Soil-cement is composed of clay domains, solid particles and cement gel, so it would seem that a similar technique could be applied here. Unfortunately, when clay is present, a physico-chemical reaction occurs between the liquid and the clay, and the degree of this reaction depends on the polarity of the liquid. To eliminate the effect of liquid polarity on clay particles, comparative tests were made using water and ethanol. These liquids have approximately the same polarity, but the molecular size of ethanol is $1\frac{1}{2}$ times that of water. The expansion of a loess soil-cement when re-wetted with water was twice that recorded when an identical sample was re-wetted with ethanol. Therefore, one can conclude that the

10.4 (cont.)

molecular size of the liquid used to re-wet a soil-cement specimen can greatly influence its swelling characteristics.

By considering a wedge-shaped void, it may be deduced that a liquid with larger molecules than water will be unable to penetrate the apex of the void, fig. (3.3). Quite strong forces exist at this apex when no liquid is present, so any penetration of a liquid into the apex will reduce these forces. Consequently, when a liquid of large molecular size is permitted to saturate a soil-cement sample, each wedge-shaped void is unable to expand to the same extent as when re-wetted with water.

10.5 Other Factors Influencing Creep

In cement paste, the total creep in tension increases as drying progresses, even though the creep deformation and the shrinkage strain are working against each other. Experiments carried out by Ruetz[123] on cement paste, show that creep is not affected by steady state moisture flow in either the liquid or the vapour phase. However, in all cases in which moisture flows either into or out of a specimen, there is a marked increase in the magnitude of the total creep strain. This increase in total creep occurs regardless of the direction of the applied stress, such that it led Ruetz to introduce a material constant, the viscosity of the hardened cement paste, which changes with the drying rate. Probably the effect of moisture on strength is one of the most well known relationships, but the understanding of this effect is one of the least researched subjects. It has been shown experimentally that provided no large rigid particles (sand sizes) are present in a soil-cement, the drier a specimen

10.5 (cont.)

becomes, the greater its strength. The proposed structure for soil-cement is capable of predicting such strength increase during drying.

As mentioned earlier in this thesis, it would appear that the change in strength with changing moisture content of a cement paste or a soil-cement specimen is the key to the increase in creep as moisture enters a sample under stress. As moisture enters a wedge-shaped void, the cohesive forces are immediately reduced, owing to water layers being adsorbed on the surface of the cement gel and/or clay particles, followed later by the formation of capillary water menisci. Therefore, if the cohesive forces holding the solid particles together are suddenly reduced by re-wetting a sample, the structural strength of the specimen as a unit is greatly reduced. Consequently, when a specimen of cement paste or soil-cement is suddenly re-wetted while under a compressive stress, a rapid expansion should take place, followed by creep of the specimen in the opposite direction as the strength of the sample reduces. This effect has been observed in laboratory experiments.

CHAPTER ELEVEN

THE DESIGN OF A SOIL-CEMENT PAVEMENT

In this Chapter, existing design techniques are discussed and compared with a proposed design method for Silverdale Road in Hamilton.

11.1 Current Pavement Design Methods for Soil-Cement

Soil-cement pavements may be considered as either flexible or rigid, depending on the design used and on their performance over a period of time. Most roading engineers have assumed, for design purposes, that soil-cement constitutes a flexible pavement; the depth of soil-cement base has been that normally used for a crushed metal base. But, if one assumes that a soil-cement pavement is flexible, one must expect the slab to break into blocks during flexure, and one must then ensure that these blocks of soil-cement are of a suitable size and durability to withstand continual movement under traffic. If the blocks are less than about 300 mm square, then pavement failure is bound to occur after a period of time as the action of traffic will cause differential elastic displacements between adjacent blocks. Pavement durability increases with increasing cement content, so it follows that a flexible soil-cement pavement designed in this way is likely to be expensive, especially if the same depth of soil-cement is used as would be needed for a good quality gravel base.

The design of a flexible pavement is normally based on the C.B.R. value for the underlying material. Using the empirical

11.1 (cont.)

charts provided by the Road Research Laboratory[120], the required pavement depth can be obtained, while the Portland Cement Association Laboratory Handbook[105] provides the cement content required.

For a sandy pumice soil-cement base, unstabilized sandy pumice sub-base and variable subgrade, as at Silverdale Road, the pavement design should be as follows:-

Material: Sandy clay subgrade. C.B.R. = 8%
Sandy pumice sub-base. C.B.R. = 55%.
Stabilized sandy pumice base. C.B.R. > 80%.

Load: 40 KN wheel load.

Thickness: Subgrade requires minimum cover = 300 mm.
Sub-base requires minimum cover = 100 mm.
Surfacing " " " = 75 mm.

If a soil-cement base is designed as a rigid pavement, i.e. the designer is assured that cracking will not occur, then less cement is generally required over the flexible pavement design. Other advantages are:-

(1) The slab is capable of bridging soft spots in the subgrade.
(2) The pavement is not affected by expansive subgrades.
(3) The design can often be carried out using known theoretical treatments, whereas for flexible pavement design, empirical methods are still required.
(4) The pavement can be constructed in a continuous run, thus eliminating many construction joints.

Disadvantages of a rigid pavement are:

(1) The pavement slab is subject to shrinkage and temperature-induced stresses.

11.1 (cont.)

(2) The pavement slab is subject to fatigue failure from repeated traffic loading.

The rigidly designed pavement may have a lower cement content, but higher costs of construction and of supervisory control must be balanced against the higher maintenance and poorer riding surface usually inherent in a flexible pavement.

Rigid pavement design, on the other hand, requires a much greater knowledge of the materials being used in the pavement, before a design technique is usable. Westergaarde made a theoretical analysis of the case of a uniform slab of isotropic elastic material resting upon an elastic sub-base. Unfortunately, he assumed that the bending stress distribution was linear and that the elastic moduli in tension and compression were the same. Bofinger[14] indicated that both these assumptions were incorrect, and made appropriate corrections for obtaining the true bending moment when using Westergaarde's formulae.

Many pavements are constructed in layers, with a base overlaying a sub-base or subgrade, so considerable attention has been paid to Burmister's analysis of multi-layered elastic systems. Burmister's original analysis has been modified by a number of research workers, so that a multi-layered pavement can now be analyzed for any surface loading, provided the elastic modulus and Poissons ratio for each layer are known. The stresses and strains at the top and bottom of each layer can then be obtained. A computer program capable of carrying out the above design calculations has been produced by Peutz et al[99] at the Shell Laboratories, Amsterdam.

11.2 Pavement Temperatures

Under a bitumen seal coat, the temperature at the top of a pavement slab may rise much higher than the atmospheric temperature, owing to solar radiation. At the same time, the temperature at the bottom of the pavement slab remains nearly constant at a much lower value. Investigations have been made into the effect of these temperature gradients on sections of the soil-cement base obtained from Silverdale Road in Hamilton, and have been described in Appendix XIII.

Interpretation of changing temperatures in terms of stresses being produced by contraction or expansion is not straightforward. The temperature at which a pavement was originally compacted must act as a reference for defining whether a pavement contracts or expands, just as the moulding moisture content, moulding density and cement content at which the pavement is placed, will dictate the shrinkage of a soil-cement. Therefore, any change in temperature from the as-constructed temperature will cause an internal stress.

For the sandy pumice soil-cement and bitumen seal, the coefficient of thermal expansion at the as-moulded moisture content was found to be 3.82×10^{-6}/unit length/°C and 3.96×10^{-6}/unit length/°C for the oven dry state.

The average earth temperature 100 mm below the surface at the time of construction of Silverdale Road (February 1965), was recorded by the Ruakura Research Station adjoining the road site, as 19°C, and this will be taken as the reference temperature for this study on Silverdale Road.

At 3.00 p.m. on 9 March 1965, the hottest day in that summer, a maximum temperature of 48.8°C was estimated (Appendix XIII)

11.2 (cont.)

at the top of the soil-cement base and a temperature of 22.6°C at the bottom of the base, giving a differential of 26.2°C. This means an expansion from the reference length of 11.3×10^{-5}/unit length at the top of the base and 1.38×10^{-5}/unit length at the bottom of the base. The temperature profile through the soil-cement base which will have existed in the early morning of 9 March 1965 would probably have been close to the as-constructed temperature, so little contraction was likely to have taken place. On the other hand, a temperature of 4°C was recorded by the thermometer, at 100 mm below the surface, on 6 July 1965. Assuming a uniform temperature profile throughout the depth of the soil-cement slab, a contraction of 6×10^{-5}/unit length should have occurred from the reference length, owing to the 15°C temperature differential between the recorded and reference temperatures.

No research was found which covered the migration of moisture in a soil-cement slab under temperature gradients, so the test program described in Appendix XIII was set up. From the laboratory tests carried out on small sections of sandy pumice soil-cement from Silverdale Road, the results shown in fig. (9.2) were obtained for moisture content profiles corresponding to 3.00 p.m. on 9 March 1965. It is evident that a marked reduction of moisture content has occurred in the upper portion of the soil-cement base while, in the lower portion, the moisture content has actually increased from the original equilibrium value. The change in moisture profile will cause considerable shrinkage at the top of the soil-cement base and a slight expansion at the bottom. These effects must be added to the natural shrinkage, brought about by net water loss from the clay, to give the total induced stresses.

11.3 Traffic Loading

An estimate of the traffic-induced stresses likely to occur at the top and bottom of the sandy pumice soil-cement base was obtained by using the computer program developed in the Shell Laboratories in Amsterdam[99]. The details of loading, and of pavement material properties, together with the predicted stresses, are given in Table (11.1). For the second set of results (Case II), the properties of the sub-base were changed, but all other parameters were held constant. An accurate value for Possions ratio could not be obtained for the unstabilized sandy pumice, but it was estimated to be between .25 and .3. Computer runs were made with both these values to examine their effect on the stresses in the base. As shown in Table (11.1), there was less than 1% difference in results, indicating that Possion's ratio had very little effect on the stresses in the base.

The stresses obtained are based on a purely elastic theory, the assumption of which seems reasonable when a dynamic state of stress is caused by moving vehicles. If the vehicle is likely to remain parked for a period of time, as in a parking lot, then some allowance for inelastic behaviour in the form of creep would be required. However, on a road, the traffic loading can be assumed to be of short duration, and therefore only elastic stresses will be induced in the soil-cement slab.

Associated with traffic loading is the problem of fatigue failure caused by repeated loading on a pavement slab. As the reduction in strength of the soil-cement slab is directly dependent on the number of repetitions of stress, it follows that a curve of tensile strength vs the number of loading cycles is required.

11.3 (cont.)

As this study was specifically directed at the shrinkage aspects of soil-cement, no experimental work was carried out to obtain such a curve; instead, work carried out by Bofinger[14] on the fatigue failure of soil-cement was used for this analysis. From his results, it was possible to obtain a reasonable estimate of the tensile strength vs number of loading cycles, fig. (11.1). One can assume that the direct tensile strength of the sandy pumice soil-cement, obtained statically, would be its ultimate strength for one load cycle. The reduction in the tensile strength as a function of the number of loading cycles has been estimated from Bofinger's[14] results on Barcaldine soil-cement. Adjustment of the one-cycle tensile strength was necessary to make it correspond with the value measured for the sandy pumice soil-cement.

The curve given in fig. 26 by Bofinger[14] appeared to be the most applicable, in that the moulding moisture content, moulding density and cement content are within the range used for the sandy pumice soil-cement. It will be noticed that the moulding moisture content, cement content and moulding density all play an important part in changing the reduction of the tensile strength. Therefore, if the moulding moisture contents, moulding densities and cement contents for two samples are very similar, the reduction in tensile strength of both samples with repetitive loading should be similar.

An allowance for changing strength with decreasing moisture content should be considered when using fig. (11.1), but the problem of an increasing strength caused by moisture loss is compounded by the loss of strength caused by fatigue . As tensile failure occurs after only a relatively small loss of

11.3 (cont.)

moisture, fig. (11.1) should be adopted without adjustment.

A traffic count of all vehicles on Silverdale Road of 1500 per week was used as a basis from which to study the frequency of heavy vehicle loadings.

As this road is situated close to a developing University site, a greater number of heavy vehicles than normally expected would use the road. A heavy traffic figure of 3% of all vehicles, that is, approximately 2500 heavy vehicles per year is reasonable under the circumstances.

11.4 Shrinkage Stresses

As established in Chapter 9, shrinkage stresses can be adequately represented by the proposed method provided the parameters causing the change in moisture content within a soil-cement base are known. From the computer program on moisture equilibrium under Silverdale Road (Chapter 8), the suctions at distances 130 mm apart covering half the road cross-section have been calculated at intervals of 2 days for the first 6 months of the pavement's life. From these changing suctions, the shrinkage strains can be calculated.

11.5 Prediction of Crack Spacing and Crack Width

Before a soil-cement slab can fail under the action of internal stress, its tensile strength must be exceeded. If we consider Silverdale Road at the stage of being an uncracked continuous slab of soil-cement, the first crack will most likely occur at a local weak point. Once this crack has developed, the stress within the slab adjacent to it will be zero, but further away from the crack in both directions, the sub-base restraint

11.5 (cont.)

(Appendix (XIV)) will be sufficient to develop the full internal stress σ_u in the base at a distance L_{max} from the crack (fig. 11.2). The slab length (L_{max}) at which the tensile stress will become critical is as follows (George[50]):

$$L_{max} = \frac{2\sigma_u}{\mu\gamma'} \qquad \ldots\ldots (11.1)$$

where σ_u = the average ultimate tensile strength across a soil-cement base.

μ = coefficient of sliding friction between slab and sub-base.

γ' = unit weight of material.

Therefore, crack spacing is heavily dependent on the stress that will cause failure. On the other hand, the crack width will be determined by the shrinkage strain developed and the strain released by overcoming sub-base friction. Consider a slab which has cracked at spacings of (L_{max}) as shown in fig. (11.2). Firstly, consider the crack width (δ) developed immediately the crack forms. Two opposing forces are involved, that is, when the base cracks a strain release occurs, but this is opposed by the sub-base friction. As failure will occur instantaneously across the width of the base, the strain release δ_1, and the elongation δ_2 maintained by sub-base friction, will be elastic. δ_1 can be obtained directly from the computer program for predicting internal stress, while

$$\delta_2 = 2\int_0^{\frac{L}{2}} \frac{\sigma_x}{Et}\,dx \qquad \ldots\ldots (11.2)$$

where σ_x is the average stress developed within the base at any given point.

$$\sigma_x = \mu\ \gamma' x$$

11.5 (cont.)

where x = distance from the centre of the crack, as shown in fig. (11.2).

After the base has cracked, shrinkage is likely to continue, thereby further increasing the crack width. This latter change in crack width σ' must occur over a period of time and the stresses developed internally within the base must therefore be subject to stress relief. Consequently, the change in strain after the base has cracked will need to be analyzed using the same computer program designed for the internal stress analysis. The total crack width

$$\delta_T = \delta_1 - \delta_2 + \delta'$$

$$\delta_T = \delta_1 - 2\int_0^{\frac{L}{2}} \frac{\sigma_x}{Et}\,dx + \delta' \qquad \ldots\ldots \quad (11.3)$$

11.6 Proposed Design for a Soil-Cement Pavement

A suitable design method for soil-cement pavements should take into account such factors as cement content, density and moisture content with respect to their performance under repeated load and their ability to shrink.

11.6.1 Design Mix Required

Before a soil-cement pavement can be built, the cement content, moulding density, moulding moisture content and precure moisture content must be specified. The precure moisture content is normally dictated in the field by the moisture content of the natural soil. Therefore, the precure moisture content can be established within a reasonable range before laboratory tests are initiated. On the other hand, the cement content, moulding density and moulding moisture content need to be varied until

11.6 (cont.)

their best combination is found with regard to minimum shrinkage and maximum tensile strength. The following series of laboratory tests should be carried out in order to establish this best combination.

Two identical sets of samples should be prepared - one is required for shrinkage measurements and the other for tensile strength tests. Both sets of samples should be prepared as follows:

From the four material properties to be investigated, namely moulding density, moulding moisture content, precure moisture content and cement content, each one of these properties should be varied while the remainder are held constant. This same procedure should be repeated with the other material properties until a series of curves is obtained as in Chapter 6, which depicts the effects of variations in material properties on both shrinkage and tensile strength. By comparing these curves, the best mix proportions should become obvious. At this stage the economics of the optimum mixture must be examined. Once these best mix proportions have been established, they should be used for all remaining laboratory tests. If the optimum cement content is subsequently found to be too low for pavement stability under repeated loads, then a re-design is necessary with a higher cement content.

11.6.2 Establishment of the Moisture Distribution Under a Road

Before a study can be made of moisture changes within a pavement slab, the environmental conditions at the site must be obtained, for at least the previous five years. This enables

11.6.2 (cont.)

a reasonably accurate prediction to be made of the likely climatic conditions that would be experienced in the years after pavement construction. A similar knowledge of the water table variations is also necessary, but only in rare cases would the ground water levels have been recorded for 5 years before construction. Nevertheless, water level measurements can usually be made for at least one year prior to construction. By comparing these levels with the rainfall in the same year, an estimate of ground water levels in preceding years can be made from the rain-records.

Before movement of moisture in soils can be predicted, the suction-moisture content relationship and the permeability and inverse differential water function must be obtained as described in Chapter 8 for each material present in the final pavement. An allowance of six months should be made to complete these tests because of the slow equilibrium rate at which the moisture contents of the samples adjust to the surrounding conditions.

When these test results have been obtained, the computer program described in Chapter 8 can be used to predict the movement of moisture in the slab for the first year after construction. Within this time, any cracking is likely to have occurred, thus eliminating the necessity for more than one year's behaviour to be predicted.

11.6.3 Predicting the Stresses in a Pavement Design

The predicted suctions for the initial post-construction period do not take into account moisture movement under temperature gradients, but only the seasonal changes in climatic conditions which occur with changing water table levels. To these predicted

11.6.3 (cont.)

suctions must be added the suction changes induced by the daily temperature gradients as discussed in section 11.2. The suction fluctuates on a daily cycle, and reverts to its equilibrium value in the early evening. From the work described in Appendix XIII it appears that temperature gradients in a slab with a bitumen seal cause considerable loss of water from the top section of the soil-cement base which, when added to any other drying effects produced by environmental changes, develops considerable shrinkage in the soil-cement base. Combining this drying shrinkage strain with contraction or expansion owing to temperature changes and with the strains induced by traffic loading gives a net strain profile through the depth of the pavement. This strain profile can be converted readily into a stress profile, and by comparing the stresses in the profile with the tensile strength, the likelihood of cracking can be determined. One must remember that a soil-cement base is subject to fatigue and an appropriate reduction factor should be applied to the tensile strength.

11.7 Proposed Pavement Design Method Applied to Silverdale Road

Using the suggested design technique in section 11.6, the following results would be obtained for Silverdale Road.

11.7.1 Design Mix for Silverdale Road

Table (6.3) compares the actual design mix used in 1965 for construction of Silverdale Road with that proposed in 1970 after carrying out the "acceptance" tests described in Chapter 6. As can be observed from these results, the design mix actually used on the road was fairly close to the proposed design mix, the only difference being the moulding density. From the acceptance tests,

11.7.1 (cont.)

it was found that the moulding density should have been less than that actually used on Silverdale Road. High density is associated with high shrinkage and low tensile strength in the range of densities considered, so it is desirable that the moulding density should be maintained as low as possible.

11.7.2 Moisture Changes in Silverdale Road

From the results presented in Chapter 8 for overall moisture changes in Silverdale Road, it can be seen that the sandy pumice soil-cement base dried out slowly from the as constructed moisture content (at the end of February 1965) to reach its minimum moisture content on 6 July 1965. However, this overall moisture change does not take into account moisture migration under a temperature gradient. When a temperature gradient is applied to the overall moisture equilibrium on 9 March 1965 and on 6 July 1965, the moisture profiles in figs. (9.2) and (11.3) are developed.

The most severe migration of moisture after completion of Silverdale Road occurred on 9 March 1965, and it was not until 9 months later, 13 December, that moisture migration again occurred to the same extent. By this time, the pavement would have gained its full strength and was therefore more able to resist cracking. It should be noted that, if the pavement was subjected to drying early in its life, the likelihood of failure would be high. It would appear that only two times need be investigated as critical, that is 9 March 1965 (warmest summer day after construction) and 6 July 1965, the coldest. By defining these elapsed times as T1 and T2 respectively, it is now possible to use these moisture content profiles to predict the internal stresses which must have developed

11.7.2 (cont.)

within the soil-cement base in Silverdale Road.

11.7.3 Stresses Predicted in Silverdale Road

A computer program was devised to predict the internal stresses induced by shrinkage and temperature strains. The daily changes in moisture content profile (Figs. (9.2) and (11.3)) and temperature gradient greatly complicate the stress analysis, but is is safe to assume that the overall strain changes within the slab are additive with the daily effects being applied only when they are detrimental to the pavement's stability.

The stresses obtained from the sum of all the strains are presented in Table (11.2). Tensile failure does not occur within the soil-cement base for time T1, but does occur for time T2 for both Case I and Case II loading. For Case I loading, it has been found that the fatigue tensile strength of the soil-cement base is less than the combined stress developed at the bottom of the slab, owing to wheel loadings, shrinkage and temperature changes. Therefore, cracking of the pavement should occur. On the other hand, Case II loading only occurs near the corner of a slab, that is after a crack has broken a continuous slab into two or more pieces. This latter type of loading is extremely severe, as shown by the high stresses predicted in the top of the soil-cement base.

From the results presented in Table (11.2), it is evident that for Silverdale Road the shrinkage stresses and the stresses caused by temperature gradients play only a minor role in causing bottom layer tension failures compared with the stresses produced by wheel loadings, and the reduction in the tensile strength of the sandy pumice soil-cement by fatigue. On the other hand,

11.7.3 (cont.)

when the wheel loading is such that tension is developed in the top of the soil-cement base, the combined effects of shrinkage and temperature gradient-induced stresses are considerable.

11.7.4 Prediction of Crack Spacing and Crack Width in Silverdale Road

Before a soil-cement slab can crack, the internally developed stresses must become equal to the tensile strength of the slab. By using the proposed shrinkage stress method (Chapter 9) the strains caused by predicted moisture changes at any time can be obtained. On combining these strain changes with the daily strain changes caused by moisture migration under temperature gradients, and with the expansion or contraction caused by temperature variations, the total strains caused by internal stresses are obtained. The strains caused by the externally applied traffic loadings can also be added to the strains caused by internal stresses. Then by using the proposed shrinkage stress method, the stresses on any day throughout the year can be obtained.

Comparing the tensile strength reduced by fatigue with the stresses predicted, it was possible to predict the time at which cracking of the slab would occur. For the sandy pumice soil-cement base used on Silverdale Road, it was found that failure should have occurred on 9 May 1965.

Under actual field conditions, cracking would have occurred over a period of time and not all exactly on 9 May, but it had been observed that cracking of Silverdale Road did in fact occur approximately seven weeks after the pavement had been completed i.e. about the end of April. These observations tie in closely

11.7.4 (cont.)

with the predicted time of cracking.

The distance between cracks (L_{max}) can be calculated from equation 11.1. For the sandy pumice soil-cement base used on Silverdale Road, the average value of L_{max} was 3.29 M. In section 8.6.2.1 it was mentioned that the average spacing of cracks on Silverdale Road was 2.98 M, which is reasonably close to the predicted value.

When a crack forms, stress is released so that the opening of a crack is controlled by the strain release and the frictional restraint to sliding between the base and the sub-base. Using equation 11.3, δ_1 was found to be 9.8 mm for the sandy pumice soil-cement base in Silverdale Road, and δ_2 was 4.6 mm. For this pavement, δ' was found to be extremely small; therefore, the total crack width δ_T would be 5.2 mm. It was difficult to measure the actual crack width in the field, but it appeared to be approximately 4 mm.

To conclude, it has been shown that the methods proposed in this chapter to predict time of crack formation, crack spacing and crack width agree with actual field occurrences. In this study of Silverdale Road, the shrinkage strains which develop are quite small compared with those predicted for a pavement base constructed of loess soil-cement; therefore, the importance of allowing for shrinkage strains has not been greatly emphasized in this study. By increasing the pavement depth from 127 mm to 152 mm cracking would not have occurred in Silverdale Road. If a full-scale loess soil-cement base had been studied, then the opposite effect would have been observed, that is, the shrinkage strains alone would have been enough to cause cracking of the base regardless of its depth.

CHAPTER TWELVE

CONCLUSIONS AND RECOMMENDATIONS

The recommended techniques for sample preparation and testing are summarized and the predictions of moisture flow, stresses and cracking in soil-cement slabs are examined. Design recommendations in the light of this research are presented.

12.1 Sample Preparation

Soil-cement samples should be compacted either by kneading action or under a static load. A kneading compactor is better for the manufacture of soil-cement samples for research work, but for routine laboratory tests statically compacted samples have been found entirely satisfactory.

Specimens 13 mm diameter are recommended for most tests, but their length depends on the test being performed - 102 mm long is most suitable for obtaining the free unrestrained shrinkage versus moisture content curve and the creep in tension with respect to moisture content and time, while 26 mm long (with 2:1 length/diameter ratio) is better for strength tests and for measuring creep in compression.

12.2 Testing Techniques Used for Determining the Suitability of a Particular Soil-Cement

It is recommended that the testing techniques from BS 1924:1967 be used to determine the suitability of a particular soil for producing soil-cement.

A soil-cement should be moulded under conditions which

12.2 (cont.)

minimize shrinkage, yet retain a high tensile strength. By carrying out the series of tests described in section 6.3, the optimum moulding conditions of precure moisture content, cement and moisture content, and density (Tables 6.2 and 6.3) can be obtained. By comparison, the present design practice for soil-cement specifies the optimum moisture content and corresponding maximum density for the moulding conditions, the cement content normally being determined as that necessary to give a specified minimum unconfined compressive strength.

12.3 Predicting Moisture Flow in Soil-Cement

If the moisture content of a particular soil-cement sample is expressed in terms of soil suction and the inverse differential water function and diffusivity function are obtained experimentally, then the diffusion equation can be used to predict moisture migration under suction gradients. The accuracy of the predictions by this method has been verified by laboratory measurements on four different sizes of specimens. The suction versus moisture content curve and the inverse differential water function for a soil-cement can be obtained experimentally with a high degree of accuracy, but the diffusivity function cannot be found by conventional experimental techniques. No satisfactory method for obtaining the diffusivity function was found in the literature; the method evolved in this project was to obtain the diffusivity coefficients from the moisture content profiles, and from these to construct the diffusivity function for a particular soil-cement. The above method yielded satisfactory results in this project, fortunately without a large amount of experimentation.

12.3 (cont.)

When the flow parameters experimentally determined for the sandy pumice soil-cement were applied in an analysis of the soil-cement base of Silverdale Road, the suction changes which were predicted were close to those which had been observed in the limited recordings made at the site. Because Silverdale Road was not built especially for this research project, and in fact was completed before this project was begun, many factors, including accurate recordings of the moisture changes and of the water table were unknown. Nevertheless, from the information obtained from Silverdale Road, it is evident that the computer program for moisture flow can be used to predict moisture changes in a pavement slab.

Probably the most important factor which has emerged from the moisture flow study in this project is the major effect of temperature gradients in causing moisture migration below a bitumen seal. Many temperature changes occur in a soil-cement slab during any year, so it is desirable that one can predict the migration of moisture with change in temperature gradient using a theoretical method, instead of relying entirely on experimental results. Some research has been carried out using temperature gradients to predict moisture migration in unstabilized soils, but an extension of this work to soil-cement was beyond the scope of this project.

12.4 Predicting Stresses in Soil-Cement

Before shrinkage stresses in soil-cement can be predicted, both the time-rate of moisture change and the absolute evaporable moisture present must be determined. It has been assumed (section 9.1.5) that any shrinkage during moist curing will have little

12.4 (cont.)

effect on the shrinkage stresses which develop within a soil-cement prism as it dries. Therefore, only drying shrinkage stresses have been considered in the theoretical method proposed in this thesis.

All the theoretical methods of shrinkage stress analysis for soil-cement which have been published to date have been shown in Chapter 7. These were found to be unreliable because of the inaccurate assumptions used to derive their theory. The use of slowly-dried, 13 mm diameter soil-cement samples to obtain the curve of free unrestrained shrinkage versus moisture content appears to be the best practical approach for obtaining a measure of the actual free unrestrained shrinkage at any position in a soil-cement prism. The strength of a soil-cement has been shown (section 9.1.9) to be related to the moisture contained in the sample, and like the free unrestrained shrinkage, it is independent of time.

On the other hand, the representation of creep in a soil-cement has caused a considerable problem as explained in Chapter 9. For a creep test both the initial moisture content of the sample and the rate at which drying occurs affect the result. Consequently, a large number of different creep tests were carried out for this project, using different combinations of initial moisture content, drying rate, and applied stress. In a soil-cement prism drying from one side, both the drying rate and the induced stress vary with time, the stress changing from tension to compression as strain reversal occurs.

The most important requirement in any experimental creep test on soil-cement is the control of the drying rate of the

12.4 (cont.)

specimen under load. Time was too limited in this project to permit the degree of control of the drying rate which would be desirable, but specially designed chambers should have been used similar to those made for the carbonation experiment, section 9.1.1.

Creep tests with constant applied stress and variable drying rates are relatively easy to perform, but if the applied stresses are to be variable, other problems arise. Measurements of creep under varying stress were made using an apparatus in which a small increment of load was added twice daily, giving a stepped loading curve. The results obtained were not good (section 9.1.8) and it is recommended that any future variable loading creep tests should be done using a constant strain-rate loading machine, with the load and deformation recorded as a function of time on a strip-chart recorder. For this project the above equipment was not available for use on this project, thus necessitating the use of the step-loading method.

From this project it has been found that the only acceptable way to represent creep strain changes in a soil-cement is by the use of a rheological model. This in turn means that any creep test which is carried out on a prismatic specimen, provided it is truly representative of the actual conditions which will exist in a large soil-cement slab, need only serve to check the validity of the rheological model and to obtain the appropriate coefficients for the model.

12.4 (cont.)

Thereafter, the process of evaluating shrinkage stresses, as proposed in this thesis, appears to be sufficiently accurate to warrant further study using other types of soil-cement. Even though the Maxwell model does not represent all the creep strain changes which occur when stresses are being released, it does accurately represent the changes in creep strains as stresses are increased. For this reason there is good correspondence between the predicted and measured shrinkage stresses for the soil-cement prisms studied in this project.

12.5 Crack Prediction for Silverdale Road

A pavement with a soil-cement base similar to that used on Silverdale Road will be subjected to many changes of stress throughout its life span. These stresses are caused by traffic loading, temperature gradients and internal strain changes within the soil-cement base. As shown in Chapter 11, it is the combined effect of all these stresses which ultimately causes failure. In many of the previously designed soil-cement pavements, only traffic loading has been used to assess the likelihood of a pavement failure. The stresses caused by traffic loading in Silverdale Road, as elsewhere, are normally much more severe than other induced stresses, but it is the combination of all stresses which eventually cause failure. For instance, it was observed on the Lyttelton Tunnel Road in Canterbury, that the loess soil-cement base cracked into approximately 2 m long slabs within 6 months of the pavement being placed. From the study of loess soil-cement made in this project it is apparent that a loess soil-cement under shrinkage induced stresses only, will fail. Therefore on the Tunnel Road which was carrying vehicles

12.5 (cont.)

it is evident that rapid failure in the form of cracking must have occurred. It can be concluded that loess soil-cement should not be used for pavement construction unless the blocks which form as a result of cracking can be regarded as acceptable for overall pavement stability.

12.6 Design Recommendations

The following testing methods and procedures for design use are recommended.

1. In a soil-cement slab design it is evident that the tensile strength is critical; therefore the indirect tension test should replace the standard unconfined compression test when testing for the acceptibility of a soil-cement.

2. Shrinkage strains should be measured for the soil-cement being used in a pavement design. Shrinkage should be measured on a drying 13 mm diameter sample and plotted with respect to its moisture content. Valuable information on the potential shrinkage of a soil-cement can be gained from this graph.

3. Designers of future soil-cement pavement slabs should specify all the tests required for the proposed shrinkage stress analysis, as presented in this thesis, but the experimental work involved may not be warranted for the design of secondary roads. Therefore, at least until further research work has been carried out, it is essential for the designer to be aware of the magnitude of potential shrinkage stresses, which can develop within a soil-cement. Even if a full analysis of all shrinkage stresses were not carried out, if a conservative estimate of the likely maximum shrinkage stress were incorporated in the

12.6 (cont.)

design, it would probably eliminate many of the failures which have previously occurred in soil-cement slabs.

12.7 Suggestions for Future Research

This project has but scratched the surface of the problems which were encountered when the internal stress build-up within a soil-cement base was investigated. Several topics for further research were found, but were not pursued since they were secondary to the main objects of this project. They are listed below.

1. The effects of differing moisture content on the elastic modulus for both tension and compression should be investigated especially in choosing a rheological model for the representation of creep.

2. As mentioned earlier in this chapter, a large amount of research still needs to be carried out on the representation of creep using rheological models. A better understanding of creep strains will almost certainly provide a better knowledge of the soil-cement structure as proposed in section 4.5. By comparing the creep curves with the characteristics of different rheological models, the most representative one for the soil-cement should be able to be found. It is quite possible that a rheological model other than the Maxwell model will be more representative of the creep characteristics.

3. Another important area of research which requires a great deal more work than time permitted in this project is on the relaxation of creep when stresses are gradually or rapidly reduced or reversed. Sudden reductions of stress occur when a soil-cement pavement slab cracks and stress reversal occurs when a pavement slab is subjected to strain reversal.

12.7 (cont.)

4. By building a full sized soil-cement pavement slab and monitoring environmental conditions, it would be possible to observe the slab's performance under field conditions and to record the time and extent of cracking. Loess soil-cement should be used since this is known to crack under internal stress build-up alone. The initial study on such a pavement should be carried out without the interference of traffic loadings. In the extension of this study, traffic loading should be introduced so that pavement failure would be accelerated. In these studies on actual pavements, cores should be removed from the soil-cement slab at different times, and cut so that the moisture content at different depths can be measured at each time. Likewise the water table level, temperatures of different depths within the base, air temperature, air humidity evaporation and rainfall would need to be recorded continually over the period of the study.

REFERENCES

1. AITCHISON, G.D. and HOLMES, J.W.: Suction profiles in soils beneath covered and uncovered areas, Proc. Fifth International Conference on S.M. and F.E., 2, 1961, pp.197-91.

2. AITCHISON, G.D. and RICHARDS, B.G.: A broad study of moisture conditions in pavement subgrades throughout Australia. Pt. 2 Techniques adopted for the measurement of moisture variables. P.191-204 Moisture equilibrium and moisture changes in soils beneath covered areas, 1965, Butterworths.

3. AITCHISON, G.D., RUSSAM, K. and RICHARDS, B.G.: Engineering concepts of moisture equilibria and moisture changes in soils. Road Research Laboratory Report No. 38.

4. ASTM D1632-59: Making and curing soil-cement compression and flexure test specimens in laboratory.

5. ASTM D560-57: Freezing and thawing soil-cement mixtures.

6. ASTM D559-57: Wetting and drying soil-cement mixtures.

7. BAŽANT, Z.P.: Constitutive equation for concrete creep and shrinkage based on thermodynamics of multi-phase systems, Materials and Structures No. 13, 1970, p.3.

8. BELCHER, D.J.: The measurement of soil moisture and density by neutron and gamma-ray scattering, Highway Research Board, Special Report 2, p.98.

9. BERNHARDT, C.T.: Creep and shrinkage of concrete, Materials and Structures, Vol. 2, No. 8, March-April 1969, pp.145-148.

10. BLACK, W.P.M., CRONEY, D. and JACOBS, J.C.: Field studies of the movement of soil moisture, Road Research Laboratory, Tech. Paper No. 41.

11. BOFINGER, H.E.: The structure of soil-cement, Australian Road Research Board, Vol. 2, No. 1, p.46.

12. BOFINGER, H.E.: Further studies of the tensile fatigue of soil-cement, Australian Road Research Board, Vol. 4, No. 1, Sept. 1969, pp.69-80.

13. BOFINGER, H.E.: The measurement of the tensile properties of soil-cement. Road Research Laboratory, Report LP 365.

14. BOFINGER, H.E.: Soil-cement as a rigid pavement material, Unpublished Ph.D. Thesis, Queensland University.

15. BOFINGER, H.E.: The creep of clay cement under steady tensile stress, Australian Road Research Board, Vol. 4, 1970, No. 3.

16. BOFINGER, H.E.: The creep of clay-cement under steady stress, ARRB, Vol. 4, 1970, No. 3.

17. BOFINGER, H.E. and SULLIVAN, G.A.: An investigation of cracking in soil-cement bases for roads. Road Research Laboratories Report, LR 379.

18. BOX, J.E.: Design and calibration of a thermocouple psychrometer which uses the Peltier effect, Humity and Moisture, Vol. 1, 1965, pp.110-121.

19. BRITISH STANDARD, 1924:1967: Methods of tests for stabilized soils.

20. CARLSON, R.W.: Drying shrinkage of large concrete members, ACI Journal Proc., Jan-Feb. 1937, Vol. 33, pp.327-336.

21. CASSEL, D.K., WARRICK, A.W., NIELSON, D.R. and BIGGAR, J.W.: Soil-water diffusivity values based upon time dependent soil-water content distributions, Proc. Soil Science Society of America, Vol. 32, No. 6, 1968, p.774.

22. CHRISTIAN, B.H. and PATTEN, B.J.F.: Multi-phase aspects of concrete drying shrinkage, Report No. R.22, University of New South Wales, 1967.

23. CICERO, L.J., DAVIDSON, D.T. and DAVID, H.T.: Strength-maturity relations of soil-cement mixtures, Highway Research Board Bulletin No. 353, pp.84-97.

24. CLEGG, B.: Kneading Compaction, Australian Road Research Board Journal, Vol. 1, No. 9, p.34.

25. COLEMAN, J.D. and MARSH, A.D.: An investigation of the pressure membrane method, J. Soil Sce. 12, (2), pp.343-62.

26. COPELAND, L.E. and CHANG.: Carbon replica in electron microscopy, Journal of the P.C.A. Research and Development Laboratories, Vol. 6, No. 3, Sept. 1964, pp.53-54.

27. CROFT, J.B.: The process involved in the lime stabilization of clay soils, Proc. Australian Road Research Board, Vol. 2, pt. 2, pp.1169-1203.

28. CROFT, J.B.: The structures of soils stabilized with cementatious agents, Engineering Geology, Vo. 2, 1967, pp.63-80.

29. CRONEY, D., COLEMAN, J.D. and BLACK, : Movement and distribution of water in soil in relation to highway design and performance, Highway Research Board, Special Report No. 40. p.226.

30. CRONEY, D., COLEMAN, J.D. and BRIDGE, P.M.: The suction of moisture held in soil and other porous materials, Road Research Laboratory, Technical Paper, 1952, No. 24.

31. DAVIDSON, D.T., PITRE, G.L., MATEOS, M. and GEORGE, K.P.: Moisture-density, moisture-strength and compaction characteristics of cement-treated soil mixtures, Highway Research Board Bulletin, No. 353, pp.42-63.

32. DAVIS, R.E. and TRAVELL, G.E.: Properties of concrete and their influence on prestress design, A.C.I. Journal, Proc. 50, 1954, pp.381-391.

33. DIAMOND, S. and KINTER, E.B.: Mechanisms of soil-lime stabilization: an interpretive review, Highway Research Board Record, 92, 1965, pp.83-95.

34. DIAMOND, S., WHITE, J.L. and DOLCH, W.L.: Transformation of clay minerals by calcium hydroxide attack, Proc. 12th Natnl. Conf. Clay and Clay Mins, 1964, pp.359-380.

35. DODD, T.A.H. and DUNLOP, R.J.: An improved kneading compaction machine, University of Canterbury, New Zealand.

36. DOERING, E.J.: Soil-water diffusivity by the one-step method, Soil Science Society of America, Vol. 99, No. 5, p.322.

37. DUMBLETON, M.J.: The suction and strength of remoulded soils as affected by composition, Road Research Laboratory, LR 306, TEI G786.

38. DUNLOP, R.J.: Laboratory testing for cement and/or lime stabilization of soil, University of Canterbury, New Zealand, Civil Engineering Department, Report, 1970.

39. DUNLOP, R.J., MOSS, P.J. and DODD, T.A.H.: Shrinkage cracking of soil-cement, R.R.U. Bulletin, No. 12, National Roads Board, New Zealand.

40. DUNLOP, R.J. and DODD, T.A.H.: Analysis of shrinkage cracking in soil-cement, New Zealand Concrete Construction, Vol. 16, No. 2, April 1972.

41. DUNLOP, R.J., MOSS, P.J. and DODD, T.A.H.: Shrinkage stresses in soil-cement pavements, Sixth Conference, Australian Road Research Board, Canberra 1972.

42. EL-RAWI, N.M.: Strength characteristics of soil-cement mixtures, Oklahoma State University, Unpublished Ph.D. Thesis, 1967.

43. EL-RAWI, N.M., HALIBURTON, T.A. and JAMES R.L.: Effect of compaction method on strength parameters of soil-cement mixtures, Highway Research Record, No. 255, p.72.

44. EL-RAWI, N.M., HALIBURTON, T.A. and JAMES, R.L.: Effect of compaction on strength of soil-cement, American Society of Civil Engineers, Vol. 93, No. S.M.6, Nov. 1967, pp.195-208.

45. FANG, H.Y.: Influence of temperature and other climatic factors on the performance of soil pavement systems, Highway Research Record, Special Report 103.

46. FELT, E.J.: Factors affecting the properties of soil-cement mixtures, Highway Research Board Bulletin, No. 108, 138-162.

47. FREEZE, R.A.: The mechanism of natural ground-water recharge and discharge 1. One-dimensional, vertical unsteady, unsaturated flow above a recharging or discharging ground waterflow system, Water Resource Research, 1969, Vol. 5, No. 1.

48. GARDNER, W.R.: Calculation of capillary conductivity from pressure plate outflow data, Proc. Soil Sci. Soc. Am., 1956, 20, pp.317-20.

49. GARY, J.W.: An instrument for in-situ measurement of soil moisture flow and suction, Soil Science Society of America Proc., 1968, Vol. 32, No. 1, p.3.

50. GEORGE, K.P.: Cracking in cement-treated bases and means for minimizing it, Highway Research Record, No. 255, pp.59-71.

51. GEORGE, K.P.: Cracking in pavements influenced by visco-elastic properties of soil-cement, Highway Research Record, No. 263, pp.47-59.

52. GEORGE, K.P.: Shrinkage cracking of soil-cement base: theoretical and model studies, Highway Research Record, No. 351, pp.115-133.

53. GEORGE, K.P.: Shrinkage characteristics of soil-cement mixtures, Highway Research Record, No. 255, pp.42-58.

54. GOPALAKRISNNAN, K.S., NEVILLE, A.M. and GHALI, A.: - Elastic and time dependent effects of aggregate-matrix interaction, Materials and Structures, 1970, Vol. 3, No. 16.

55. GRIM, R.E.: Clay mineralogy, McGraw-Hill, 2nd. Ed.

56. GRIMER, F.J. and KRAWCZYK, J.: Relations between strength and age for soil-cement, with particular reference to the prediction of later strengths from earlier strengths, Magazine Concrete Research, 1963, Vol. 15, No. 43.

57. GRIMER, F.J. and ROSS, N.F.: The effect of pulverization on the quality of clay cement, Proc. of the 4th Inter. Conf. Soil Mech. and Found. Engnrg., 1957, Vol. 2, pp.109-113.

58. HANNANT, D.J.: The mechanism of creep in concrete, Materials and Structures, 1968, Vol. 1, No. 5, p. 403.

59. HANSEN, T.C.: Surface cracking of mass concrete structures at early form removal, Extrait du Bulletin Rilem, Sept., No. 28, pp.145-153.

60. HANSEN, T.C.: Creep of concrete, Swedish Cement and Concrete Research Institute, Stockholm, Bulletin No. 33, 1958, p.48.

61. HARMATHY, T.Z.: Moisture and heat transport with particular reference to concrete, Highway Research Record, No. 342, p.5.

62. HARMATHY, T.Z.: Simultaneous moisture and heat transfer in porous systems with particular reference to drying, I. and E.C. Fundamentals, 1969, Vol. 8, No. 1.

63. HERZOG, A.: The structure of clay cement, C.S.I.R.O. Research Report, No. 85, Paper 2, pp.2-1.

64. HERZOG, A.: Evidence for a skeleton-matrix structure in clays stabilized with Portland cement, Proc. 5th Australian and New Zealand Conf. S.M. and F.E., pp.55-61.

65. HUDSON, W.R. and KENNEDY, T.W.: An indirect tensile test for stabilized materials, Center for Highway Research, University of Texas at Austin Research, Report No. 98-1, January 1968.

66. ILLSON, J.M.: The creep of concrete under uniaxial tension, Magazine of Concrete Research, June, 1965, Vol. 17, No. 51.

67. INGLES, O.G.: Advances in soil stabilization, C.S.I.R.O. Division of Soil Mechanics Research, 1961-67, Paper No. 108.

68. ISHAI, O.: The time dependent deformation behaviour of cement paste mortar and concrete, The Structure of Concrete (Proc.), 1965, p.345.

69. JACKSON, R.D., VAN BAVEL, C.H.M. and REGINATO, R.J.: Examination of pressure-plate outflow method for measuring capillary conductivity, Soil Science, Vol. 96, p.249.

70. JOHNSTON, C.D. and SIDWELL, E.H.: Influence of drying on strength of concrete specimens, A.C.I. Journal, Sept. 1969, p.748.

71. KALOUSEK, G.L.: Fundamental factors in the drying shrinkage of concrete block, Pro. A.C.I., Vol. 51, 1955, p.233.

72. KAWAMURA, M.: Shrinkage stresses in concrete as a visco-elastic material, A.C.I. Journal Proc., Vol. 66, No. 12, Dec. 1969, pp.968-971.

73. KAWAMURA, M.: Fundamental studies on the fabric of soil-cement mixture and its mechanical properties, Unpublished Ph.D. Thesis, Koyto University, 1970.

74. KENNEDY, T.W. and HUDSON, W.R.: Application of the indirect tensile test to stabilized materials, Highway Research Record, No. 235, pp.36-48.

75. KEZDI, A. and NAGYVATI, B.: Strength of stabilized soils, Asta Technica (Budapest), Vol. 62, No. 1-2, 1968, pp.75-95.

76. KLUG, P. and WITTMANN, F.: The correlation between creep deformation and stress relaxation in concrete, Materials and Structures, Vol. 3, No. 14, 1970, p.75.

77. KLUTE, A.: A numerical method for solving the flow equation for water in unsaturated materials, Soil Sci., 1952, 72, pp.105-16.

78. KUNZE, R.J. and KIRKHAM, D.: Simplified accounting for membrane independence, Soil Science Society of America Proc., Vol. 26, No. 5, p.421.

79. LAMBE, T.W.: The structure of compacted clay, Journal Soil Mechanics and Foundations Division, American Society of Civil Engineers, Vol. 84, No. SM2, 1958, p. 1654.

80. LEE, E.H.: Stress analysis in viscoelastic bodies, Quarterly of Applied Mathematics, Vol. 13, No. 2, pp.183-190.

81. L'HERMITE, R.G.: Volume changes of concrete, Proc. Fourth Inter. Symp. on the Chemistry of Cement, Washington D.C., No. 2, 1960, pp.659-694.

82. METCALF, J.B.: The effect of high curing temperatures on the unconfined compressive strength of a heavy clay stabilized with lime and with cement, Fourth Australian and New Zealand Conf. S.M. and F.E.

83. METCALF, J.B. and FRYDMAN, S.: A preliminary study of the tensile stresses in stabilized soil pavements, Australian Road Research Board Proc., 1962, Vol. 1, Part 2, p.1048.

84. METCALF, J.B. and FRYDMAN, S.: A preliminary study of the tensile stresses in stabilized soil Pavements, Proc. First Conf. Australian Road Research Board, 1962, Vol. 1, Part 2, p.1048.

85. MEYERS, B.L. and SLATE, F.O.: Creep and creep recovery of plain concretes as influenced by moisture conditions and other variables, Magazine Concrete Research, 1970, Vol. 22, No. 70.

86. MILLER, E.E. and ELRICK, D.E.: Dynamic determination of capillary conductivity extended for non-negligible membrane impedance, Proc. Soil Sci. Soc. Am., 22, (6), 1958, p.483-6.

87. MILLS, R.H.: Influence of water in areas of restricted adsorption on properties of concrete, Materials and Structures, 1968, Vol. 1, No. 6, p.553.

88. MITCHELL, N.B. Jr.: The indirect tension test for concrete, Materials Research and Standards, ASTM, October 1961, Vol. 1, No. 10, pp.780-787.

89. MITZEL, A.: Concrete creep and shrinkage, Bldg. Science, Nov. 1967, Vol. 2, No. 3, pp.259-265.

90. MITZEL, A. and KLAPOC, M.: On superposition of shrinkage and creep deformations Bldg. Science, Nov. 1967, Vol. 2, No. 3, pp.267-271.

91. MOORE, R.K., KENNEDY, T.W. and HUDSON, W.R.: Factors affecting the tensile strength of cement treated material, Highway Research Record, No. 315, p.64.

92. NAKAYAMA, H. and HARDY, R.L.: Factors influencing shrinkage of soil-cement, Highway Research Record, No. 86, pp.15-27.

93. NEVILLE, A.M.: Current problems in shrinkage of concrete as affected by cement paste, Civil Engineering (Lond.), Nov. 1968, Vol. 63, No. 748, pp.1223,1225,1227,1229,1231.

94. NEVILLE, A.M.: The measurements of creep of mortar under fully controlled conditions, Magazine of Concrete Research, 1957, Vol. 9, No. 25, p.3.

95. NEVILLE, A.M.: Creep of concrete: plain, reinforced and prestressed, Amsterdam, North-Holland Publishing Co., 1970.

96. NEVILLE, A.M. and MEYERS, B.L.: Creep of concrete: influencing factors and prediction, Symp. on Creep of Concrete, SP.9, ACI TI M678.

97. NEVILLE, A.M., STAUNTON, M.M. and BONN, G.M.: A study of the relation between creep and gain of strength of concrete, Symp. on Structure of P.C. Paste and Concrete. Highway Research Board S.P. 90, pp.186-203.

98. OKADA, K. and KAWAMURA, M.: Some considerations on drying shrinkage stresses of soil-cement, Transactions of the Japan Society of Civil Engineers (In Japanese), 1967, No. 142, pp.37-45.

99. PEUTZ, M.G.F., JONES, A. and VAN KEMPON, H.P.M.: Computer program. Layered systems under normal surface loads, Shell Laboratory, Amsterdam, 1968.

100. PICKETT, G.: Shrinkage stresses in concrete, A.C.I. Journal Proc., 1946, Vol. 42, Part 1, p.165; Part 2, p.361.

101. PICKETT, G.: The effects of change in moisture content of the creep of concrete under sustained load, A.C.I. Vol. 13, No. 4, 1942, p.333.

102. PICKETT, G.: Effect of aggregate on shrinkage of concrete and a hypothesis concerning shrinkage, Journal A.C.I., 1956, Vol. 27, No. 5, pp.581-590.

103. PLASTER, R.W. and NOBLE, D.F.: Reactions and strength development in Portland cement-soil mixtures, Highway Research Record, 315, 1970, pp.46-63.

104. POLLARD, J.S.: The inter-relation of atmospheric, binder and road surface temperature, 1967 New Zealand Roading Symposium.

105. PORTLAND Cement Association, Laboratory Handbook, 1959, 5th Edition, Chicago.

106. POWERS, T.C.: Mechanisms of shrinkage and reversible creep of hardened cement paste, The Structure of Concrete Proc., 1965, p.319.

107. POWERS, T.C.: Causes and control of volume change, P.C.A. Journal Research and Development Labs., 1959, Vol. 1, No. 1, pp.29-39.

108. PRETORIUS, P.C. and MONISMITH, C.L.: Prediction of shrinkage stresses in pavements containing soil-cement bases, Highway Research Record, No. 362.

109. RAWLINS, S.L. and DALTON, F.N.: Psychrometric measurements of soil water potential without precise temperature control, Proc. Soil Science Society of America, 1967, Vol. 31, No. 3, p.297.

110. REDWARD, J.W.: Design of a kneading compactor, Project Report, Soil Mechanics, 1968, University of Canterbury.

111. RICHARDS, B.G.: Review of measurement of soil water variables and flow parameters, C.S.I.R.O. Div. of S.M. Research Paper No. 106. Reprinted from Proc. 4th Conf. A.R.R.B., 1968, Vol. 4, Part 2, pp.1843-1861.

112. RICHARDS, B.G.: A review of methods for the determination of the moisture flow properties of unsaturated soils, C.S.I.R.O. Soil Mechanics Section, Tech. Memo. No. 5, 1967.

113. RICHARDS, B.G.: A mathematical model for moisture flow in Horsham clay, C.S.I.R.O. Div. of S.M., Research Paper No. 109.

114. RICHARDS, B.G.: The solution of the two-dimensional moisture flow equation applied to road subgrade soil conditions, C.S.I.R.O. Div. of S.M., Research Paper No. 96.

115. RICHARDS, B.G.: Psychrometric techniques for measuring soil water potential, C.S.I.R.O. Div. of S.M., Tech Report No. 9, 1969.

116. RICHARDS, B.G.: Determination of the unsaturated permeability and diffusivity functions from pressure plate outflow data with non-negligible membrane impedance, Moisture equilibria and moisture changes in soils beneath covered areas, Butterworths, 1965.

117. RICHARDS, B.G. and CHAN, C.Y.: Theoretical analyses of subgrade moisture under Australian environmental conditions and their practical implications, Australian Road Research, 1971, Vol. 4, No. 5.

118. RICHARDS, L.A. and RICHARDS, P.L.: Radial flow cells for soil-water measurements, Proc. Soil Sci. Soc. Am., 1962, Vol. 26, No. 6, pp.515-8.

119. RIJTEMA, P.E.: Calculation of capillary conductivity from pressure plate outflow data with non-negligible membrane impendance. Heth. J. Agric. Sci., 1959, 7, pp.209-15.

120. ROAD RESEARCH LABORATORY,: Soil Mechanics for Road Engineers, H.M. Stationery Office, London, p.81 and p.407.

121. ROPER, N.: Dimensional change and water adsorption studies of cement paste, Highway Research Record SP 90.

122. RUBIN, J.: Theoretical analysis of two dimension transient flow of water in unsaturated and partly unsaturated soils, Soil Science Society of America Proc., 1968, Vol. 32, No. 5.

123. RUETZ, W.: A hypothesis for the creep of hardened cement paste and influence of simultaneous shrinkage, The Structure of Concrete (Proc.), 1965, p.365.

124. RUFF, C.G. and HO, C.: Time-temperature-strength-reaction product relationships in lime-bentonite-water mixtures, Highway Research Board Record, 1966, 139, pp.42-60.

125. RUSSAM, K.: Subgrade moisture studies by the British Road Research Laboratory, Highway Research Record No. 301.

126. SCHOFIELD, R.K.: The pF of the water in soil, Trans. 3rd Internat. Congr. Soil. Sci., 1935, 2, pp.37-48.

127. SEED, N.B. and CHAN, C.K.: Strength characteristics of compacted clays, Journal Soil Mechanics and Foundation Division, American Society of Civil Engineers, 1959, Vol. 85, No. SM5.

128. SLOANE, R.L.: Early reaction determination in two hydroxide-kaolinite, Systems by Electron Microscopy and Diffraction Proc. 13th Natnl. Conf. Clays and Clay Mins., 1966, pp.331-339.

129. STOCKER, P.T.: Diffusion and diffuse cementation in lime and cement-stabilized clayey soils, Ph.D. Thesis to University of Queensland, 1968.

130. STOCKER, P.T.: Private Communications, 1971.

131. STOCKER, P.T.: Diffusion and diffuse cementation in lime and cement-stabilized clayey soils, Private Communications.

132. STOCKER, P.T.: The interaction of inorganic additives with soils, C.S.I.R.O. Research paper, No. 85, p.6-5.

133. SWARTZENDRUBER, D.: The applicability of Darcy's law, Proc. Soil Science Society of America, 1968, Vol. 32, No. 1, p.11.

134. TEST METHOD NO. CALIF. 901-B: Method of Operation and Calibration of the Mechanical Compactor.

135. The Structure of Concrete Conference.: The structure of concrete and its behaviour under load, Proc. of an International Conference, London, Sept. 1965. Published by the Cement and Concrete Association.

136. THOM, H.C.S.: Quantative evaluation of climatic factors in relation to soil moisture regime, Highway Research Record No. 301.

137. THOMPSON, M.R.: Split-tensile strength of lime-stabilized soils, Highway Research Record No. 92, pp.69-82.

138. VERBECK, G.J.: Carbonation of hydrated Portland cement, Portland Cement Assoc. Bulletin, No. 87.

139. WALLO, E.M.: Prediction of creep in concrete, Unpublished Ph.D. Thesis, University of Illinois, 1967.

140. WATSON, K.K.: Non-continuous porous media flow, Report No. 84, 1965, University of New South Wales.

141. WHISLER, F.D., KLUTE, A. and PETERS, D.B.: Soil water diffusivity from horizontal infiltration, Proc. Soil Science Society of America, 1968, Vol. 32, No. 1, p.6.

142. WITTMANN, F.: Surface tension shrinkage and strength of hardened cement paste, Materials and Structures, Nov.-Dec. 1968, p.547.

143. ZOLLINGER, W.D., CAMPBELL, G.S. and TAYLOR, S.A.: A comparison of water potential measurements made using two types of thermocouple psychrometers, Soil Science, Vol. 102, No. 4, p.231.

GLOSSARY OF SPECIAL TERMS

C.B.R. - California Bearing Ratio.

CRACK INTENSITY - Signifies the number of cracks per unit length.

CRACKING - When the internal stress build-up within a soil-cement prism or soil-cement pavement exceeds the tensile strength of the soil-cement cracking occurs.

CREEP - Defined as the excess deformation over shrinkage of a loaded sample.

DIFFUSE CEMENTATION - The diffusion of lime in solution throughout the matrix and lumps in a soil-cement.

DISJOINTING PRESSURE - The extra pressure which developes in areas of hindered adsorption.

DRYING SHRINKAGE STRESSES - The stresses which develop from strain changes caused by drying of a soil-cement.

FATIGUE FAILURE - Failure of a soil-cement at a stress lower than the ultimate strength because of the repetition of loads applied.

FLEXIBLE PAVEMENT - A pavement which carries little traffic load by beam action, but relys on a consistent load bearing ability of the sub-base and sub-grade.

HINDERED ADSORPTION - An area at the apex of a wedge shaped void which does not permit adsorption of the full number of water molecules available.

MOIST CURE SHRINKAGE - The measured change in length caused by self desiccation as a sample moist cures in the absence of an applied load.

MOLECULAR SIEVE DEVICE - The use of different sized liquid molecules to determine the approximate void spacing.

OUTFLOW DATA - The outflow in cuesecs from a pressure membrane cell.

PF - Common logarthm of the height in cm of a water column which the suction would support.

PRECURE MOISTURE CONTENT - The moisture content at which the natural soil is stored before being mixed with cement and water.

PRIMARY REACTION - The hydration of cement to form hydration products in which skeletal formation occurs.

PULVERIZATION - The breaking down of soil lumps to a fine grading.

RHEOLOGICAL MODEL - A mechanical model usually composed of dashpots and springs and used to represent both elastic and non-elastic changes in a material.

RIGID PAVEMENT - A pavement which sustains traffic loading almost entirely by beam action.

SECONDARY REACTION - The release of lime and its reaction with the clay particles.

SELF-DESICCATION - In a sealed system the loss of moisture from a soil lump to the surrounding matrix with consequent shrinkage of the soil lump.

SHRINKAGE - The measured change in length caused by moisture loss in the absence of an applied load.

SHRINKAGE STRESS BUILD-UP - The internal build-up of stress caused by shrinkage strain changes in either a small soil-cement prism of a soil-cement pavement.

STRAIN REVERSAL - The point at which the strains in a prism change sign.

STRUCTURE OF SOIL-CEMENT - The development of bonds and the physical distribution of constituents of soil-cement.

SUCTION - A measure of the energy of retention of moisture retained in a material.